



UNIVERSITAT
POLITÈCNICA
DE VALÈNCIA

DEPARTAMENTO DE MÁQUINAS Y MOTORES TÉRMICOS

DOCTORAL THESIS

**STUDY OF DIFFERENT
STRATEGIES TO IMPROVE THE
INTERNAL COMBUSTION ENGINE
(ICE) OPERATING AT COLD
CONDITIONS**

Presented by: MR. MIGUEL ÁNGEL BERNAL MALDONADO
Supervised by: DR. VICENTE DOLZ RUIZ

Valencia, December 2022

DOCTORAL THESIS

**Study of Different Strategies to Improve the Internal Combustion
Engine (ICE) Operating at Cold Conditions**

AUTHORS

Presented by: MR. MIGUEL ÁNGEL BERNAL MALDONADO
Supervised by: DR. VICENTE DOLZ RUIZ

Ph.D. ASSESSORS

DR. OCTAVIO ARMAS VERGEL
DR. ÓSCAR GARCÍA AFONSO
DR. FRANCISCO VERA GARCÍA

DEFENSE COMMITTEE

Chairman: DR. HÉCTOR CLIMENT PUCHADES
Secretary: DR. FRANCISCO VERA GARCÍA
Member: DR. JUAN JOSÉ HERNÁNDEZ ADROVER

Valencia, December 2022

Abstract

Current and future legislations, regarding pollutant emissions reduction and green mobility, will continue fixing a difficult stage for the development and improvement of internal combustions engines (ICEs). The Real Driving Emissions (RDE) parameters, the changes of altitude, and the extreme ambient temperature conditions in operation, are the major challenges to fulfill under these new legislations. By these reason, academy and automotive manufacturers continue working in collaboration, trying to develop more efficient and less polluting powertrains.

In this experimental research work, the main results of a collaboration project between the private company Valeo Systèmes Thermiques and the Universitat Politècnica de València are presented. Exhaust gas recirculation (EGR), in both configurations, high-pressure and low-pressure, and Cylinder Deactivation (CDA), are the main strategies studied in this work due to its high potential and low-cost implementation. These strategies are evaluated in a Light-duty Diesel engine, fitted in a climatic test bench and operating under low ambient temperature (-7°C).

The first strategy is the High-pressure EGR activation from the beginning of the engine start and the development of a simple condensation model able to predict whether or not there is condensation inside the EGR line under these conditions. In particular, the humidity ratio and the internal engine conditions that characterize the appearance of this phenomenon are estimated by the model. This model is validated by means of cameras fitted on the EGR rail in order to visualize the condensation evolution. The humidity ratio estimate and the condensation behavior observed through the cameras, shows that during an engine cold start, condensation conditions in the gases are present until reach approximately 50°C , while in solid walls and components, the conditions remains until reach approximately 30°C . In the second strategy, a new compact line fitted with a bypass system for the cooler is used with the aim of accelerating the engine warm-up process as compared to the original low-pressure EGR line. The aim of this strategy is to evaluate the impact on the engine behavior of performing Low-pressure EGR at cold conditions and to activate the bypass system in order to disable the cooler. Following this strategy, a noticeable NO_x emissions reduction of approximately 60% with respect to a reference case without low-pressure EGR has been achieved. In addition, the engine warm-up process has been reduced in approximately 60 seconds and the engine intake temperature has been increased 30°C , leading a CO emissions reduction of approximately 12%. In the third strategy, the impact of using a new cylinder deactivation configuration with the aim of improving the engine warm-up process is evaluated. The results show an increase of the exhaust temperatures of around 100°C , which allows to reduce the diesel oxidation catalyst light-off by 250 seconds besides of reducing the engine warm-up process in approximately 120 seconds. This allows to reduce the CO and HC emissions by 70% and 50%, respectively. And finally, the last experimental strategy evaluates the impact of using

the high-pressure exhaust gas recirculation while the diesel particulate filter is under active regeneration mode. Following these possible engine calibration conditions, a NO_x emissions reduction of approximately 50% with respect to a reference case without high-pressure EGR during a DPF regeneration process has been achieved. CO and HC emissions has been also reduced due to the improvements in combustion efficiency and fuel consumption. However, performing high-pressure EGR at cold conditions could contribute to the DPF saturation and degradation, due to the increased difference pressure in the DPF and therefore an increment in the EGR rate and EGR temperatures.

Resumen

Las actuales y futuras normativas, en términos de emisiones contaminantes y movilidad sostenible, continuarán fijando una difícil etapa para el desarrollo y mejoramiento de los motores de combustión interna alternativos (MCIA). Los nuevos parámetros conocidos como, emisiones reales de conducción, los cambios de altitud y las condiciones extremas de operación a bajas temperaturas, son los mayores desafíos para cumplir bajo estas nuevas normativas. Por esta razón, la academia y los fabricantes de la industria de la automoción continúan trabajando en colaboración, tratando de desarrollar más eficientes y menos contaminantes sistemas de propulsión.

En este trabajo experimental de investigación, los principales resultados de un proyecto de colaboración llevado a cabo entre la empresa Valeo Systèmes Thermiques y la Universitat Politècnica de València son presentados. La recirculación de gases de escape, en sus dos configuraciones, de alta y de baja presión, y la desactivación de cilindros, son las principales estrategias que se estudiarán en este trabajo, debido a su alto potencial y su bajo costo de implementación. Estas estrategias son evaluadas en un motor Diesel, instalado en una cámara de ensayos climática y operando a bajas temperaturas ambiente (-7°C).

La primera estrategia, es la activación de la EGR de alta presión desde el inicio de un arranque de motor y el desarrollo de un modelo de condensación simple capaz de predecir si hay o no condensación dentro de la línea de EGR bajo estas condiciones. En particular, el ratio de humedad y las condiciones internas del motor que caracterizan la aparición de este fenómeno son calculadas por el modelo. Este modelo es validado por medio de cámaras instaladas en el rail de EGR con el objetivo de visualizar la evolución de la condensación dentro de los componentes. El ratio de humedad calculado y el comportamiento de la condensación observado a través de las cámaras, muestran que durante un arranque de motor en frío, las condiciones de condensación en los gases están presentes hasta que se alcanzan aproximadamente 50°C , mientras que en las paredes sólidas y en los componentes, las condiciones se mantienen hasta que se alcanzan aproximadamente 30°C . En la segunda estrategia, una nueva línea de EGR compacta, equipada con un sistema de bypass para el intercambiador de calor es usada con el objetivo de acelerar el proceso de calentamiento del motor en comparación a la línea de EGR de baja presión original del motor. El objeto de esta estrategia es evaluar el impacto en el comportamiento del motor de realizar EGR de baja presión a bajas temperaturas con la activación del sistema de bypass para deshabilitar el intercambiador de calor. Siguiendo esta estrategia, una notable reducción en emisiones de NO_x de aproximadamente 60% con respecto a un caso de referencia sin activación de la EGR de baja presión es lograda. Además, el proceso de calentamiento del motor ha sido reducido en aproximadamente 60 segundos y la temperatura de admisión del motor ha sido aumentada en 30°C , liderando una reducción en las emisiones de CO de aproximadamente

12%. En la tercera estrategia, el impacto de usar una nueva configuración de la desactivación de cilindros con el propósito de acelerar el proceso de calentamiento del motor es evaluada. Los resultados muestran un incremento en la temperatura de escape de alrededor de 100°C, el cual permite reducir la activación del catalizador en 250 segundos además de reducir el proceso de calentamiento del motor en aproximadamente 120 segundos. Esto permite reducir las emisiones de CO y HC en un 70% y 50%, respectivamente. Y finalmente, la última estrategia experimental realizada, evalúa el impacto de usar la EGR de alta presión mientras el filtro de partículas está en el modo activo de regeneración. Siguiendo esta posible condición de calibración de motor, una reducción en emisiones de NO_x de aproximadamente 50% con respecto a un caso de referencia sin activar la EGR de alta presión ha sido alcanzada. Las emisiones de CO y HC han sido también reducidas debido a la mejora en la eficiencia de la combustión y el consumo de combustible. Sin embargo, realizar EGR de alta presión a bajas temperaturas puede contribuir a la saturación y degradación del filtro de partículas, debido al incremento en el diferencial de presión en el filtro y como consecuencia el incremento en la tasa de EGR y las temperaturas de EGR.

Resum

Les actuals i futures normatives, en termes d'emissions contaminants i mobilitat sostenible, continuaran fixant una difícil etapa per al desenvolupament i millorament dels motors de combustió interna alternatius (MCIA). Els nous paràmetres coneguts com, emissions reals de conducció, els canvis d'altitud i les condicions extremes d'operació a baixes temperatures, són els majors desafiaments per a complir les noves normatives. Per aquesta raó, l'acadèmia i els fabricants de la indústria de l'automoció continuen treballant en col·laboració, tractant de desenvolupar més eficients i menys contaminants sistemes de propulsió.

En aquest treball experimental d'investigació, es presenten els principals resultats d'un projecte de col·laboració dut a terme entre l'empresa Valeo Systèmes Thermiques i la Universitat Politècnica de València. La recirculació de gasos del motor, en les seues dues configuracions, d'alta i de baixa pressió, i la desactivació de cilindres, són les principals estratègies que s'estudiaran en aquest treball, a causa del seu alt potencial i el seu baix cost d'implementació. Aquestes estratègies són avaluades en un motor Dièsel, instal·lat en una cambra d'assajos climàtica i operant a baixes temperatures ambient (-7°C).

La primera estratègia, és l'activació de la EGR d'alta pressió des de l'inici d'una arrancada de motor i el desenvolupament d'un model de condensació simple capaç de predir si hi ha o no condensació dins de la línia de EGR. En particular, el ràtio d'humitat i les condicions internes del motor que caracteritzen l'aparició d'aquest fenomen són calculades pel model. Aquest model és validat per mitjà de càmeres instal·lades a el rail de EGR amb l'objectiu de visualitzar l'evolució de la condensació dins dels components. El ràtio d'humitat calculat i el comportament de la condensació observat a través de les càmeres, mostren que durant una arrancada de motor en fred, les condicions de condensació en els gasos són presents fins que s'aconsegueixen aproximadament 50°C , mentre que a les parets i als components, les condicions es mantenen fins que s'aconsegueixen aproximadament 30°C . En la segona estratègia, una nova línia de EGR compacta, equipada amb un sistema de bypass per a l'intercanviador de calor és usada amb l'objectiu d'accelerar el procés de calfament del motor en comparació a la línia de EGR de baixa pressió original del motor. L'objecte d'aquesta estratègia és avaluar l'impacte en el comportament del motor de realitzar EGR de baixa pressió a baixes temperatures amb l'activació del sistema de bypass per a evitar l'intercanviador de calor. Seguint aquesta estratègia, s'aconsegueix una notable reducció en emissions de NO_x d'aproximadament 60% respecte a un cas de referència sense activació de la EGR de baixa pressió. A més, el procés de calfament del motor ha sigut reduït en aproximadament 60 segons i la temperatura d'admissió del motor ha sigut augmentada en 30°C , produint una reducció en les emissions de CO d'aproximadament 12%. Per a la tercera estratègia, és avaluat l'impacte d'usar una nova configuració de la desactivació de cilindres amb el propòsit d'accelerar el procés de calfament del motor. Els

resultats mostren un increment a la temperatura dels gasos de al voltant de 100°C, el qual permet reduir l'activació del catalitzador en 250 segons a més de reduir el procés de calfament del motor en aproximadament 120 segons. Això permet reduir les emissions de CO i HC en un 70% i 50%, respectivament. Finalment, l'última estratègia experimental realitzada, avalua l'impacte d'usar la EGR d'alta pressió mentre el filtre de partícules està en la manera activa de regeneració. Seguint aquesta possible condició de calibratge de motor, ha sigut aconseguida una reducció en emissions de NO_x d'aproximadament 50% respecte a un cas de referència sense activar la EGR d'alta pressió. Les emissions de CO i HC han sigut també reduïdes a causa de la millora en l'eficiència de la combustió i el consum de combustible. No obstant això, realitzar EGR d'alta pressió a baixes temperatures pot contribuir a la saturació i degradació del filtre de partícules, a causa de l'increment en el diferencial de pressió en el filtre i com a conseqüència l'increment en la taxa de i les temperatures de EGR.

List of publications

The following papers form the basis of this thesis have been published:

- “High-pressure exhaust gas recirculation line condensation model of an internal combustion diesel engine operating at cold conditions” by Luján, Dolz, Monsalve, and Bernal [1].
- “Advantages of using a cooler bypass in the low-pressure exhaust gas recirculation line of a compression ignition diesel engine operating at cold conditions” by Galindo, Dolz, Monsalve, Bernal, and Odillard [2].
- “EGR cylinder deactivation strategy to accelerate the warm-up and restart processes in a Diesel engine operating at cold conditions” by Galindo, Dolz, Monsalve, Bernal, and Odillard [3].
- “Impacts of the exhaust gas recirculation (EGR) combined with the regeneration mode in a compression ignition diesel engine operating at cold conditions” by Galindo, Dolz, Monsalve, Bernal, and Odillard [4].

Other publications

The following list presents other publications in which the author of this thesis was involved during the researches leading to the present work. Although not directly present in this document, they have provided a deeper insight into Diesel Engine improvements.

- “Exhaust gas recirculation combined with regeneration mode in a compression ignition diesel engine operating at cold conditions” by Galindo, Dolz, Monsalve, Bernal, and Odillard [5].

To my wife, with love.

Acknowledgements

First of all, I want to express my gratitude to the CMT Motores Térmicos team, for giving me the opportunity of growing up as a professional and as a person during these last years. Especially to my friend, colleague and tutor, Mr. Vicente Dolz Ruiz. Thank you Vicente for giving me your support and sharing with me and your students all your great knowledge and wisdom.

Guille, Alberto, Nico, Pau and Lucas, thank you for greeting this foreign and make him part of your group. We only know how is the road and the efforts to travel it. Juancho and Fabio, do not fall, go ahead and take pride in what we are achieving far away from home.

I want to dedicate this work to my family, my mother Doris, my father Suley and my brother Juanpis. You have done the main contribution to this work with your love, your support, your dedication and your sacrifices. This success is also yours.

Thank you to my whole family, specially to Guanita, Fanny, Jorge Mario, Sergio, Diana, Camilita, Elsa, Julia, Álvaro, Jovita, Blanquita, Gerver, Nelson, Andrés and Beatriz. Missing all of you has been one of the biggest challenges to overcome every day. You are always present in my mind. Thank you also to Alex and Maria Isabel, I feel fortunate of being part of your family.

I want to dedicate some words to my best friends and the people who have joined to my road along these years. Carmen, Johannita, Yuddy, John Jairo, Lippe, Tavo, you know you have a special place in my heart. Ali, Cris, Noe and Miquel, you are my support, my family and another success in this process.

My love, you have this place, because it is the most important. I can not find the words to tell you how much I love you and how much I recognize your patience, your support, your effort and your incredible love for me. Estefanía, my wife and life partner, my happiness is to share my life with you and the moments that we traveled together. Let's continue writing this story of love.

Funding acknowledgements

Miguel Ángel Bernal Maldonado has been partially supported through contract FPI-S1-2017-2377 of "Programa de Ayudas de Investigación y Desarrollo (PAID-01-17) de la Universitat Politècnica de València". The support of Valeo Systèmes Thermiques through projects CN-2016-99 and CN-2018-08 is also greatly acknowledged.

*Go back to the root and you will find the meaning
(Sengcan)*

Contents

Contents	xv
List of Figures	xvii
List of Tables	xix
Nomenclature	xxi
1 Introduction	1
1.1 Background	2
1.2 Motivation	2
1.3 Objectives	3
1.4 Methodology	4
1.5 References	6
2 Literature Review	7
2.1 Engines Pollutant Emissions Overview	8
2.2 High-pressure EGR	9
2.3 Low-pressure EGR	10
2.4 Cylinders Deactivation	12
2.5 Diesel Particulate Filter Regeneration with High-pressure EGR	12
2.6 References	15
3 Experimental Testbench	21
3.1 Introduction	22
3.2 Experimental Setup	23
3.3 Engine Cycle and Methodologies	26
3.4 Engine Configuration Strategies	28
3.5 Summary	35
3.6 References	36
4 High-pressure EGR Condensation Model	37
4.1 Introduction	38
4.2 Methodology and Strategies	39

4.3	Condensation Model	40
4.4	Results and Model Validation	43
4.5	Summary	52
4.6	References	53
5	Low-pressure EGR Bypass	55
5.1	Introduction	56
5.2	Methodology and Strategies	57
5.3	Results and Discussions	58
5.4	Condensation and Fouling Analysis	63
5.5	Summary	71
5.6	References	72
6	Cylinder Deactivation Strategy	73
6.1	Introduction	74
6.2	Methodology and Strategies	75
6.3	Experimental study at ambient temperature (20°C)	78
6.4	Experimental study at cold conditions (-7°C)	83
6.5	Summary	87
6.6	References	88
7	DPF Regeneration with High-pressure EGR	89
7.1	Introduction	90
7.2	Methodology and Strategies	91
7.3	Results and Discussions	92
7.4	Summary	102
7.5	References	103
8	Conclusions and Future Works	105
8.1	Introduction	106
8.2	Main contributions	107
8.3	Future works	112
	Bibliography	113

List of Figures

3.1	Engine Configuration and Instrumentation	24
3.2	Engine fitted in the climatic test-bench	25
3.3	Profile of the cycle performed	27
3.4	EGR rate measure	27
3.5	High-pressure EGR circuit configuration	29
3.6	Cameras Configuration and Field of View	30
3.7	Engine configuration with the Low-pressure EGR bypass fitted	31
3.8	Low-pressure EGR Bypass Prototype	31
3.9	Engine Set-up, Cameras Configuration and Field of View	32
3.10	a) Standard Engine Configuration b) EGR DEACT Configuration	33
4.1	HP EGR activation since engine cold start	39
4.2	IC engine scheme with water mass flows	42
4.3	Sample of the images captured by the cameras at the cylinder intake ports in the EGR	43
4.4	Measured engine speed, fuel consumption, torque and EGR% during the first 400 sec of the cycle	44
4.5	Measured pressures during the first 400 sec of the cycle	45
4.6	Measured temperatures during the first 400 sec of the cycle	46
4.7	Water mass flow estimate and HC mass flow during the first 400 sec of the cycle	47
4.8	Estimated relative humidity during the first 400 sec of the cycle	48
4.9	Video frames of the 4 cylinder cameras in the second 1, 100, 200, 300 and 400. In these pics φ_g is the relative humidity in the gas side and φ_w is the relative humidity in the wall side	49
4.10	Estimated relative humidity from the second 400 to the second 1200 of the cycle	50
4.11	Video frames of the 4 cylinder cameras in the second 400, 600, 800, 1000 and 1200. In these pics φ_g is the relative humidity in the gas side and φ_w is the relative humidity in the wall side	51
5.1	Low-pressure EGR rate from cold start conditions with the modified calibration	57
5.2	Compressor Outlet Temperature and Intake Manifold Temperature	58
5.3	Exhaust Temperature with Zoom	59
5.4	Engine Coolant Temperature with Zoom	60
5.5	Accumulated Pollutant Emissions. Continuous line: Engine-out emissions. Dashed line: Tailpipe emissions	61
5.6	Combustion Efficiency and Accumulated Fuel Consumption	63

LIST OF FIGURES

5.7	Video frames comparing two tests performed without (left) and with (right) bypass activation in the second 100, 200, 300 and 400	64
5.8	Video frames comparing two tests performed without (left) and with (right) bypass activation in the second 500, 600, 700 and 800	65
5.9	LP EGR Cooler Outlet Temperature (Gas Temperature)	66
5.10	Thermal Gravimetric Analysis (TGA) Profile	67
5.11	Pictures of fouling conditions after tests performed with and without bypass activation	69
5.12	Detail of fouling observed on the bypass flap	70
5.13	Initial (left) and final (right) conditions of the LP EGR cooler	70
6.1	Standard and EGR DEACT Fuel Injection Strategy	76
6.2	Torque limitations as function of VGT and EGR DEACT Valve position – 1500rpm	77
6.3	Indicated Diagram Profile (P – V) for the EGR DEACT Configuration	78
6.4	Torque at 20°C	81
6.5	Engine coolant and turbine outlet temperature at 20°C	81
6.6	Engine pollutant emissions at 20°C	83
6.7	Torque at -7°C	85
6.8	Engine coolant and turbine outlet temperature at -7°C	85
6.9	Engine pollutant emissions at -7°C	86
7.1	Profile of the tests performed	91
7.2	Engine intake temperature	93
7.3	HP EGR rate performed	94
7.4	Turbocharger behavior	94
7.5	DPF difference pressure	95
7.6	DPF inlet temperature	96
7.7	Pressure drop dimensionless coefficient	97
7.8	Raw pollutant emissions measurements	98
7.9	Combustion efficiency and BSFC	99
7.10	Fouling observed on the HP EGR valve	100
7.11	Fouling observed on the section of the HP EGR rail	100

List of Tables

3.1	Engine Specifications	23
3.2	Instrumentation Accuracy	26
4.1	Ratio of hydrogen mass in an alkane hydrocarbon of single bonds . .	41
5.1	Gas Chromatography – Mass Spectroscopy (GC – MS) Results	68
6.1	Indicated work and pumping losses estimation	79
6.2	Engine performance at 20°C	80
6.3	EGR rate limitations	82
6.4	Engine performance at -7°C	84

Nomenclature

\dot{m}	Mass flow rate [kg/s]	V	Dead volume [m ³]
$\dot{m}_{(H_2O/air)}$	Water mass flow from air	W	Work [J]
$\dot{m}_{(H_2O/exh)}$	Water mass flow at cylinders	w	Humidity Ratio
$\dot{m}_{(H_2O/fuel)}$	Water mass flow from combustion	1D	One Dimensional
η_{Comb}	Combustion Efficiency	AC	Alternative Current
$\tau_{(H/fuel)}$	Ratio of hydrogen mass in fuel	BDC	Bottom Dead Center
$\tau_{(H/H_2O)}$	Ratio of hydrogen mass in water	BSFC	Brake Specific Fuel Consumption
$\tau_{(H_2O/fuel)}$	Water ratio in fuel	CDA	Cylinder Deactivation
CO_2	Carbon Dioxide	CFD	Computational Fluid Dynamics
i	Number of cylinders	CMT	Centro de Motores Térmicos
n	Speed [rpm]	CO	Carbon Monoxide
$n^{\circ}C$	Number of Carbon Atoms	DOC	Diesel Oxidation Catalyst
$n^{\circ}H$	Number of Hydrogen Atoms	DPF	Diesel Particulate Filter
NO_x	Nitrogen Oxides	DPI	Dots per Inch
P	Pressure [bar]	ECU	Electronic Control Unit
R	Universal Gas Constant	EGR	Exhaust Gas Recirculation
T	Temperature [°C]	ET	Exhaust Throttle
		EU	European Union

NOMENCLATURE

FPS	Frames per Second	VGT	Variable Geometry Turbine
GC-MS	Gas Chromatography - Mass Spectroscopy	VOC	Volatile Organic Compound
GHG	Green House Gases	VVT	Variable Valve Timing
GPF	Gasoline Particulate Filter	WCAC	Water Charge Air Cooler
HC	Hydrocarbons	WLTC	Worldwide harmonized Light vehicles Test Procedures
HEV	Hybrid Electric Vehicle		
HP	High-pressure		
ICE	Internal Combustion Engine		
IMEP	Indicated Mean Effective Pressure		
LDV	Light Duty Vehicle		
LP	Low-pressure		
MR	Mid-route		
NEDC	New European Driving Cycle		
OEM	Original Equipment Manufacturer		
P-V	Pressure-Volume		
PID	Proportional Integral Derivative Controller		
PM	Particulate Matter		
RLS	Road Load Simulation		
SCR	Selective Catalyst Reduction		
TDC	Top Dead Center		
TGA	Thermal Gravimetric Analysis		
VC	Volume Coefficient		

Greek Symbols

α	Leaks Coefficient
Δ	Increment
η	Efficiency
ρ	Density [kg/m ³]
τ	Ratio
φ	Relative Humidity

Subscripts

<i>air</i>	Air
<i>amb</i>	Ambient
<i>boost</i>	Boost Pressure
<i>comb</i>	Combustion
<i>eng</i>	Engine
<i>exh</i>	Exhaust Gases Side
<i>fuel</i>	Fuel
<i>i</i>	Indicated
<i>int</i>	Inlet Conditions
<i>out</i>	Outlet Conditions
<i>rate</i>	Ratio
<i>theor</i>	Theoretical Value
<i>vol</i>	Volumetric

CHAPTER **1**

Introduction

1.1 Background

TODAY, the automotive industry is in a transition process where the IC engine, specially, the light-duty diesel engine, is being replaced by new technologies like hybrid and fully electric vehicles. This situation has been derived from the daily-daily more stringent environmental regulations implemented by the governments of the European Union (EU). The current normative, Euro 6d Temp, effective from 2020, considers the engine operation under a wide range of temperatures and conditions, from -7°C to 35°C and altitudes from 0 to 1200 meters. A future normative, Euro 7, targeted for 2025, could increase the range of these limitations with more stringent conditions and could impose a NO_x emissions reduction up to 50% less with respect to the current Euro 6d normative.

Despite these circumstances, current mobility is still highly dependent of fossil fuels, and consequently, of internal combustion engines (ICEs), besides, recent studies have shown that the transition from diesel to electric motor power, is being progressive and slower than expected. Even though it is estimated that half of new cars sold will be electric in the year 2030, it will still take many more years after to make a significant dent in greenhouse gas emissions [6]. Meanwhile, conventional technologies like exhaust gas recirculation (EGR) and new technologies like biofuels and water injection strategies in IC engines can reduce the carbon foot print while electric vehicle technology is further developed and institutionalized.

By these reasons, people and goods transport is a fundamental activity for the development of modern societies, and to achieve this goal, it is necessary to continue developing efficient light vehicles with low fuel consumption and low pollutant emissions levels.

1.2 Motivation

For the last ten years, environmental normatives and legislations around the world have stated a difficult stage for the internal combustion engines (ICE). Greenhouse gas emissions and Euro regulations have represented an industrial race for developing the more efficient technologies and the more ecological solutions. In this race, the automotive industry has led a great effort in the development of more sustainable technologies, such as hybrid and completely electric powertrain. Moreover, diesel and gasoline technologies, continue taking precedence and due to their still high presence in the automotive market, are presented as an important part of the procedure and as mentioned before, a possible contributor to reduce the carbon foot print in the planet.

Following this motivation, and due to the cost reduction of this kind of projects, widely use techniques as the exhaust gas recirculation (EGR) and more recent techniques as the cylinder cutout or cylinder deactivation, are presented as possible candidate solutions for NO_x emissions constraints and engine warm-up advance with the aim to fulfill the current and future environmental legislations. This thesis contributes to the knowledge and evaluation of these strategies implemented in an IC Engine when it is operated at -7°C . The thesis is based on different experimental works carried out on a diesel engine coupled to a climatic test-bench.

This work is part of a research project named “Further researches of a Euro 6 diesel engine running under -7°C environment temperature” funded by a Collaboration Project with reference CN-2018-08 between the Universitat Politècnica de València and the international private company Valeo Systèmes Thermiques. In this research work several tests were performed to evaluate the different experimental strategies and its impact on the IC engine performance.

1.3 Objectives

The main objective of this research work is to evaluate and analyze the potential of different experimental strategies to improve the internal combustion engine (ICE) working under low ambient temperatures (-7°C). The aim of this work is to achieve an improvement of the IC engine in terms of pollutant emissions, specially NO_x emissions, combustion efficiency and thermal behavior. Therefore, the main objective can be divided in four partial objectives.

Experimental evaluation of the different strategies In order to quantify the potential of each strategy, a light-duty diesel engine is installed in a climatic test bench at CMT - Motores Térmicos, which can reach temperatures up to -20°C and allow to test different driving conditions. Four experimental strategies were developed:

- High-pressure EGR condensation model: To develop and validate experimentally a condensation model able to estimate whether or not there is condensation inside the High-pressure EGR line of an IC engine operating at cold conditions (-7°C).
- Low-pressure EGR Bypass prototype: To analyze the impact of a new compact line of Low-pressure EGR fitted with a cooler bypass on the engine warm-up process, the regulated diesel emissions, NO_x and soot, as well as on the thermal engine efficiency when it is activated at cold conditions (-7°C). In addition, to visualize and characterize chemically the

condensation phenomena and the fouling inside the Low-pressure EGR line.

- **Cylinder Deactivation strategy:** To evaluate a new method of the cylinder deactivation strategy, named “EGR DEACT”, the pumping losses presented when a cylinder works only under compression and expansion processes, and the impact on the engine behavior at steady-state and transient conditions under standard ambient temperature (20°C), to subsequently reply this strategy and evaluate the effects of using the EGR DEACT strategy at steady-state conditions and during the engine cold start (-7°C) on the regulated diesel emissions and the engine thermal efficiency.
- **Diesel Particulate Filter (DPF) Regeneration with High-pressure EGR activation:** To analyze the impact on the engine response in the regulated diesel emissions, NO_x and fuel consumption, as well as on the combustion engine efficiency, of performing High-pressure EGR while the DPF is under regeneration mode at cold conditions (-7°C). To visualize, characterize and estimate the amount of soot produced under these particular conditions.

1.4 Methodology

The methodology used in this research work has been focused on the literature review of the potential of the exhaust gas recirculation (EGR), in its two configurations, high-pressure and low pressure, and the deactivation cylinder technique as low cost effective solutions in diesel engine applications. The main advantages and disadvantages, operating conditions and pollutant emissions results are reviewed in [Chapter 2](#). Subsequently, the experimental methodology is split, as in the objectives, into four different parts.

The aim of the experimental methodology presented in [Chapter 3](#) is to obtain an experimental understanding of the different strategies performed with the IC engine.

- **Develop a High-pressure EGR condensation model** able to predict under which particular conditions the condensation phenomena appears inside the EGR line of an IC engine working at cold conditions. A simple mathematical model able to calculate the relative humidity in different points of the EGR line was developed. The High-pressure EGR rail was fitted with endoscope cameras in order to visualize and validate experimentally the condensation model results. This will be presented in [Chapter 4](#).

- Evaluate the impact on the engine behavior of a Low-pressure EGR cooler bypass working at cold conditions. A new compact Low-pressure EGR line fitted with a bypass system for the cooler was installed on the engine. The first part of the [Chapter 5](#) will present the engine behavior under two configurations, activating the bypass or not together with the Low-pressure EGR along a representative driving cycle. The second part of the [Chapter 5](#) will present the condensation conditions observed on the engine components, by means of endoscope cameras and chemical analyzing a sample of this residual particles.
- Evaluate a new proposal of cylinder deactivation named “EGR DEACT”, as a solution to improve the engine warm-up process operating at cold conditions. The High-pressure EGR line was modified in order to deactivate two of the four cylinders of the engine and evaluate its response in terms of pumping losses, thermal behavior and pollutant emissions reduction. The first part of the [Chapter 6](#) will present the main results of this study under standar ambient conditions (20°C). The second part of the [Chapter 6](#) will present the impacts of this strategy working at low ambient temperature (-7°C).
- Analyze the impact of performing High-pressure EGR together with DPF regeneration process under cold operating conditions. The standar engine calibration was modified with the aim of testing this possible engine scene and its impacts on the thermal engine behavior and performance. In addition, an approach estimation of the amount of soot produced under this conditions was realized. The main results of this experimental work will be presented in [Chapter 7](#)

1.5 References

- [6] U. of Michigan Michigan Engineering. *Video: 100% renewable diesel cars can reduce carbon emissions while waiting for electric vehicles*. 2021. URL: <https://news.engin.umich.edu/2021/09/100-renewable-diesel-cars-can-reduce-carbon-emissions-while-waiting-for-electric-vehicles/> (cit. on p. 2).

CHAPTER **2**

Literature Review

2.1 Engines Pollutant Emissions Overview

The introduction of the current regulations for the vehicles homologation has imposed new challenges to the car manufacturers and research institutions in this field. In this sense, the fuel consumption reduction, altitude variations, real driving emissions and cold operating conditions are considered guidelines in the current and future legislations [7]. Furthermore, the consequent reduction in the pollutant emissions levels is a second challenge to achieve for the automotive industry. Apart from the imperative reduction of the carbon dioxide (CO₂) and carbon monoxide (CO) emissions, the nitrogen oxides (NO_x) emissions reduction in diesel engines will be a major concern in future regulatory stages [8]. In order to fulfil these regulations, the internal combustion engine architecture is being continuously studied and improved by testing different strategies and systems that allow to reduce the impact of these pollutant emissions in the environment [9], [10].

The operation conditions of the test drive for these new regulations will consider the effect of running at lower ambient temperature [11]. For example, the recent Euro 6d regulation includes the engine operation at -7°C. Considering this context, the fuel consumption and pollutant emissions during the engine warm-up become as critical parameters. According to the literature [12] [13], unburned hydrocarbons (HC) and carbon monoxide (CO) are mainly emitted when the engine temperatures remain low due to the strong temperature dependence of the after-treatment systems to reach its maximum efficiency. This is particularly important in the hybrid electric vehicles (HEV), in which the shut-off and engine restart occur more often, introducing a key challenge to keep the aftertreatment temperature at the pertinent levels. Another consequence of operating at low ambient temperature is the exhaust gas recirculation (EGR) limitations and its dependency with the nitrogen oxides (NO_x) concentration and the particulate matter (PM) and condensation generated at these conditions [14]. In this sense, it is proved that accelerating the warm-up process and increasing the engine temperatures can provide benefits such as HC and CO emissions reduction, combustion noise control and engine stability improvement after the cold start, besides of the possibility of implement different and enhanced warm-up and EGR calibration strategies [15].

The exhaust gas recirculation (EGR) is a widely used technique to reduce the nitrogen oxides (NO_x) from internal combustion engines (ICE), especially in diesel engines [16]. Many engine manufacturers have invested time and resources trying to optimize this technique due to its effectivity to reduce these kind of emissions [17]. A recent solution implemented by the manufacturers of current diesel engines was the use of two independent EGR circuits. Although making complex the engine architecture, this was found to be an effective

solution to reduce the NO_x levels in different engine operating points [18] [19]. The first circuit, is the conventional EGR circuit, known as high-pressure (HP) EGR, where the EGR rates are limited by the pressure difference among the inlet and outlet manifolds. The second circuit, is an innovative solution known as low-pressure (LP) EGR, which has been introduced as a cleaner EGR, with higher values of EGR rates and the same effectivity to reduce NO_x emissions [20]. For these reasons, the use of EGR could be mandatory to comply with the current and future approval regulations.

2.2 High-pressure EGR

The use of exhaust gas recirculation (EGR) to reduce the NO_x levels presents some issues, as per example the condensation that can appear inside the components when the engine is running at low temperatures. The gas coming from the fuel combustion has important water content as well as other products of the combustion process [21]. Thus, if the gas temperature is reduced below the dew point, the partial condensation of the water vapor will occur. In this sense, condensation deposits may appear in the engine components through which the EGR flows, contributing to the fouling processes on these elements. Even more, with the moisture, some acids and hydrocarbon (HC) species coming from the fuel composition may condensate corroding these components and reducing their life [22] [23]. Furthermore, these hydrocarbon species could affect in-cylinder processes during the combustion [24]. For instance, Furukawa et al. [25] studied the deposits resulting from high concentration of hydrocarbons due to the exhaust gas recirculation on control valves. The author identified the chemical components of each type of hydrocarbons present and their dew points in order to determine the conditions in which valve sticking occurs in engines. On the other hand, the liquid water injected into the cylinders can improve the engine behavior considering different injection-combustion strategies [26] [27].

The condensation phenomenon has been widely studied by many authors in the past, however the detailed models proposed in the literature are difficult to parameterize and validate [28]. This fact makes interesting the study of semi-empirical models for different cases.

In automotive applications, it is not usual that the EGR temperature falls below the dew point when a high-pressure (HP) EGR layout is used. However, the condensation of the moisture contained in the burnt gas can occur during cold start phases. As soon as the coolant temperature warms-up ($\approx 80^\circ\text{C}$) the condensation becomes almost unreachable [29]. By contrast, with a low-pressure (LP) EGR arrangement, the condensation may occur even after engine warm-up, mainly when the humid stream of EGR is mixed with a cold (typically below 0°C) stream of fresh air before the compressor [30] [31].

Some researchers have studied the condensation phenomenon inside the heat exchangers used to cool down the EGR in internal combustion (IC) engines applications. Yang et al. [32] presented a CFD model coupled with a 1-D heat and mass transfer model to study the most important physical aspects of the condensation process inside a typical EGR cooler in a heavy-duty diesel engine operating under off-road conditions. The model may be used to give accurate predictions of the water vapor, sulfuric acid and nitric acid corrosion in equipment with complicated geometry such as the EGR coolers. Waley et al. [33] developed a 1-D model to simulate the soot deposition, soot removal and condensation of several HC species inside EGR coolers operating at normal conditions. This model predicts the mass distribution in the deposit layer on the tube walls and the condensation of different HC species. Furthermore, these authors visualized the condensation of the water vapor and hydrocarbons at the outlet of the EGR cooler over a range of coolant temperatures in the EGR cooler, concluding that the condensation of water or hydrocarbons is not observed for coolant temperatures above 40 °C [34]. However, temperatures below 40 °C produce the condensation of water and hydrocarbons, besides, soot formation inside the EGR cooler.

Many authors have investigated the soot formation inside the EGR coolers used in diesel engines, specially characterizing and analyzing its composition and features [35] [36]. , Few studies have been carried out regarding the condensation provoked by the EGR because of its complexity and magnitude of the work [37]. A recently work performed by Qiu et al. [38] present the in-cylinder condensation processes observed in optically accessible engine experiments and a phase transition model to determine when the mixtures coming from low temperature combustion become unstable and a new phase is formed. The experiments reveal the importance of fuel condensation on the emission characteristics of low temperature combustion.

2.3 Low-pressure EGR

The use of the Low-pressure EGR concept could be mandatory to fulfill the future approval regulations applied to vehicles equipped with IC engines, which are becoming more stringent with the years.

The benefits of the Low-pressure EGR system in the engine behavior are the lower temperature of the exhaust gas, the higher amount of energy available to the turbine and the smaller pressure difference needed to move the gas [39]. Nevertheless, the use of EGR presents some issues, as per example the condensation phenomenon at low temperatures. At these conditions, the condensates can produce fouling deposits inside the EGR line components [30]. Condensation is produced due to the fact that the exhaust gas coming from the

combustion has important water content as well as other products like acids and hydrocarbon (HC) species [21]. When the temperature decreases in this gas with high humidity ratios, the condensation phenomenon appears. The condensate liquids contribute to the fouling processes on these elements, which reduces their useful life [37]. On the other hand, the important rates of HC species in the exhaust gas during the engine warm-up could affect the actuation of these elements due to the accumulation of deposits on the elements of the EGR line (i.e. valves and coolers) [40].

Many works presented in the literature highlight the importance of the EGR to fulfill the current and future emissions regulations and many researchers have studied how to continue taking advantage of this system. For example, Lapuerta et al. [41] presented a comparison of the effectiveness of both exhaust gas recirculation systems on the improvement of the NO_x particulate matter emission on an Euro 6 turbocharged diesel engine. In this work, different combinations of engine speed and torque, at transient and steady conditions with different coolant temperature strategies were performed. Results shown that the Low-pressure is more efficient than the High-pressure EGR to reduce the NO_x emissions due to the higher recirculation potential and the lower temperature of the recirculated gas. In addition, during the engine warm-up, switching from High-pressure to Low-pressure EGR at an intermediate coolant temperature is also beneficial for the emissions. Dimitriou et al. [42] evaluated the potential of introducing an alternative EGR route in a two stage boosted engine. The authors proposed a Mid-route (MR) EGR system to combine the benefits of the High-pressure and Low-pressure EGR systems in order to increase the EGR rates and reduce the transportation delay of the exhaust gases. Besides, the performance of different components (i.e. compressor, turbine and cooler) with this proposed configuration was examined. The study demonstrated that MR EGR could provide high EGR rates, particularly at high and low engine speeds. The reduction in the EGR response time was found to be around 50% and the study related to the sizing of the cooler revealed that a Low-pressure EGR cooler is unnecessary whereas the MR EGR cooler can also be omitted from the system.

Few studies have been carried out regarding the condensation and deposits phenomena. In this sense, Furukawa et al. [25] presented a chemical analysis of the hydrocarbons deposits that produce the sticking of the EGR valves and a method to avoid this issue when the EGR operating range in a diesel engine is expanded. The analysis revealed that the type of hydrocarbons collected, and their dew points, are the major factors in the sticking process of these valves. Furthermore, a control method to maintain the temperature of the EGR valve walls above the critical temperature necessary to produce these deposits was proposed.

2.4 Cylinders Deactivation

In the recent years, different strategies have been developed to improve the thermal efficiency of the IC engine and accelerate its thermal transient. Some of these strategies are the cylinder cutout [43] or the variable valve timing (VVT) [44] [45], which can be combined with novel strategies as the cylinder ventilation [46]. Another strategy that offers good results is the cylinder deactivation (CDA) [47] [48]. This strategy helps to reduce the fuel consumption and increase the exhaust temperature up to 100°C, thus activating the aftertreatment systems in shorter times. The oxidation catalyst and selective catalytic reduction (SCR) systems have strong temperature dependencies, even, the diesel and gasoline particulate filter (DPF, GPF) must be periodically regenerated with high exhaust gases temperatures [49] [50]. By this reason, CDA strategy could be presented as a reasonable operating condition for modern ICEs working at very low ambient temperatures (-7°C).

Several authors have considered this strategy with different objectives. Zammit et al. [51] studied this strategy on a 2.2 l diesel engine by deactivating two of the four cylinders at steady-state conditions at 1500, 2000, and 2500 rpm. The authors concluded that the CDA strategy has no effect or improvement on the brake specific fuel consumption (BSFC) and NO_x emissions levels, but it can reduce the HC and CO emissions and increase the exhaust temperature by up to 120°C. Another group of authors, Gritzenko et al [52], performed a theoretical and experimental study on a 2 l diesel engine by using three different cylinder deactivation strategies. The objective of these strategies was to evaluate the engine efficiency at different stationary regimes from 1200 to 2350 rpm. The results of this work reported benefits in fuel consumption due to improvements in combustion efficiency.

2.5 Diesel Particulate Filter Regeneration with High-pressure EGR

The conventional High-pressure EGR circuit, where the EGR rates are limited by the pressure difference among the inlet and outlet manifolds, is a low cost and effective solution due to its simple architecture and high potential to reduce the NO_x emissions [53]. Taking this into account, the evaluation of this strategy, in combination with other engine working conditions, as per example, the particulate filter regeneration, is a necessary study point for manufacturers and researchers. This regeneration process consists of increasing the temperature of the exhaust gas and is controlled by the electronic control unit (ECU) in order to burn off and remove the particulate matter (PM) and soot depositions collected in the after treatment system of gasoline and diesel engines [54], [55]. When

saturation conditions are detected by the ECU, active regeneration strategies as per example post injection and separate diesel injection are performed [56]. These strategies lead to higher pollutant emissions levels and deposits due to the additional fuel mass required to cause this regeneration [57]. For these reasons, a possible scenario in which the engine is working at cold conditions, activating the HP EGR for reducing the NO_x emissions and carrying out a diesel particulate filter (DPF) or gasoline particulate filter (GPF) regeneration due to a saturation condition in the filter has not been studied before, but it is very interesting to be evaluated from an experimental point of view.

Nevertheless, the use of High-pressure EGR to reduce the NO_x levels presents some issues, as per example the appearance of condensation and fouling depositions resulted of a degraded combustion, specially working at low temperatures [14]. The soot particles can affect the main components of the EGR line (i.e. EGR valve, EGR cooler, intake manifold) reducing its life span [58]. In addition, it could contribute to accelerate the DPF loading, thus affecting its normal operation [59]. Lapuerta et al. investigated the effect of the soot accumulation in a DPF of a common rail diesel engine on the combustion process and pollutant emissions, reproducing a New European Driving Cycle (NEDC) [60], [61]. The investigation concluded that performing a DPF regeneration without controlling the injection settings parameters and the EGR ratio could increase the NO_x emissions around 60% and the fuel consumption around 4%. This is caused by the higher back pressure and the higher temperature of the recirculated gas, which modifies the combustion process and moves the engine operation away from its optimum conditions.

Afterwards, the authors carried on evaluating these issues and presented some strategies for the active DPF regeneration modifying the engine control parameters. The selected parameters to be studied were the injection timing, exhaust gas recirculation and amount of post injected fuel. In this case, the work was performed at steady-state conditions at 2000 rpm of engine speed and 94 Nm of torque, as a representative point of the NEDC cycle. The relevant findings of the authors were that eliminating the EGR during the regeneration process is an optimal option for a fast DPF regeneration and reduced fuel consumption. However, low values of EGR rate could contribute to avoid excessively fast or uncontrolled regeneration in the cases of very high soot load at the DPF and to reduce NO_x emissions. Regarding the injection timing and the amount of post injected fuel, it was concluded that keeping the optimal temperature conditions is essential for an efficient DPF regeneration.

Regarding the impact of fouling depositions in the EGR line components and its characterization, several studies have been performed in the literature. Arnal presented the characterization of five different types of diesel soot, which were collected from several high pressure EGR coolers working at different

conditions (engine bench and vehicle) [36]. The authors highlighted the fact that the fouling depositions on the EGR components, as EGR coolers and valves, decreases their thermal efficiency and increases the pressure drop producing the malfunctioning of the device, implying the non-compliance of the NO_x standard regulations. In addition, these depositions are composed of adsorbed compounds like lube oil and unburned fuel that could aggravate this issue.

2.6 References

- [7] Z. Yang, Y. Liu, L. Wu, S. Martinet, Y. Zhang, M. Andre, and H. Mao. “Real-world gaseous emission characteristics of Euro 6b light-duty gasoline- and diesel-fueled vehicles”. In: *Transportation Research Part D: Transport and Environment* 78.– (2020), p. 102215 (cit. on p. 8).
- [8] N. Hooftman, M. Messagie, J. Van Mierlo, and T. Coosemans. “A review of the European passenger car regulations – Real driving emissions vs local air quality”. In: *Renewable and Sustainable Energy Reviews* 86.– (2018), pp. 1–21 (cit. on p. 8).
- [9] J. M. Luján, B. Pla, P. Bares, and V. Pandey. “Adaptive calibration of Diesel engine injection for minimising fuel consumption with constrained NOx emissions in actual driving missions”. In: *International Journal of Engine Research* 22.6 (2021), pp. 1896–1905 (cit. on p. 8).
- [10] C.-A. A, H. J, R.-F. J, L. M, R. A, and B. J. “Effect of advanced biofuels on WLTC emissions of a Euro 6 diesel vehicle with SCR under different climatic conditions”. In: *International Journal of Engine Research* 22.12 (2021), pp. 3433–3446 (cit. on p. 8).
- [11] E. U. Parliament. *REGULATION (EU) 2019/631 OF THE EUROPEAN PARLIAMENT AND OF THE COUNCIL*. 2019. URL: <https://eur-lex.europa.eu/legal-content/EN/TXT/?uri=CELEX%3A32019R0631&qid=1666123169654> (cit. on p. 8).
- [12] J. M. Luján, H. Climent, S. Ruiz, and A. Moratal. “Pollutant emissions and diesel oxidation catalyst performance at low ambient temperatures in transient load conditions”. In: *Applied Thermal Engineering* 129.– (2018), pp. 1527–1537 (cit. on p. 8).
- [13] F. J. Arnau, J. Martín, P. Piqueras, and Ángel Auñón. “Effect of the exhaust thermal insulation on the engine efficiency and the exhaust temperature under transient conditions”. In: *International Journal of Engine Research* 22.9 (2021), pp. 2869–2883 (cit. on p. 8).
- [14] J. Galindo, R. Navarro, D. Tarí, and F. Moya. “Development of an experimental test bench and a psychrometric model for assessing condensation on a low-pressure exhaust gas recirculation cooler”. In: *International Journal of Engine Research* 22.5 (2021), pp. 1540–1550 (cit. on p. 8, 13).
- [15] A. J. Torregrosa, A. Broatch, P. Olmeda, and C. Romero. “Assessment of the Influence of Different Cooling System Configurations on Engine Warm-up, Emissions and Fuel Consumption”. In: *International Journal of Automotive Technology* 9.4 (2008), pp. 447–458 (cit. on p. 8).

- [16] F. Millo, P. F. Giacominetto, and M. G. Bernardi. “Analysis of different exhaust gas recirculation architectures for passenger car Diesel engines”. In: *Applied Energy* 98.– (2012), pp. 79–91 (cit. on p. 8).
- [17] J. Thangaraja and C. Kannan. “Effect of exhaust gas recirculation on advanced diesel combustion and alternate fuels - A review”. In: *Applied Energy* 180.– (2016), pp. 169–184 (cit. on p. 6).
- [18] J. M. Desantes, J. M. Luján, B. Pla, and J. A. Soler. “On the combination of high-pressure and low-pressure exhaust gas recirculation loops for improved fuel economy and reduced emissions in high-speed direct-injection engines”. In: *International Journal of Engine Research* 14.1 (2013), pp. 3–11 (cit. on p. 9).
- [19] J. M. Luján, C. Guardiola, B. Pla, and A. Reig. “Switching strategy between HP (high pressure)- and LPEGR (low pressure exhaust gas recirculation) systems for reduced fuel consumption and emissions”. In: *Energy* 90.– (2015), pp. 1790–1798 (cit. on p. 9).
- [20] Y. Park and C. Bae. “Experimental study on the effects of high/low pressure EGR proportion in a passenger car diesel engine”. In: *Applied Energy* 133.– (2015), pp. 308–316 (cit. on p. 9).
- [21] S. Moroz, G. Bourgoïn, J. M. Luján, and B. Pla. “Acidic Condensation in Low Pressure EGR Systems using Diesel and Biodiesel Fuels”. In: *SAE International Journal of Fuels and Lubricants* 2.2 (2010), pp. 305–312 (cit. on pp. 9, 11).
- [22] R. D. Chalgren, G. G. Parker, O. Arici, and J. H. Johnson. “A Controlled EGR Cooling System for Heavy Duty Diesel Applications Using the Vehicle Engine Cooling System Simulation”. In: *SAE Technical Paper 2002-01-0076*. United States, 2002, p. 28 (cit. on p. 9).
- [23] S. Magand, E. Watel, M. Castagné, D. Soleri, O. Grondin, S. Devismes, and S. Moroz. “Optimization of a Low NOx Emission HCCI Diesel Prototype Vehicle”. In: *Proceedings of the THIESEL Congress 2008*. Valencia, Spain, 2008, pp. – (cit. on p. 9).
- [24] X. Yu, S. Yu, and M. Zheng. “Hydrocarbon impact on NO to NO₂ conversion in a compression ignition engine under low-temperature combustion”. In: *International Journal of Engine Research* 20.2 (2019), pp. 216–225 (cit. on p. 9).
- [25] N. Furukawa, S. Goto, and M. Sunaoka. “On the mechanism of exhaust gas recirculation valve sticking in diesel engines”. In: *International Journal of Engine Research* 15.1 (2014), pp. 78–86 (cit. on pp. 9, 11).

- [26] M. R. Boldaji, A. Sofianopoulos, S. Mamalis, and B. Lawler. “Computational fluid dynamics investigations of the effect of water injection timing on thermal stratification and heat release in thermally stratified compression ignition combustion”. In: *International Journal of Engine Research* 20.5 (2019), pp. 555–569 (cit. on p. 9).
- [27] A. Vaudrey. “Thermodynamics of indirect water injection in internal combustion engines: Analysis of the fresh mixture cooling effect”. In: *International Journal of Engine Research* 20.5 (2019), pp. 527–539 (cit. on p. 9).
- [28] T. Tsuruta and G. Nagayama. “A microscopic formulation of condensation coefficient and interface transport phenomena”. In: *Energy* 30.6 (2005), pp. 795–805 (cit. on p. 9).
- [29] X. Tauzia, A. Maiboom, H. Karaky, and P. Chesse. “Experimental analysis of the influence of coolant and oil temperature on combustion and emissions in an automotive diesel engine”. In: *International Journal of Engine Research* 20.2 (2019), pp. 247–260 (cit. on p. 9).
- [30] J. R. Serrano, P. Piqueras, E. Angiolini, C. Meano, and J. D. L. Morena. “On Cooler and Mixing Condensation Phenomena in the Long-Route Exhaust Gas Recirculation Line”. In: *SAE Technical Paper 2015-24-2521*. United States, 2002, p. 15 (cit. on pp. 9, 10).
- [31] J. Serrano, P. Piqueras, R. Navarro, D. Tarí, and C. Meano. “Development and verification of an in-flow water condensation model for 3D-CFD simulations of humid air streams mixing”. In: *Computers Fluids* 167 (2018), pp. 158–165 (cit. on p. 9).
- [32] B.-J. Yang, S. Mao, O. Altin, Z.-G. Feng, and E. E. Michaelides. “Condensation Analysis of Exhaust Gas Recirculation System for Heavy-Duty Trucks”. In: *ASME. J. Thermal Sci. Eng. Appl.* 3.4 (2011), p. 9 (cit. on p. 10).
- [33] A. Warey, S. Balestrino, P. Szymkowicz, and M. Malayeri. “A One-Dimensional Model for Particulate Deposition and Hydrocarbon Condensation in Exhaust Gas Recirculation Coolers”. In: *Aerosol Science and Technology* 46.2 (2012), pp. 198–213 (cit. on p. 10).
- [34] A. Warey, D. Long, S. Balestrino, P. Szymkowicz, and A. S. Bika. “Visualization and Analysis of Condensation in Exhaust Gas Recirculation Coolers”. In: *SAE Technical Paper 2013-01-0540*. United States, 2013, p. 12 (cit. on p. 10).

- [35] Y. Bravo, J. L. Lázaro, and J. L. García-Bernad. “Study of Fouling Phenomena on EGR Coolers due to Soot Deposits. Development of a Representative Test Method”. In: *SAE Technical Paper 2005-01-1143*. United States, 2005, p. 8 (cit. on p. 10).
- [36] C. Arnal, Y. Bravo, C. Larrosa, V. Gargiulo, M. Alfè, A. Ciajolo, M. U. Alzuet, Ángela Millera, and R. Bilbao. “Characterization of Different Types of Diesel (EGR Cooler) Soot Samples”. In: *SAE Technical Paper 2015-01-1690*. United States, 2015, p. 11 (cit. on pp. 10, 14, 68).
- [37] A. Warey, A. S. Bika, D. Long, S. Balestrino, and P. Szymkowicz. “Influence of water vapor condensation on exhaust gas recirculation cooler fouling”. In: *International Journal of Heat and Mass Transfer* 65 (2013), pp. 807–816 (cit. on pp. 10, 11).
- [38] L. Qiu, R. Reitz, E. Eagle, and M. Musculus. “Investigation of Fuel Condensation Processes under Non-reacting Conditions in an Optically-Accessible Engine”. In: *SAE Technical Paper 2019-01-0197*. United States, 2019, p. 12 (cit. on p. 10).
- [39] V. Bermúdez, J. M. Lujan, B. Pla, and W. G. Linares. “Effects of low pressure exhaust gas recirculation on regulated and unregulated gaseous emissions during NEDC in a light-duty diesel engine”. In: *Energy* 36.9 (2011), pp. 5655–5665 (cit. on p. 10).
- [40] M. J. Lance, Z. G. Mills, J. C. Seylar, J. M. Storey, and C. S. Sluder. “The effect of engine operating conditions on exhaust gas recirculation cooler fouling”. In: *International Journal of Heat and Mass Transfer* 126 (2018), pp. 509–520 (cit. on p. 11).
- [41] M. Lapuerta, Ángel Ramos, D. Fernández, and I. González. “High-pressure versus low-pressure exhaust gas recirculation in a Euro 6 diesel engine with lean-NO_x trap: Effectiveness to reduce NO_x emissions”. In: *International Journal of Engine Research* 20.1 (2019), pp. 155–163 (cit. on p. 11).
- [42] P. Dimitriou, J. Turner, R. Burke, and C. Copeland. “The benefits of a mid-route exhaust gas recirculation system for two-stage boosted engines”. In: *International Journal of Engine Research* 19.5 (2018), pp. 553–569 (cit. on p. 11).
- [43] K. R. Vos, G. M. Shaver, A. K. Ramesh, and J. M. Jr. “Impact of Cylinder Deactivation and Cylinder Cutout via Flexible Valve Actuation on Fuel Efficient Aftertreatment Thermal Management at Curb Idle”. In: *Frontiers in Mechanical Engineering* 5.52 (2019), pp. 1–18 (cit. on p. 12).

- [44] F. J. Arnau, J. Martín, B. Pla, and Ángel Auñón. “Diesel engine optimization and exhaust thermal management by means of variable valve train strategies”. In: *International Journal of Engine Research* 22.4 (2020), pp. 1196–1213 (cit. on p. 12).
- [45] K. R. Vos, G. M. Shaver, M. C. Joshi, A. K. Ramesh, and J. M. Jr. “Strategies for using valvetrain flexibility instead of exhaust manifold pressure modulation for diesel engine gas exchange and thermal management control”. In: *International Journal of Engine Research* 22.3 (2021), pp. 755–776 (cit. on p. 12).
- [46] D. B. Gosala, G. M. Shaver, J. M. Jr., and T. P. Lutz. “Fuel-efficient thermal management in diesel engines via valvetrain-enabled cylinder ventilation strategies”. In: *International Journal of Engine Research* 22.2 (2021), pp. 430–442 (cit. on p. 12).
- [47] D. B. Gosala, C. M. Allen, A. K. Ramesh, G. M. Shaver, J. M. Jr., D. Stretch, E. Koeberlein, and L. Farrell. “Cylinder deactivation during dynamic diesel engine operation”. In: *International Journal of Engine Research* 18.10 (2017), pp. 991–1004 (cit. on p. 12).
- [48] A. K. Ramesh, D. B. Gosala, C. Allen, M. Joshi, J. M. Jr., L. Farrell, E. D. Koeberlein, and G. Shaver. “Cylinder Deactivation for Increased Engine Efficiency and Aftertreatment Thermal Management in Diesel Engines”. In: *SAE Technical Paper 2018-01-0348*. United States, 2018, p. 10 (cit. on p. 12).
- [49] J. McCarthy. “Cylinder deactivation improves Diesel aftertreatment and fuel economy for commercial vehicles”. In: *17. Internationales Stuttgarter Symposium. Proceedings*. Springer Vieweg, Wiesbaden, 2017, pp. 1013–1039 (cit. on p. 12).
- [50] C. M. Allen, M. C. Joshi, D. B. Gosala, G. M. Shaver, L. Farrell, and J. M. Jr. “Experimental assessment of diesel engine cylinder deactivation performance during low-load transient operations”. In: *International Journal of Engine Research* 22.2 (2021), pp. 606–615 (cit. on p. 12).
- [51] J. Zammit, M. McGhee, P. Shayler, and I. Pegg. “Internal Combustion Engines: Performance, Fuel Economy and Emissions”. In: Woodhead Publishing, 2013 (cit. on pp. 12, 75).
- [52] A. V. Gritsenko, K. V. Glemba, and A. A. Petelin. “A study of the environmental qualities of diesel engines and their efficiency when a portion of their cylinders are deactivated in small-load modes”. In: *Journal of King Saud University - Engineering Sciences* 33.1 (2021), pp. 70–79 (cit. on p. 12).

- [53] G. Zamboni and M. Capobianco. “Experimental study on the effects of HP and LP EGR in an automotive turbocharged diesel engine”. In: *Applied Energy* 94 (2012), pp. 117–128 (cit. on p. 12).
- [54] V. Bermúdez, A. García, D. Villalta, and L. Soto. “Assessment on the consequences of injection strategies on combustion process and particle size distributions in Euro VI medium-duty diesel engine”. In: *International Journal of Engine Research* 21.4 (2020), pp. 683–697 (cit. on p. 12).
- [55] S. Fontanesi, M. D. Pecchia, V. Pessina, S. Sparacino, and S. D. Iorio. “Quantitative investigation on the impact of injection timing on soot formation in a GDI engine with a customized sectional method”. In: *International Journal of Engine Research* 23.4 (2022), pp. 624–637 (cit. on p. 12).
- [56] W. Kang, S. Pyo, and H. Kim. “Comparison of intake and exhaust throttling for diesel particulate filter active regeneration of non-road diesel engine with mechanical fuel injection pump”. In: *International Journal of Engine Research* 22.7 (2021), pp. 2337–2346 (cit. on p. 13).
- [57] Z. Liu, A. N. Shah, Y. Ge, Y. Ding, J. Tan, L. Jiang, L. Yu, W. Zhao, C. Wang, and T. Zeng. “Effects of continuously regenerating diesel particulate filters on regulated emissions and number-size distribution of particles emitted from a diesel engine”. In: *Journal of Environmental Sciences* 23.5 (2011), pp. 798–807 (cit. on p. 13).
- [58] M. Abarham, T. Chafekar, J. W. Hoard, A. Salvi, D. J. Styles, C. S. Sluder, and D. Assanis. “In-situ visualization of exhaust soot particle deposition and removal in channel flows”. In: *Journal of Environmental Sciences* 87 (2013), pp. 359–370 (cit. on p. 13).
- [59] J. Fang, Z. Meng, J. Li, Y. Du, Y. Qin, Y. Jiang, W. Bai, and G. G. Chase. “The effect of operating parameters on regeneration characteristics and particulate emission characteristics of diesel particulate filters”. In: *Applied Thermal Engineering* 148 (2019), pp. 860–867 (cit. on p. 13).
- [60] M. Lapuerta, J. Rodríguez-Fernández, and F. Oliva. “Effect of soot accumulation in a diesel particle filter on the combustion process and gaseous emissions”. In: *Energy* 47.1 (2012), pp. 543–552 (cit. on p. 13).
- [61] M. Lapuerta, J. J. Hernández, and F. Oliva. “Strategies for active diesel particulate filter regeneration based on late injection and exhaust recirculation with different fuels”. In: *International Journal of Engine Research* 15.2 (2014), pp. 209–221 (cit. on p. 13).

CHAPTER **3**

Experimental Testbench

3.1 Introduction

IN the previous chapter, a literature review regarding experimental and theoretical works performed on Internal Combustion Engines (ICE) operating at low ambient temperatures was presented. In this chapter, the experimental setup of this work, and its main configurations are described.

The chapter is divided in three sections:

- **section 3.2** describes the main characteristics of the internal combustion engine and the engine test-bench used in this study.
- **section 3.3** shows the engine cycle and the methodologies and strategies performed at transient and steady state conditions.
- **section 3.4** presents the different engine configurations and new components utilized on each experimental study.

3.2 Experimental Setup

This section presents a detailed description of the light-duty diesel engine used in this research study, which is prepared inside of an special engine test-bench fitted with a climatic chamber able to reach low temperatures up to -20°C .

3.2.1 Description of the Internal Combustion Engine

To perform this theoretical-experimental work, an in-line 4 cylinders, 1.6 liter, turbocharged, diesel engine Euro V was used. Table 3.1 summarizes the technical features of the engine. The engine is fitted with a common rail direct injection system, high-pressure and low-pressure exhaust gas recirculation (EGR), and an intake cooling system equipped with a Water Charge Air Cooler (WCAC).

Table 3.1: Engine Specifications

Parameter	Value	Units
Number of Cylinders	4	-
Number of Valves	16	-
Bore x Stroke	80 x 79.5	mm
Total Displacement	1598	cc
Maximum Power	96/4000	kW/rpm
Maximum Torque	320/1750	Nm/rpm
Compression Ratio	15.4:1	-

As was mentioned above, the engine has two EGR circuits. The first one is the High-pressure EGR circuit, in this case, the exhaust gas is directly cooled in the cylinder head and mixed with the fresh air that comes from the intake line. Fig. 1 shows the HP EGR line and its instrumentation. This circuit consists of an internal duct that guides the exhaust gases coming from the exhaust manifold through a compact section of the cylinder head (without EGR cooler) to reduce its temperature, a HP EGR valve controlled by the electronic control unit (ECU) of the engine, and a HP EGR rail, where the exhaust gases are driven and distributed to the engine intake manifold and mixed with the air at the intake of the four cylinders. The second circuit is the Low-pressure EGR, in this case, the exhaust gas passes through the catalyst and the particulate filter, and then is redirected into the turbo compressor. Fig. 1 shows the LP EGR line and its instrumentation. This circuit introduces the exhaust gas coming from the turbine into the after treatment systems. First, using a diesel oxidation catalyst (DOC), the CO and HC emissions are oxidized. Then, using a diesel particulate filter (DPF), the particulate matter (PM) coming from the combustion process is trapped. When the exhaust gas is treated by these systems, a LP EGR cooler is used to reduce its temperature and a LP EGR valve controlled by the ECU of the

engine sets the LP EGR rate. The LP EGR cooler is cooled by the own engine coolant circuit. Finally, the exhaust gas is driven and distributed to the engine intake line and mixed with the air at the compressor inlet. This gas mixture is compressed and directed to the engine intake manifold where is introduced into the four cylinders. The water charge air cooler (WCAC) is positioned at the inlet of the intake manifold.

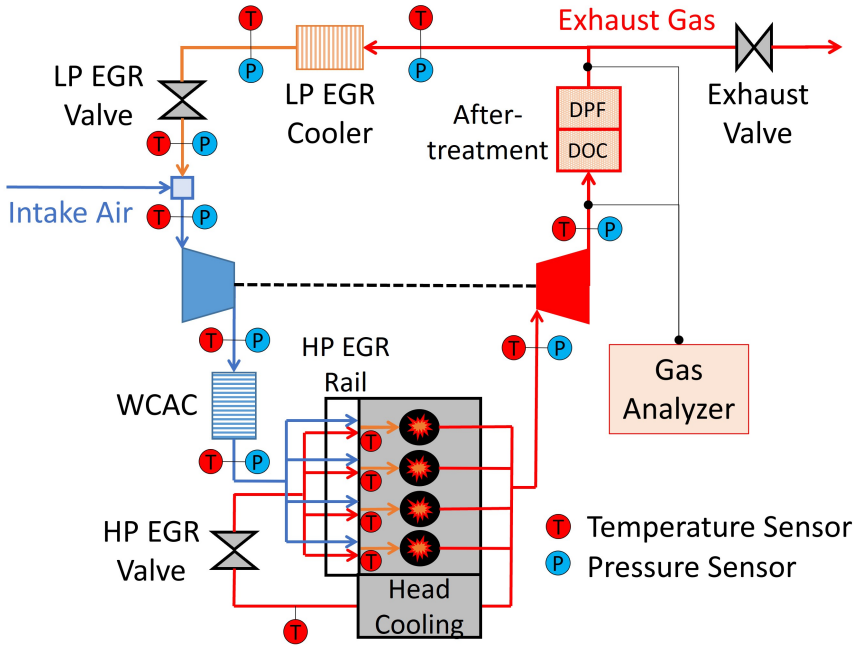


Figure 3.1: Engine Configuration and Instrumentation

The engine is instrumented with K Type thermocouples, due to its low cost and a high range of measure (-200°C to 1250°C), and piezoresistive sensors P40, due to its capacity of measure static pressures from 0 to 10 bars. Figure 3.1 shows the engine configuration and its main instrumentation for this study. In addition, a Horiba Mexa 7100 DEGR was used to measure, carbon monoxide (CO), carbon dioxide (CO_2), nitrous oxides (NO_x) emissions and oxygen concentration (O_2), using a non-dispersive infrared analyzer, and unburned hydrocarbons (HC_s) with a chemiluminescent detector. The error of the gas analyzer is in the range of 2%. Two measurement points are located on the after-treatment system with the aim of measure upstream and downstream emissions.

3.2.2 Description of the Test-bench

To carry out the experiments at cold conditions, the engine was installed in a climatic test-bench, where the temperatures of the test-bench air, fuel and coolant are under control. The test-bench is instrumented to measure the torque, speed, temperatures and pressures at different engine points. The injected fuel mass and the air mass flow through the intake line are also measured.

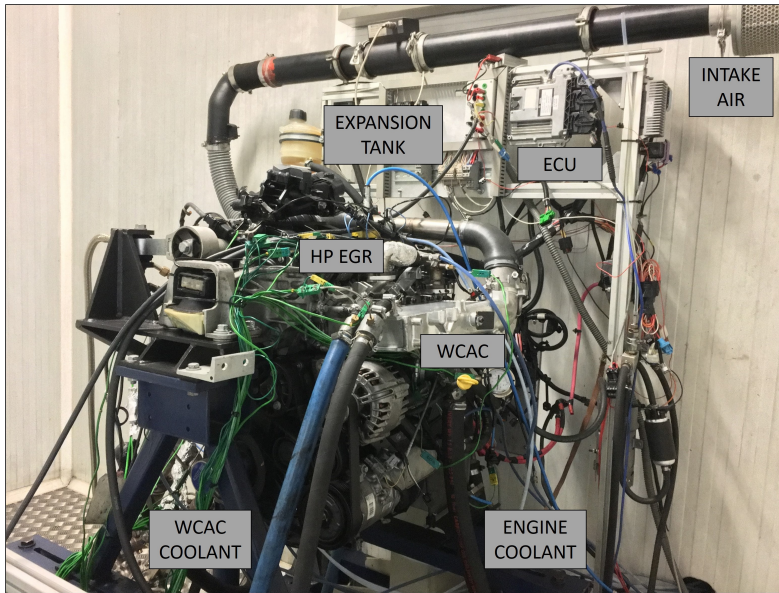


Figure 3.2: Engine fitted in the climatic test-bench

Figure 3.2 shows the diesel engine fitted in the climatic test bench, where some components like the High-pressure EGR rail, the WCAC and the engine instrumentation can be observed. Moreover, the engine is coupled to an Alternating Current (AC) Dynamometer specially designed for simulation of legislative test cycles like WLTP or NEDC as well as Road Load Simulation (RLS) and driver and vehicle simulation.

In order to control the temperatures of the test-bench air, fuel and coolant, a refrigeration and ventilation system, an AVL gravimetric fuel balance and a water-glycol deposit positioned into the climatic chamber are used. Operating these systems, the ambient temperature inside the climatic chamber and the fuel and coolant temperatures, can be set at -7°C . In addition, the air mass flow through the intake line of the engine is measured by means of a hot wire anemometer with a measurement error of 1% and the fuel consumption during an engine cycle is measured via the AVL fuel balance, which has measurement error of 0.2%.

A high quantity of engine parameters have been measured to assess the engine performance and analyze the impact of the proposed strategies. The measured parameters together with the sensor features are presented in Table 3.2. These information is handled using the HORIBA STARS Engine 1.8 System, by means of data acquisition, software control and monitoring.

Table 3.2: Instrumentation Accuracy

Sensor	Variable	Accuracy [%]	Range
Thermocouples type K	Temperature	1	-200°C-1250°C
Pressure sensor	Pressure	0.3	0-10bar
Gravimetric fuel balance	Fuel mass flow	0.2	0-150kg/h
Hot wire meter	Air mass flow	1	0-720kg/h
Dynamometer brake	Torque	0.1	0-480Nm

3.3 Engine Cycle and Methodologies

This section describes the engine cycle profile performed in these studies and the methodologies and particular strategies to carry out the different experiments.

3.3.1 Engine Cycle Description

A transient engine cycle named “EGR Cycle”, with special characteristics in terms of NO_x emissions generation and soot formation inside the EGR components of a diesel engine running at cold conditions was tested. The low ambient temperature and the real urban driving conditions are critical states for the engine warm-up process and the after-treatment efficiency. The aim of this cycle is to simulate these adverse and real characteristics under operation. Figure 3.3 shows the profile of the cycle performed for these experiments. This cycle is characterized by low-middle load points with important EGR rates and sudden accelerations.

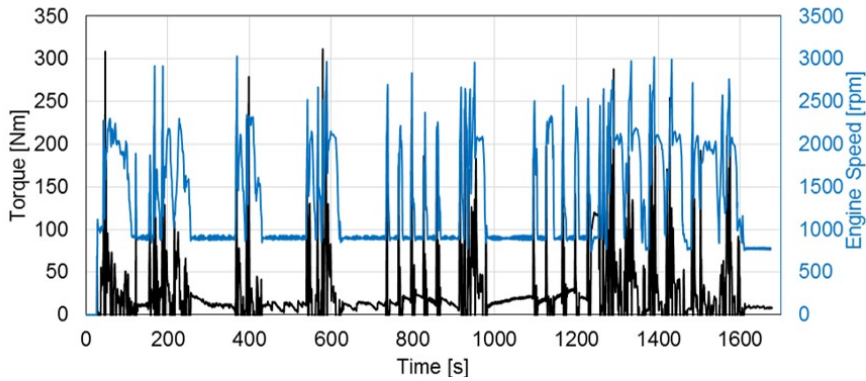


Figure 3.3: Profile of the cycle performed

The transient cycle was selected as representative for these experiments due to the important EGR rates capable to introduce in the engine under cold conditions operation. Figure 3.4 shows the EGR rate. Rates up to 40%, performing both, high-pressure and low-pressure EGR, are representative for the study and could indicate a considerable NO_x emissions reduction under these particular conditions.

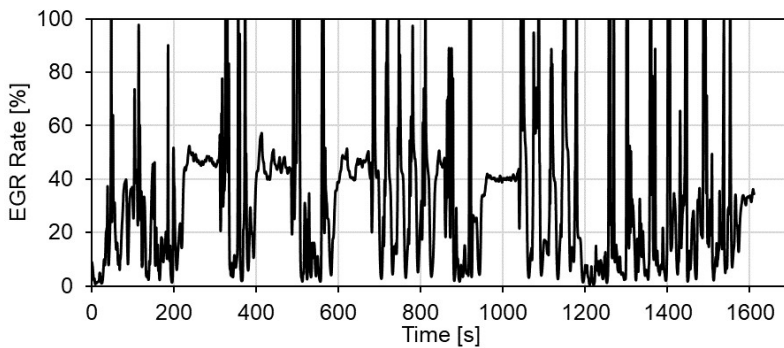


Figure 3.4: EGR rate measure

3.3.2 Methodologies and Strategies

When the Low-pressure EGR is activated in the different studies, the EGR rate is obtained experimentally from CO₂ measurement in exhaust and intake manifolds. By means of the HORIBA gas analyzer and using the following expression Equation 3.1, the Low-pressure EGR rate is assessed:

$$EGR_{rate} = \frac{[CO_2]_{Int} - [CO_2]_{Amb}}{[CO_2]_{Exh} - [CO_2]_{Amb}} \quad (3.1)$$

This difference allows to obtain a theoretical calculation of the percentage of EGR that is re-introduced in the engine. However, when the High-pressure is activated, due to the complexity of the line, the gas analyzer is not able to do this estimate. In this case, a mathematical approach is performed using the engine volumetric efficiency for each engine configuration and taking as a reference the standard engine configuration and its volumetric efficiency without using EGR.

Equation 3.2 shows the engine volumetric efficiency as a function of the air mass flow (\dot{m}_{air}), the engine parameters (engine speed, displacement, etc.), the boost pressure (P_{boost}) and the intake temperature (T_{intake}) [62]. When the volumetric efficiency is assessed, the theoretical air mass flow is calculated with the measured boost pressure ($P_{boostEGR}$) and intake temperature ($T_{intakeEGR}$) at active EGR mode Equation 3.3. Finally, it is possible to obtain the EGR rate as a relation between the air mass estimated theoretically by using the volumetric efficiency and the air mass flow measured. Equation 3.4 shows the High-pressure EGR rate estimation.

$$\eta_{vol} = \frac{\dot{m}_{air}}{\frac{P_{boost}}{R \cdot T_{intake}} \cdot V_{eng} \cdot n \cdot i} \quad (3.2)$$

$$\dot{m}_{theor} = \eta_{vol} \cdot \frac{P_{boostEGR}}{R \cdot T_{intakeEGR}} \cdot V_{eng} \cdot n \cdot i \quad (3.3)$$

$$EGR_{rate} = \frac{\dot{m}_{theor} - \dot{m}_{air}}{\dot{m}_{theor}} * 100 \quad (3.4)$$

3.4 Engine Configuration Strategies

This section presents the engine experimental setup and configuration for the four strategies studied in this research work.

3.4.1 High-Pressure EGR Configuration

This strategy evaluates the High-pressure EGR activation from an engine cold start at -7°C and following the transient engine cycle named ‘‘EGR Cycle’’, described before. This strategy is performed with the aim of observing the condensation phenomena inside the High-pressure EGR circuit of the engine and consequently, develop a condensation model to predict the conditions under which phenomenon emerge.

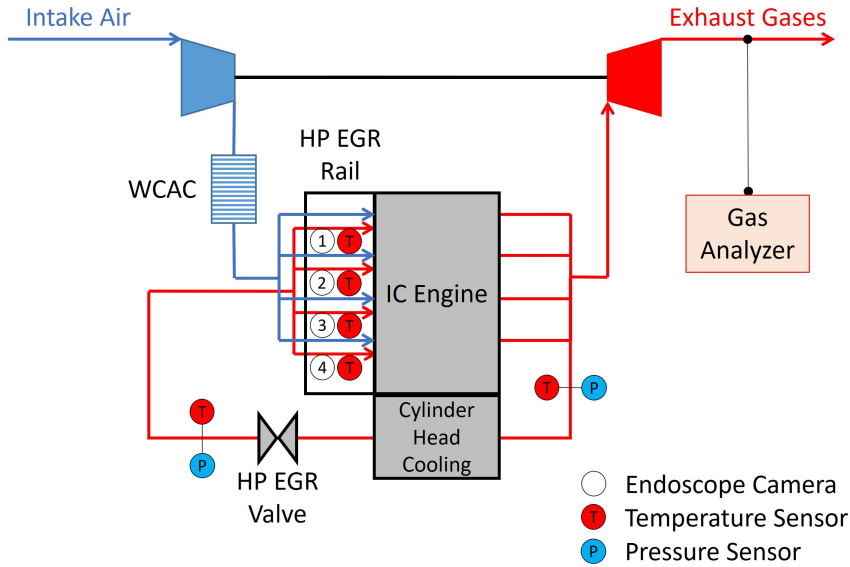


Figure 3.5: High-pressure EGR circuit configuration

Figure 3.5 shows the High-pressure EGR line and its instrumentation for this strategy. In order to perform the data acquisition for the condensation model, the HP EGR line is instrumented to measure the pressure and temperature before the turbine, at the outlet of the HP EGR valve and on the HP EGR rail, just at the inlet of each of the four cylinders of the engine. The thermocouples used to measure the temperature at the inlet of the four cylinders of the engine have been installed in two different configurations. First, introducing the thermocouples to the central area of the inlet ducts to the cylinders (gas side), and second, placing the thermocouples just in the wall surface of these ports (wall side).

The pollutant emissions measurement point is located downstream the turbine and upstream of the after-treatment systems. In order to validate the condensation model experimentally, four endoscope cameras were placed on the HP EGR rail cover to visualize inside the rail at the inlet side of the cylinder ports. Figure 3.6 shows the locations of these cameras on the engine experimental set up as well as the field of view that is observed and recorded during the experiments. These cameras allow to record videos and pictures at high quality (30 fps and 96 dpi).

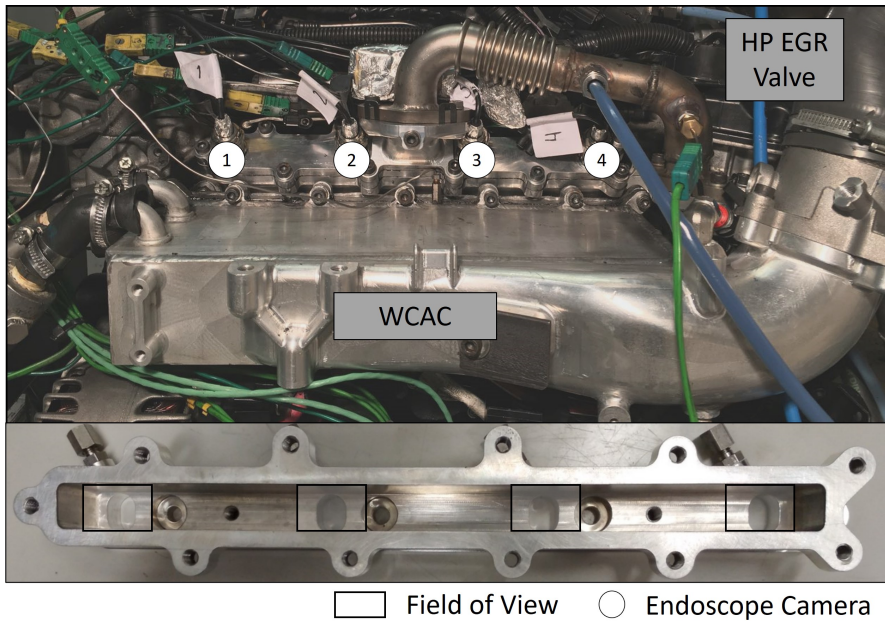


Figure 3.6: Cameras Configuration and Field of View

3.4.2 Low-Pressure EGR Bypass Configuration

This strategy evaluates the impact of a new Low-pressure EGR bypass system implemented in the engine with the aim of accelerate the warm-up process under cold conditions operation at -7°C . The transient engine cycle named “EGR Cycle” is performed in this study. The High-pressure EGR is disabled and the WCAC is with 0 flow inside during cold start operation.

The Low-pressure EGR cooler bypass prototype tested in this experimental work can be observed in [Figure 3.7](#) and [Figure 3.8](#). This is a compact concept of the whole Low-pressure EGR line of the engine. This bypass has an electronically controlled flap valve in order to guide the exhaust gas through the cooler and then to the mixer, or directly to the mixer through a parallel circuit with the aim of increasing the engine intake temperature during the cold start operation. In addition, this compact bypass has been instrumented with three endoscope cameras and two light sources in order to locally observe the condensation phenomenon inside the circuit and a sampling point coupled to a beaker in order to collect part of the condensates produced during the experiments. Two measurement points for pollutant emissions are located upstream and downstream of the after-treatment system.

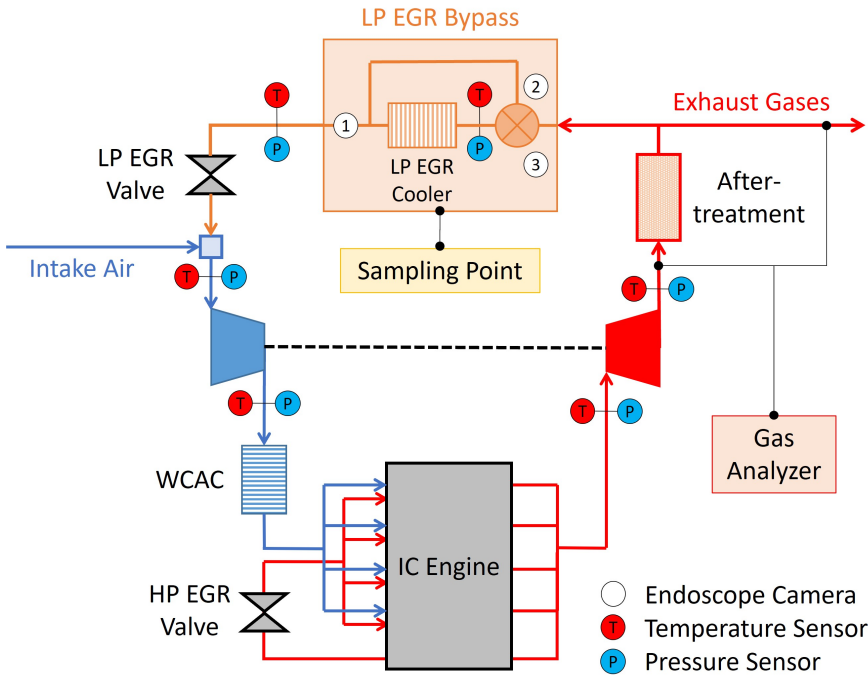


Figure 3.7: Engine configuration with the Low-pressure EGR bypass fitted

Figure 3.9 shows the locations of the prototype and the cameras on the engine experimental set-up as well as the field of view that is observed and recorded during the experiments. These endoscope cameras allow to record videos and pictures with a quality of 30 fps and 96 dpi.

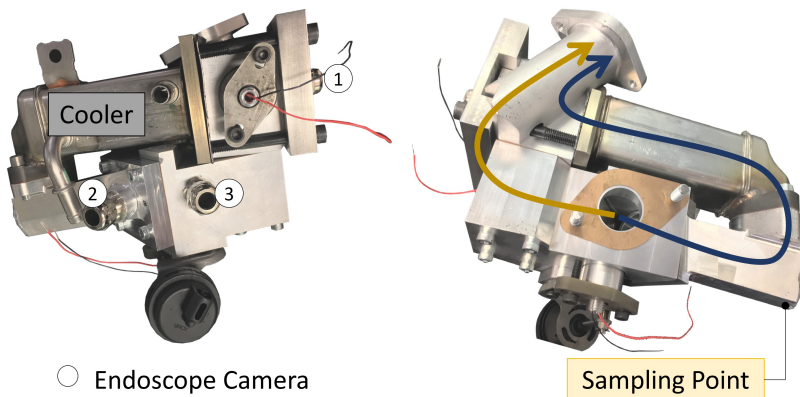


Figure 3.8: Low-pressure EGR Bypass Prototype

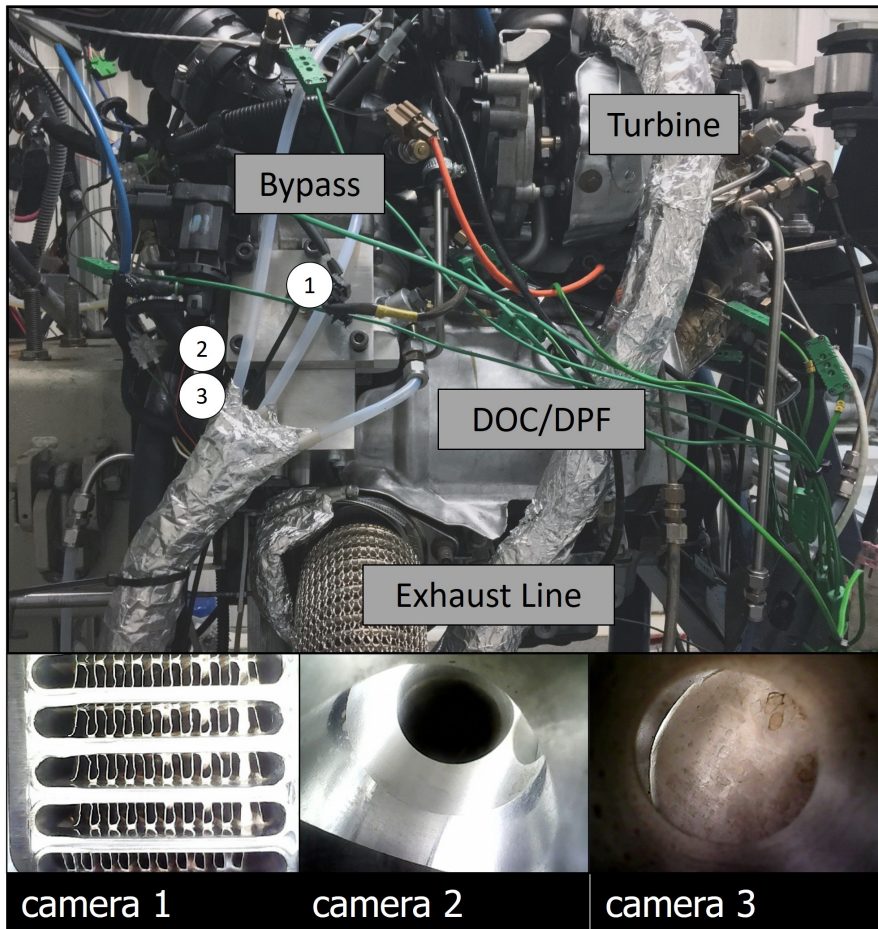


Figure 3.9: Engine Set-up, Cameras Configuration and Field of View

3.4.3 Deactivation Cylinder Configuration

This strategy evaluates a new proposal for the cylinder cutout or cylinder deactivation, named “EGR DEACT”. This strategy is performed as an alternative method to improve the engine warm-up process operating at -7°C .

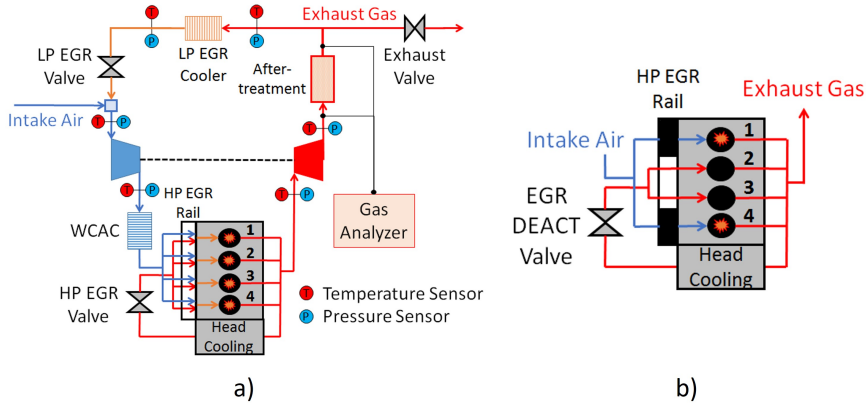


Figure 3.10: a) Standard Engine Configuration b) EGR DEACT Configuration

Figure 3.10 a) shows the standard engine configuration and its instrumentation. Figure 3.10 b) shows the EGR DEACT configuration, fired cylinders (1 and 4) and deactivated cylinders (2 and 3). In order to deactivate the cylinders 2 and 3, the injectors has been unplugged and two external injectors has been plugged to the electronic control unit (ECU) connector. In addition, the engine intake manifold and the HP EGR rail have been modified, closing the air inlet of the cylinders 2 and 3 and closing the HP EGR inlet of the cylinders 1 and 4 with the aim of reducing pumping losses in the circuit. The HP EGR valve (renamed as EGR DEACT valve) is now controlled manually through a proportional integral derivative (PID) controller and an external valve has been fitted to the ECU connector in order to avoid mistakes in the engine calibration due to the valve position measurement. In the fired cylinders 1 and 4, only the LP EGR is enabled and the whole intake air is distributed to the cylinders inlet.

In-cylinder pressure data was acquired using a Kistler 6537A4Q59 piezoelectric pressure sensor fitted with a standard water-cooled Kistler 7061B precision pressure transducer and coupled to a Kistler 4603 piezoresistive amplifier. The pressure signal from these transducers is normally converted to an absolute value by referencing the signal at the inlet bottom dead center (BDC) to the intake manifold pressure. The pressure data was sampled every 0.5° crank angle by the shaft encoder and ensemble averaged over 50 cycles. This data was recorded using the NI LabVIEW software, and post-processed to determine

the Indicated mean effective pressure (IMEP) and the pumping losses. The pollutants emissions measurement point is located downstream the turbine and upstream of the after-treatment systems. The WCAC is with 0 flow inside during cold start operation.

3.4.4 Diesel Particulate Filter Regeneration Configuration

This strategy uses the standard engine configuration presented in [Figure 3.1](#). The Low-pressure EGR is not activated under this configuration and the High-pressure EGR is forced in combination with the DPF regeneration mode. In addition, the water charge air cooler (WCAC) is activated with a constant regulation in order to control the engine intake temperature due to the higher temperatures reached during the DPF regeneration process. The measurement point for the pollutant emissions is located upstream of the after-treatment system in order to show the raw emissions levels.

The aim of performing this strategy is to evaluate the impacts of introducing exhaust gas recirculation (EGR) while the diesel particulate filter (DPF) is under regeneration process working at low ambient temperatures (-7°C).

3.5 Summary

This chapter presented the complete experimental setup, description and characterization of the different engine configurations performed in this study. The internal combustion engine description, the test-bench description and the engine configuration for each strategy was showed.

The results are summarized in the next points:

- The engine is prepared inside a climatic test bench and instrumented for recording all significant parameters as temperatures, pressures, mass flows and signals. This allows to evaluate the engine performance and its response under each experimental strategy.
- The engine cycle performed is a representative transient cycle in terms of NO_x generation and EGR levels. EGR rates up to 40% can be reached following this profile at low ambient temperature.
- The four different engine configurations and the new components and modifications installed on the engine are presented and described.

3.6 References

- [62] F. Payri and J. M. Desantes. *Motores de Combustión Interna Alternativos*. 1st ed. Editorial Reverté, 2011 (cit. on p. 28).

CHAPTER **4**

**High-pressure EGR
Condensation Model**

4.1 Introduction

IN the previous chapter, the experimental testbench description, methodologies and configuration of each strategy was presented. The objective of this chapter consist of the mathematical overview and experimental validation of the High-pressure EGR line condensation model of an internal combustion engine operating at cold conditions (-7°C). The use of exhaust gas recirculation (EGR) could be necessary from the engine starting at cold conditions. In this context, condensation inside the EGR line could appear, affecting in several ways to the engine components and their life span.

The main parts of this experimental campaign are summarized below:

- [section 4.2](#) describes the different methodologies and strategies followed to perform the physical experiments.
- [section 4.3](#) presents the main assumptions and mathematical description of the condensation model.
- [section 4.4](#) shows the experimental results and the model validation. The condensation behavior along a representative driving cycle has been visualized by means of cameras fitted on the HP EGR rail.

4.2 Methodology and Strategies

The transient engine cycle named “EGR Cycle”, described in the subsection 3.3.1, was conducted along this study under low ambient temperature (-7°C). This cycle is characterized by low-middle load points with important EGR rates and sudden accelerations. For this particular study, the Low-pressure EGR was disabled and only the High-pressure EGR has been activated.

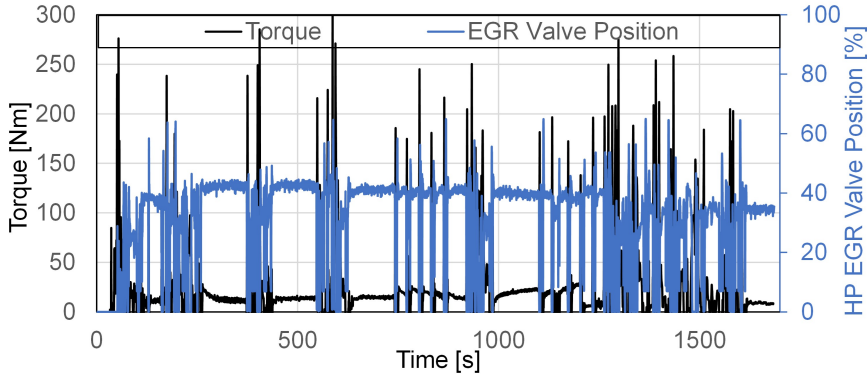


Figure 4.1: HP EGR activation since engine cold start

The standard engine calibration is not configured to perform High-pressure EGR under these particular conditions (-7°C). Under this engine calibration, once the temperature of the coolant reaches 60°C , the High-pressure EGR is activated. For this reason, it was necessary to modify the standard engine calibration in order to activate the High-pressure EGR during the complete cycle, from the beginning of the warm-up process. Figure 4.1 shows the activation of the High-pressure EGR by showing the EGR valve position during the complete cycle. This modification was done with the purpose of introducing a similar EGR rate to the standard engine calibration at ambient conditions (20°C) when the warm-up process finishes (approx. 40%) and to check under which conditions during the warm up process at -7°C the condensation is produced.

4.3 Condensation Model

For the purpose of estimate whether or not there is condensation in the High-pressure EGR line of the engine, a simple condensation model has been defined. The condensation model has as input parameters the temperature, pressure and humidity at ambient conditions, the air mass flow through the intake line of the internal combustion engine and the amount of fuel injected into the cylinders (air-fuel ratio). Based on these data, the model calculates the amount of water (humidity ratio) that is available at the cylinders outlet, assuming that the combustion efficiency is 100%. With this value of humidity ratio, and considering the local temperature and pressure at different points of the High-pressure EGR line, the relative humidity at these points is estimated as the output parameter of the model. In the following subsection, the model is described and the hypotheses on which it is based are established.

4.3.1 Mathematical Description

Four main hypothesis are considered for the condensation model:

- Quasi-steady conditions in the intake line, IC engine and High-pressure EGR line.
- Although condensation conditions could appear, it is assumed that the condensed water is entrained by the exhaust gas mass flow and it is not accumulated at different points of the IC engine outlet or the High-pressure EGR line.
- All the water present in the High-pressure EGR line comes from the ambient, from the combustion process and from the recirculated gases itself.
- The combustion efficiency is 100%, it means that all the injected fuel burns and the combustion process transforms this injected fuel, combined with oxygen, into water and CO_2 .

Based on the input variables of the model and the previously defined hypotheses, the following equations allow the estimation of relative humidity values at different points of the exhaust gas recirculation line.

First, considering the chemical composition of the fuel, the atomic mass of a hydrogen atom and the atomic mass of a carbon atom, the ratio of Hydrogen mass in a fuel molecule can be calculated following the [Equation 4.1](#):

$$\tau_{(H/fuel)} = \frac{(n^o H)(1.00794)}{(n^o H)(1.00794) + (n^o C)(12.0107)} \quad (4.1)$$

Where $n^{\circ}H$ is the number of hydrogen atoms, $n^{\circ}C$ is the number of carbon atoms and 1.00794 and 12.0107 are the atomic mass of the hydrogen and carbon atoms, respectively.

Table 4.1 shows the ratio of hydrogen mass in a fuel molecule for different alkanes of single bonds. If alkane hydrocarbons of single bonds are considered, a particularity of this hypothesis is that this ratio remains practically constant (~ 0.15) when the number of carbon atoms increase from nine onwards ($n^{\circ}C \geq 9$). In Diesel fuel, the typical hydrocarbon molecule will be higher than this alkane of 9 carbons and lower than a molecule of 25 carbons. For all these cases, it is possible to consider the approximation of 0.15 for this ratio as an acceptable value.

Table 4.1: Ratio of hydrogen mass in an alkane hydrocarbon of single bonds

$n^{\circ}C$	1	3	6	9	12	15	18	21	24
$n^{\circ}H$	4	8	14	20	26	32	38	44	50
$\tau_{(H/fuel)}$	0.215	0.183	0.164	0.157	0.154	0.152	0.151	0.150	0.149

Considering the atomic mass of a hydrogen atom, the atomic mass of an oxygen atom is 15.9994 and that a water molecule is made up of two hydrogen atoms and one oxygen atom, the ratio of Hydrogen mass in a water molecule is shown in the Equation 4.2:

$$\tau_{(H/H_2O)} = \frac{(2)(1.00794)}{(2)(1.00794) + (15.9994)} = 0.11 \quad (4.2)$$

This means that 11% of the mass of a water molecule corresponds to the mass of the hydrogen atoms. Considering that all the hydrogen in the fuel reacts with oxygen to produce water, that the mass ratio of hydrogen in water is 0.11 and the mass ratio of hydrogen in the fuel is 0.15, it is possible to obtain the water ratio in the fuel with the Equation 4.3:

$$\tau_{(H_2O/fuel)} = \frac{\tau_{(H/fuel)}}{\tau_{(H/H_2O)}} = \frac{0.15}{0.11} = 1.336 \quad (4.3)$$

This means that considering a perfect combustion, as described in the hypothesis, for each gram of fuel burned, 1.336 grams of water are produced. From this expression, and considering the injected fuel mass, it can be obtained the mass flow of water at the IC engine outlet coming from the combustion process as in Equation 4.4:

$$\dot{m}_{(H_2O/fuel)} = (\dot{m}_{fuel})(\tau_{(H_2O/fuel)}) \quad (4.4)$$

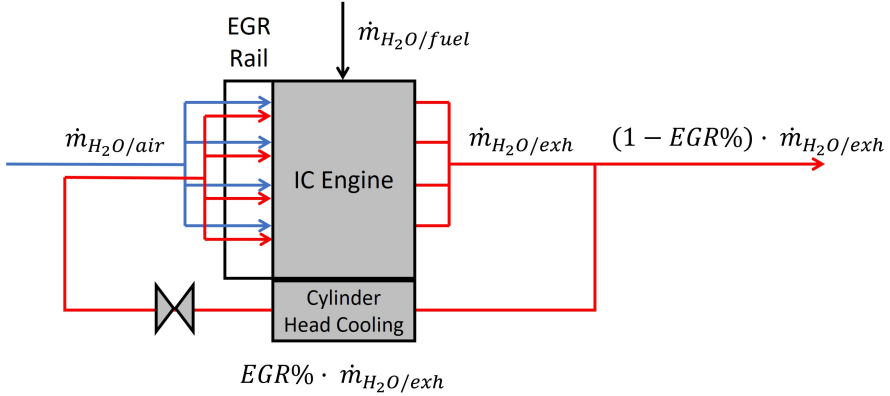


Figure 4.2: IC engine scheme with water mass flows

On the other hand, to estimate the amount of water coming from the intake air due to the ambient humidity, the “Humidity Ratio” (w_{air}) can be calculated. The air humidity ratio is a relation between the mass of water vapor per mass of dry air [63]. It is possible to calculate this ratio by using a psychrometric diagram from the conditions of pressure, temperature and relative humidity in ambient conditions. From these data, and knowing the air mass flow through the intake line, it is possible to obtain the water vapor mass per dry air mass as shown in Equation 4.5

$$\dot{m}_{(H_2O/air)} = \frac{(\dot{m}_{air})(w_{air})}{1 + w_{air}} \quad (4.5)$$

Adding the two previous terms, that is, the water mass flow coming from the combustion process through the EGR loop and the water mass flow coming from the ambient conditions, it is possible to estimate the total water mass flow at the cylinders outlet taking into account the EGR rate. Considering the scheme of the IC engine with an EGR circuit of the Figure 4.2, it is possible to estimate the water mass flow at the cylinders through the Equation 4.6:

$$\dot{m}_{(H_2O/exh)} = \left[\frac{1}{1 - EGR\%} \right] [\dot{m}_{(H_2O/fuel)} + \dot{m}_{(H_2O/air)}] \quad (4.6)$$

Considering this water mass flow at the cylinders outlet and knowing that the total mass flow at this point is the sum of the intake air mass flow and the mass flow of fuel, the humidity ratio at the cylinders outlet (w_{exh}) can be calculated as shown in Equation 4.7:

$$w_{exh} = \left[\frac{\dot{m}_{(H_2O/exh)}}{\frac{\dot{m}_{air} + \dot{m}_{fuel}}{1 - EGR\%} - \dot{m}_{(H_2O/exh)}} \right] \quad (4.7)$$

Finally, using the psychometric diagram, it is possible to obtain the relative humidity (φ_x) at a local point by using the humidity ratio at the cylinders outlet and the local conditions of pressure and temperature at this local point of the HP EGR line.

4.4 Results and Model Validation

The IC engine used is instrumented to measure pressure and temperature before the turbine, at the outlet of the High-pressure EGR valve and on the High-pressure EGR rail, just at the inlet of each of the four cylinders of the engine. The thermocouples used to measure the temperature at the inlet of the four cylinders of the engine have been installed in two different configurations. Firstly, introducing the thermocouples to the central area of the inlet ducts to the cylinders (gas side) and then, introducing the thermocouples just at the wall of the rail (wall side). In all these places, the relative humidity has been estimated using the model described in the previous section. On the other hand, the four cameras installed in the EGR rail at the inlet of the cylinders have been used to validate this model by comparing the images of these cameras with the condensation conditions estimated by the model.

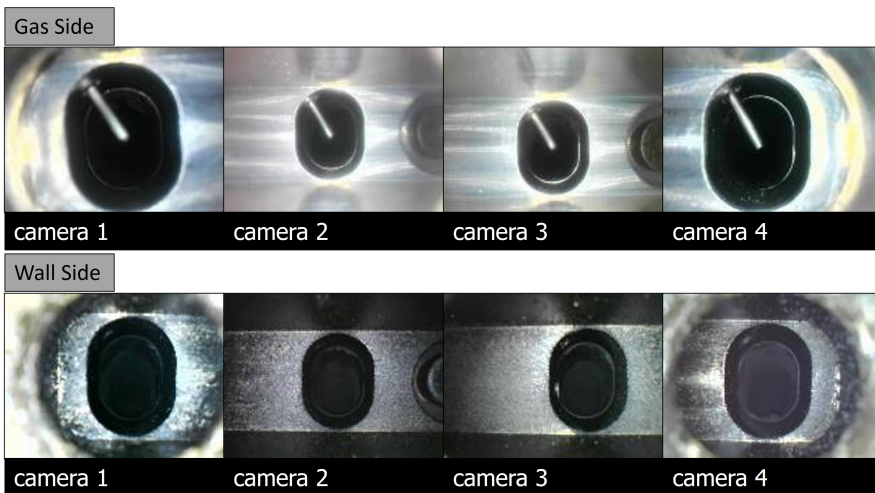


Figure 4.3: Sample of the images captured by the cameras at the cylinder intake ports in the EGR

Figure 4.3 shows a sample of the images of the EGR rail obtained by these four cameras. The top of the figure shows the position of the thermocouples in the gas side, while the bottom of the figure present the pictures with the thermocouples positioned in the wall side, just at the middle of the surface. The

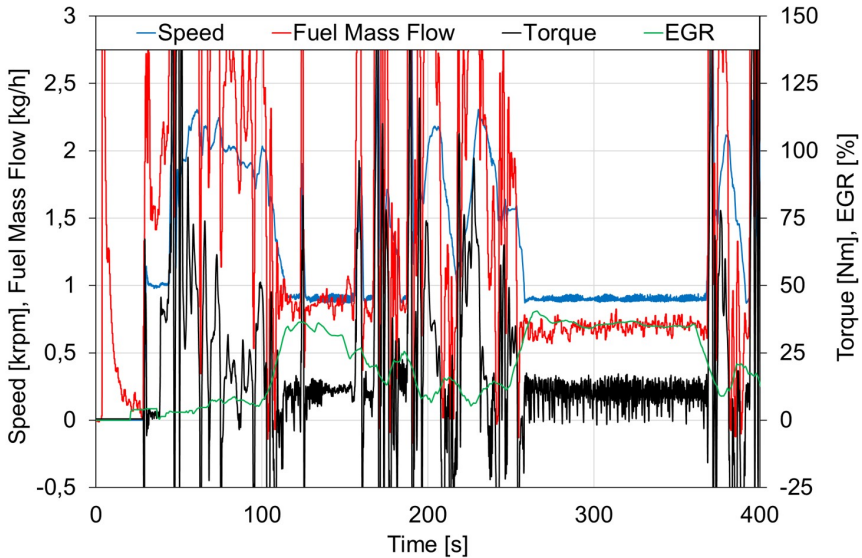


Figure 4.4: Measured engine speed, fuel consumption, torque and EGR% during the first 400 sec of the cycle

instrumentation of these sensors was mechanized in the HP EGR Rail used for the experiments and placed to measure the exhaust gases temperature before the mixture at the intake cylinders.

Figure 4.4 shows some measured parameters of the IC engine during the first part of the cycle. As can be seen in the graph, the cycle is composed of transient periods with severe accelerations and decelerations and other periods in steady conditions with smoother engine operating conditions. To take into account the operating conditions of the IC engine in new homologation cycles, the ambient temperature in the engine test bench has been set to -7°C and high EGR rates have been forced from the very beginning of the cycle. The initial temperature of the engine block is -7°C and the EGR rates in this first stage of the cycle reach values that reach up to 40%, especially in periods of steady conditions. These conditions at the beginning of the cycle force severe conditions of condensation that will be analyzed in next paragraphs.

Figure 4.5 shows the pressure measured at the turbine inlet and the pressure at the High-pressure EGR line outlet during the first part of the cycle. As can be seen in the figure, the transient periods have pressure peaks which reach up to 4 bar and periods in steady conditions with pressure values close to the ambient pressure. In order to estimate the condensation conditions in the High-pressure EGR line, the engine outlet pressure will be considered a uniform value from

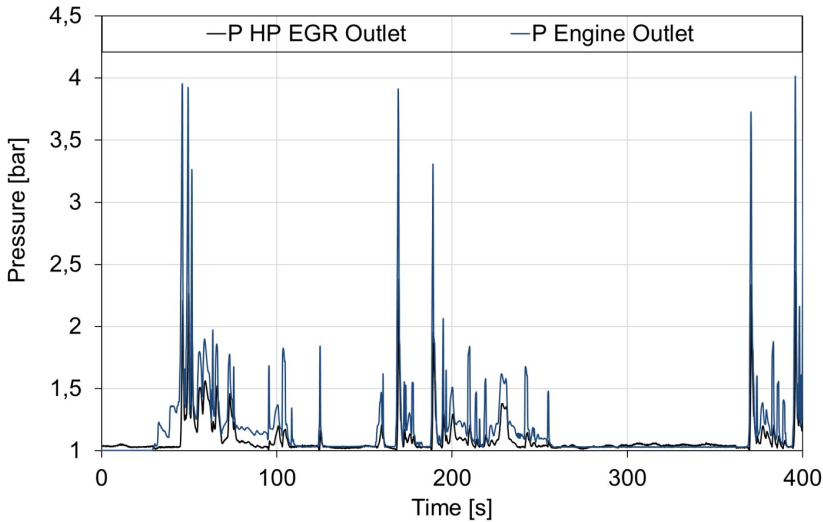


Figure 4.5: Measured pressures during the first 400 sec of the cycle

the engine outlet to the HP EGR valve inlet, and the HP EGR outlet pressure will be considered a uniform value from the HP EGR valve outlet to the four cylinders inlets.

Figure 4.6 shows the measured temperature during the cycle at the engine outlet, at the HP EGR valve outlet and at the four cylinders inlet. Temperatures at cylinders inlet have been measured at two different points, the “gas side” by placing the thermocouple approximately in the center of the cylinders inlet ports and the “wall side” by placing the thermocouple just in the wall surface of these ports. As can be seen from Figure 4.6, the temperature at the engine outlet increases quickly, avoiding the condensation conditions (red line in Figure 4.6). However, at the final part of the HP EGR line, these temperatures are lower, specially close to the wall (thick blue and purple lines in Figure 4.6) of cylinders inlet ports, where temperatures remain with values lower than 40°C during the first part of the cycle. Furthermore, due to the heat transfer efficiency in this final part of the EGR line, temperatures in the gas side (thin blue and purple lines in Figure 4.6) are considerably higher than close to the wall. These lower temperatures will produce condensation conditions close to these ports during the first part of the cycle. It is interesting to note that the temperatures recorded at the inlet of cylinders 1 and 4 (located at the extremes of the EGR rail) are lower than the temperatures measured in cylinders 2 and 3 (located in the central part of the rail). This is because the conditions for the heating of the

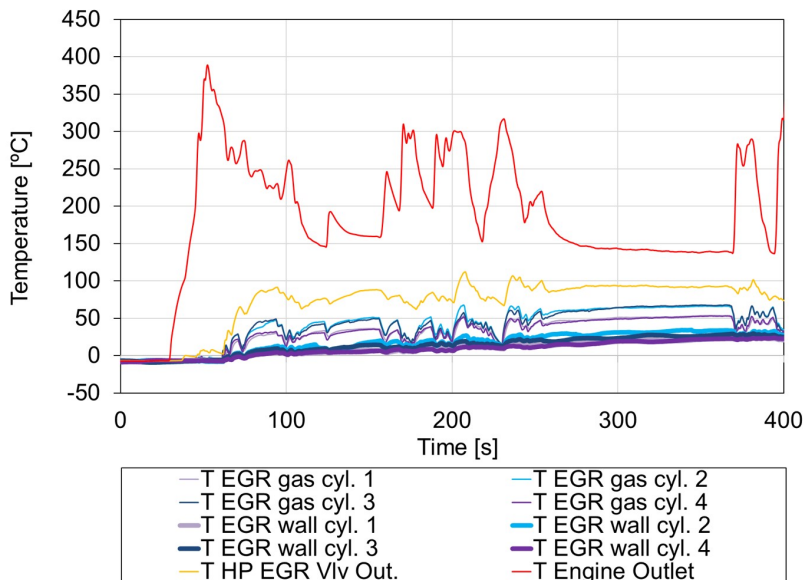


Figure 4.6: Measured temperatures during the first 400 sec of the cycle

EGR rail ducts by the hot exhaust gases and the heat transfer from the engine block are less severe in the ducts located at the extreme of the EGR rail.

Figure 4.7 shows the mass flow of water and hydrocarbons during the first seconds of the cycle. Hydrocarbons mass flow was measured through the gas analyzer and the total water mass flow at the cylinders outlet was estimated through the Equation 4.6 described in the mathematical description. As can be seen in the graph, most of the products coming from the combustion process and from the ambient conditions can be considered as water and approximately a 2% of this mass flow corresponds to hydrocarbon species.

The condensation model has been used to calculate the relative humidity at different points of the High-pressure EGR line, considering the pressures and temperatures of previous figures, air and fuel mass flows and the ambient conditions. Figure 4.8 shows the results of the model to estimate relative humidity at different points of the HP EGR line. As can be seen in this figure, the relative humidity at the engine outlet and at the HP EGR valve outlet drops to values below 50% before the second 80 of the cycle, avoiding condensation conditions at these points. However, at the cylinders inlet, these values remain well above 100% due to the low temperatures at these points. It is necessary to wait until 250 seconds to avoid the condensation conditions (relative humidity less than 100%) in the central part of the inlet ducts to the cylinders. However,

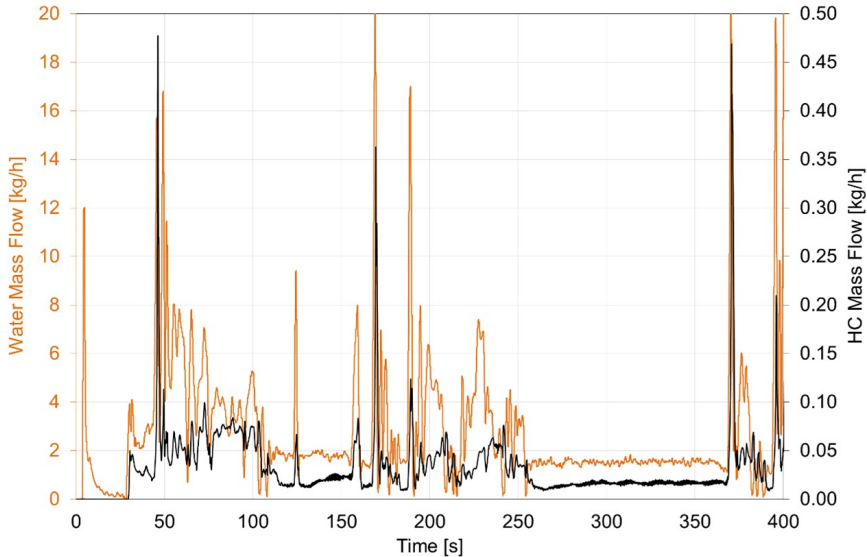


Figure 4.7: Water mass flow estimate and HC mass flow during the first 400 sec of the cycle

this does not prevent it from being followed in conditions of condensation near the walls.

For the qualitative validation of the condensation model, these results are compared with the videos recorded. [Figure 4.9](#) shows a sequence of frames of the four videos recorded at the inlet of the four cylinders. The first frame (top of the figure) corresponds to a frame of the initial conditions at the beginning of the cycle. The second frame of the figure shows the images of the four ports at 100 seconds. At this point in time, a severe fog appears on the four ports and first drops precipitate on the EGR rail surface, as shown the bright spots on the surface of the camera 2 and 3. The third frame shows the images at 200 seconds. As [Figure 4.8](#) shows, at this time the temperatures in the gas side of the EGR rail have increased enough to avoid condensation conditions. However, close to the EGR rail surface, temperatures are lower and condensation conditions appear. As the two central cylinders present higher temperatures, it is possible to observe a reduction in the fog in these two central cylinders and a dense fog in the two cylinders at the ends of the EGR rail. Also, an increment in the quantity of drops on the EGR rail surface can be observed in this frame. The fourth and fifth frames show the images at 300 seconds and at second 400. At this point, the fog practically disappears and only a little fog appears on camera 4 because the glass of the camera was fogged up. As [Figure 4.8](#) shows, although

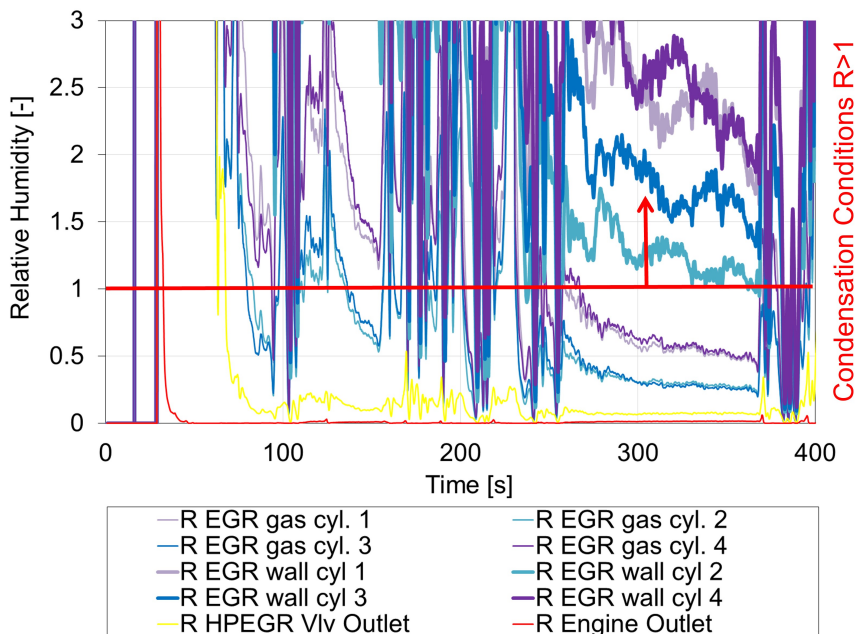


Figure 4.8: Estimated relative humidity during the first 400 sec of the cycle

the temperature of the gas has increased considerably at these moments and no fog is formed in the gas side, temperatures in the EGR rail wall continue to be low and the dew conditions cause a film of water on the surface of the rail.

Figure 4.10 shows the results of the model to estimate the relative humidity from the 400 to the 1200 seconds of the cycle. As can be seen in this figure, the relative humidity in the gas side is lower than 50% avoiding condensation conditions in the central part of the ducts. However, the EGR wall remains at low temperatures and dew conditions continue in the two central cylinders before the 800 seconds and the two ends cylinders remain in dew conditions practically until the 1200 seconds.

Figure 4.11 shows a sequence of frames of the four videos at the four cylinders inlet. The first frame (top of the figure) corresponds to a frame at the 400 seconds. Although at this time there are no condensation conditions on the gas side, dew conditions are produced in all the EGR wall and water drops appear in the EGR surface. The second frame of the figure shows the images of the four ports at the 600 seconds. At this time, the warm-up process of the two central cylinders reduce the relative humidity and dew conditions begin to disappear. It is possible to observe in the two central images a reduction in the quantity of liquid in the EGR wall, especially in camera 3. The last three frames, third, fourth and fifth, show the images at the 800, 1000 and 1200 seconds respectively.

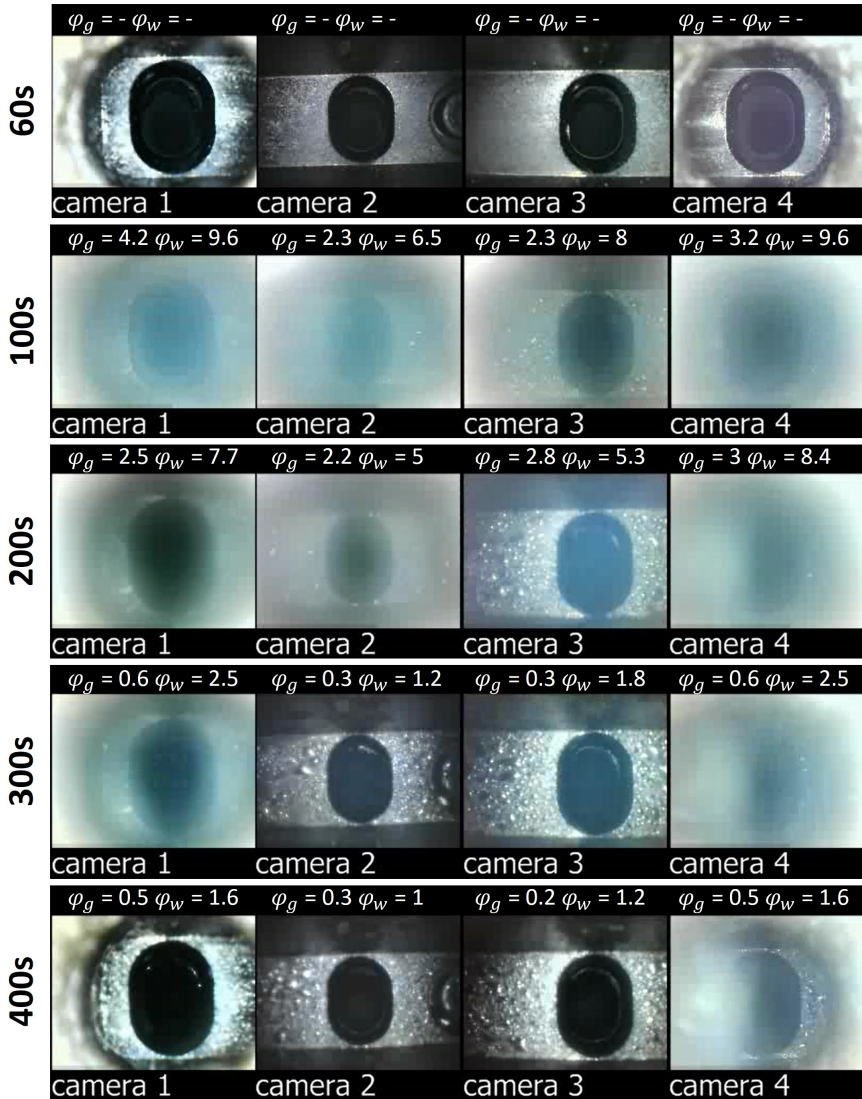


Figure 4.9: Video frames of the 4 cylinder cameras in the second 1, 100, 200, 300 and 400. In these pics φ_g is the relative humidity in the gas side and φ_w is the relative humidity in the wall side

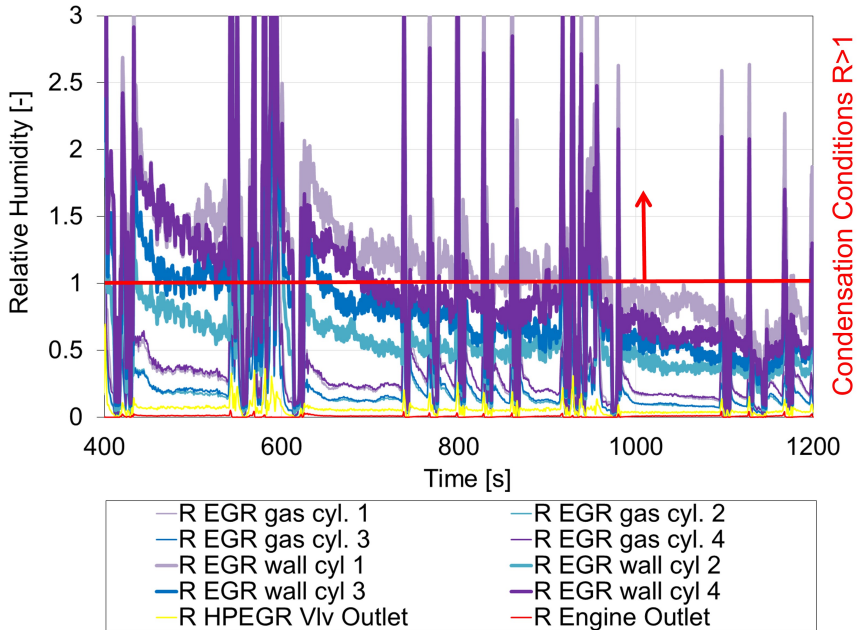


Figure 4.10: Estimated relative humidity from the second 400 to the second 1200 of the cycle

These images show a progressive reduction of the liquid drops in the EGR rail surface. This reduction is clear in the two central cylinders and it is less clear in the two ends cylinders where the relative humidity remains at high values practically until the last frame at the 1200 second. The results observed in the cameras have an important relationship with the values of relative humidity in the wall estimated by the model shown in the [Figure 4.10](#).

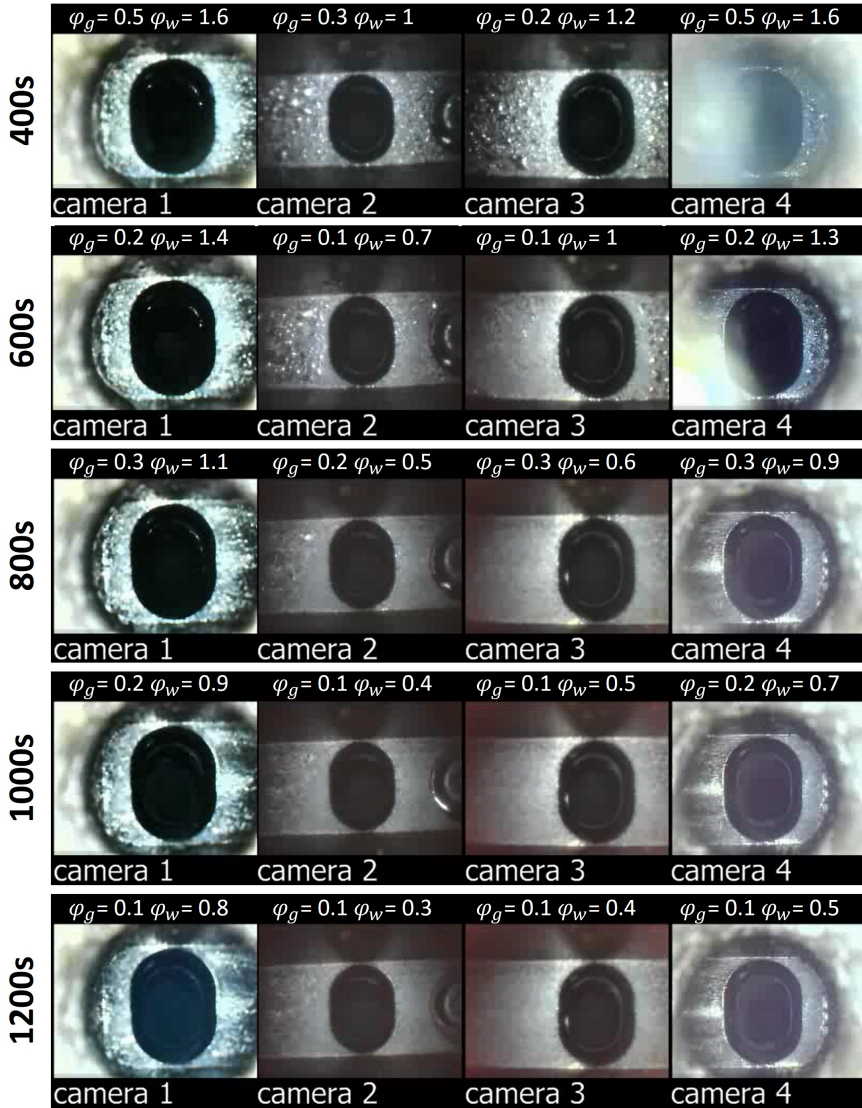


Figure 4.11: Video frames of the 4 cylinder cameras in the second 400, 600, 800, 1000 and 1200. In these pics φ_g is the relative humidity in the gas side and φ_w is the relative humidity in the wall side

4.5 Summary

This chapter presented a simple condensation model, capable to estimate the physical and thermodynamic conditions that produce the condensation phenomenon inside the High-pressure EGR line of an IC engine. This model has been validated visualizing in real time, the condensation behavior inside the engine component. This validation process shows that the predictions made by the model are in good agreement with the results obtained from the experimental tests.

The results are summarized in the next points:

- A mathematical model is developed with the aim of predicting the conditions that produce the condensation phenomenon to appear inside the EGR circuits of an internal combustion engine working at low ambient temperatures (-7°C).
- The humidity ratio and the internal engine conditions that characterize the appearance of this phenomenon are estimated by the model. Values of humidity ratio below one, and temperatures above 30°C , set a reference to avoid condensation conditions in the EGR circuits.
- The model is validated experimentally visualizing the condensation behavior along a representative driving cycle by means of cameras fitted on the EGR rail. Results shows that after 300 seconds in the gas side and 800 seconds in the wall side, condensation is avoided.

4.6 References

- [63] T. H. Kuehn, J. Ramsey, and J. L. Threlkeld. *Thermal Environmental Engineering*. 3rd ed. Pearson, 1998 (cit. on p. 42).

CHAPTER 5

Low-pressure EGR Bypass

5.1 Introduction

IN the previous chapter, due to the High-pressure EGR activation in an engine cold start, a simple condensation model has been developed and its experimental validation was presented. In this chapter, a different strategy using a Low-pressure EGR cooler bypass during the engine warm-up process under cold conditions is evaluated. The use of a bypass system in the Low-pressure EGR line avoids the passage of the gas through the LP EGR cooler. This strategy could lead to a higher temperature at the engine intake line, improving the engine warm-up process.

The main parts of this experimental study are summarized below:

- [section 5.2](#) describes the different methodologies and strategies followed to perform the physical experiments.
- [section 5.3](#) presents the impacts of the proposed strategy on the engine behavior in terms of the warm-up process, pollutant emissions, combustion efficiency and fuel consumption.
- [section 5.4](#) shows the condensation and fouling analysis. The condensation behavior along a representative driving cycle and the fouling deposits have been visualized and chemically analyzed.

5.2 Methodology and Strategies

The transient engine cycle named “EGR Cycle”, described in the [subsection 3.3.1](#), was conducted along this study under fixed low ambient temperature (-7°C). For this experimental work, a total of 30 tests have been performed at -7°C and activating the Low-pressure EGR during the whole cycle. 20 of these tests were performed with the bypass system activated in order to check the repeatability of the experiments and to check the engine response under this new configuration. The remaining 10 cycles were performed with the bypass deactivated to make a comparison and to evaluate the engine behavior when the Low-pressure EGR is activated and passing through the cooler.

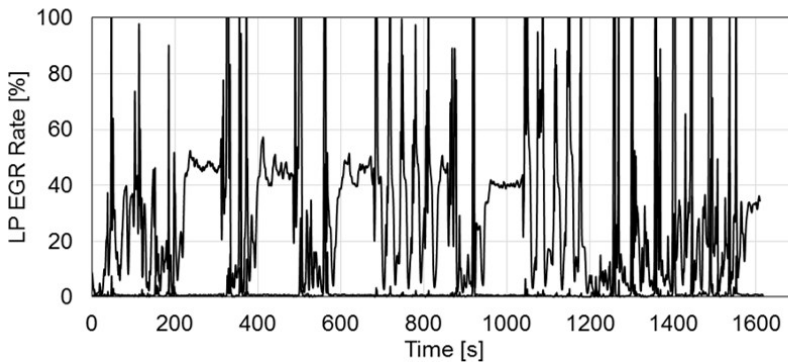


Figure 5.1: Low-pressure EGR rate from cold start conditions with the modified calibration

Additionally, it was necessary to modify the standard engine calibration, in order to activate the Low-pressure EGR and deactivate the High-pressure EGR during the complete cycle, because the ECU is not configured to perform Low-pressure EGR under these particular conditions. At cold conditions, only the High-pressure EGR is activated using the standard calibration. In order to perform realistic EGR rates during the warm-up process, the ECU was modified to introduce similar EGR rates to those of the engine running after the completion of the warm-up process. [Figure 5.1](#) shows the Low-pressure EGR rate along the entire cycle measured with the Horiba gas analyzer.

5.3 Results and Discussions

With the goal of presenting how the implementation of a bypass in the Low-pressure EGR line could improve the engine behavior and its performance under cold operating conditions, this section is divided into two different parts. In the first part [subsection 5.3.1](#), the impact of this configuration on the intake and exhaust temperatures, pollutant emissions and fuel consumption is presented. In the second part [section 5.4](#), the condensation and the chemical composition of the deposits is analyzed and the fouling phenomena evolution inside the engine components is presented.

5.3.1 Impact of the LP EGR bypass on the engine behavior

In order to show the main results of this work in terms of repeatability and dispersion between tests, a group of five tests is selected. First, a reference test performed at -7°C without activating the LP EGR and without using the bypass system. Later, two tests are performing using LP EGR and without bypass. Finally, two tests are performed using LP EGR with the bypass system activated.

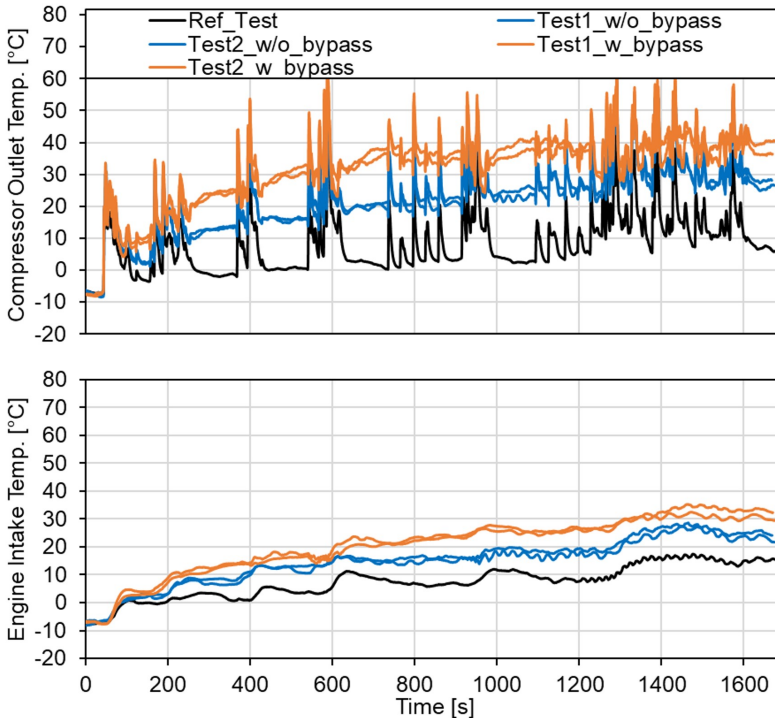


Figure 5.2: Compressor Outlet Temperature and Intake Manifold Temperature

Figure 5.2 shows the compressor outlet temperature and the engine intake temperature measured in the intake manifold. After the first 100 seconds, comparing the reference test to the two tests performing only Low-pressure EGR, it can be observed how the compressor outlet temperature increases approximately by 5°C . Furthermore, an additional increment of approximately 5°C is observed when the bypass system is activated in combination with the Low-pressure EGR, that is, when the exhaust gas is driven directly to the intake line without passing through the Low-pressure EGR cooler. Due to the WCAC deactivation during cold start operation, it can be observed in the bottom of the figure how the engine intake temperature increases progressively with respect to the reference test. These higher temperatures could increase the in-cylinder temperature and accelerate the warm-up process of the engine, improving the engine combustion efficiency.

As in the case of the intake temperature, Figure 5.3 shows how the exhaust temperature increases also progressively when performing LP EGR in combination with the bypass activation. From literature, it is known that an increase of 15°C in the intake temperature leads to a proportional increase in the exhaust temperature, affecting the combustion process and as a consequence, the engine pollutant emissions [64][65].

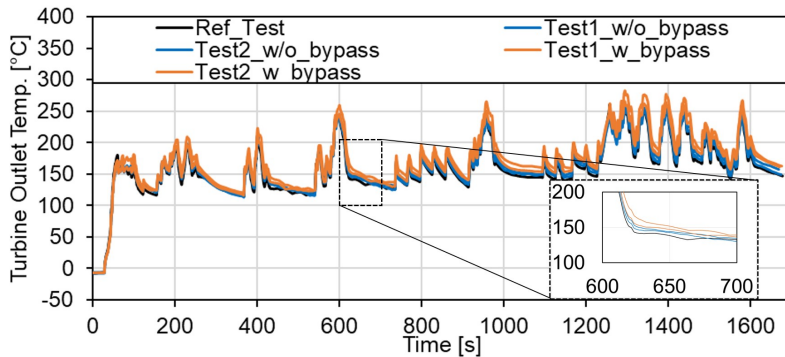


Figure 5.3: Exhaust Temperature with Zoom

As is usual in the IC engines calibration, the engine coolant temperature is used as a reference parameter in order to set different control strategies as per example the injection timing, the EGR activation and the engine cooling. Figure 5.4 shows this temperature and how the time to heat-up the engine coolant is reduced due to the abovementioned increase of the intake and exhaust temperatures. For this experimental work, the coolant temperature where the Electronic Control Unit (ECU) changes the EGR calibration strategy for an engine cold start is set at 60°C . During the experiments, it has been observed

that the tests performed with LP EGR and without bypass reach earlier a higher temperature reducing the time for heating the coolant, while tests performed with LP EGR and bypass work better than the reference test, but have a delay for the coolant temperature of thirty seconds approximately with respect to the previous case. This effect is expected to be due to the cooling engine configuration, where the coolant inside the engine circuit is recirculated to the LP EGR cooler in order to cool down the exhaust gas coming from the after-treatment. For this reason, the tests performed with LP EGR and passing the exhaust gas through the cooler (without bypass) allow to cool down the EGR gas and at the same time to heat the coolant inside the cooling circuit contributing to improve the global engine warm-up. This is something relevant in terms of engine calibration in order to know the effects that the implementation of a bypass system could produce in the aforementioned engine control strategies and also could be used a reference parameter to follow the engine warm-up process.

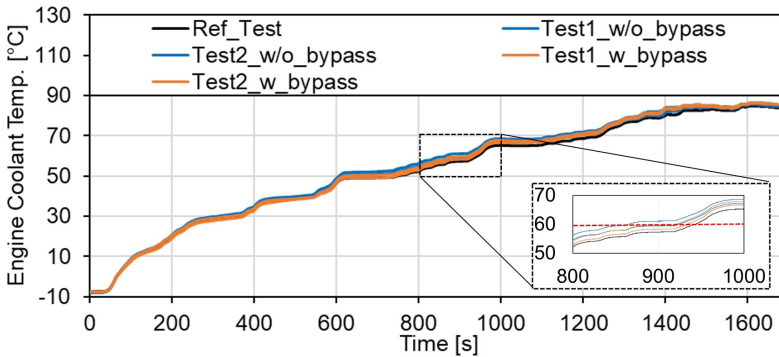


Figure 5.4: Engine Coolant Temperature with Zoom

5.3.1.1 Pollutant Emissions

Accumulated values of NO_x , HC and CO emissions measured upstream (continuous lines) and downstream (dashed lines) of the after-treatment system are presented in Figure 5.5. These values are calculated using aggregated data of each variable during the whole experimental cycle. The aim of performing EGR is to obtain a significant NO_x emissions reduction to both during the warm-up in cold operating conditions and after the warm-up process. Nevertheless, one disadvantage of this strategy is the combustion degradation, increasing the unburned HCs and PMs.

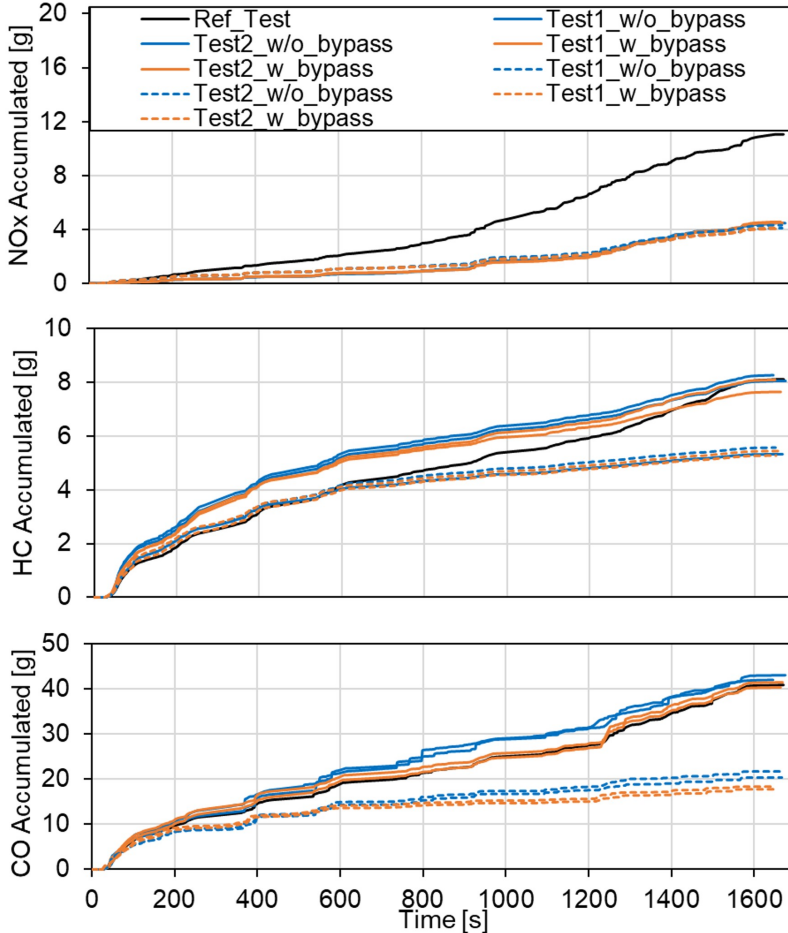


Figure 5.5: Accumulated Pollutant Emissions. Continuous line: Engine-out emissions. Dashed line: Tailpipe emissions

The top graph of Figure 5.5 shows the accumulated value of NO_x emissions. The accumulated value at the end of the cycle for this polluting emission is reduced from 11 g, in the case of reference test, to approximately 4.5 g, by activating the Low-pressure EGR from the beginning of the cycle for both configurations (with and without bypass). This reduction represents a reduction of 60% approximately. In terms of HC and CO emissions, a slight increase is observed during the first part of the cycle, when the engine is working in cold conditions. The increment in these emissions is due to the combustion degradation caused by the EGR gas introduced into the cylinders. However, this increase in HC and CO, during the first part of the test, disappears in the second part of the test, due to the reduction of the engine warm-up duration when

EGR is performed during the test. This positive phenomenon (reduction of the warm-up process period) compensates the negative phenomenon (exhaust gas introduced into cylinders) and at the end of the cycle, the accumulated emissions are practically the same in the two cases, with and without EGR.

When comparing the raw emissions (Continuous curve) to the final emissions (Dashed curve), by using the engine after-treatment system, the total HC emissions are reduced approximately 30% during the whole cycle (accumulated reduction at the end of the cycle). Regarding CO emissions, the reduction in accumulated emissions is practically a 50% at the end of the cycle.

In addition, the higher intake temperature reached when activating the LP EGR cooler bypass could help to slightly reduce the CO emissions, as it can be observed by comparing the CO cumulative in these two cases with and without bypass. At the end of the cycle, comparing the cumulative CO emissions after the catalyst in these two cases, it is possible to estimate an approximate reduction of 12% when the LP EGR is performed with the bypass activated.

5.3.1.2 Combustion Efficiency and Fuel Consumption

Figure 5.6 shows the combustion efficiency and the accumulated fuel consumption for the whole cycle. Using the air mass flow, the fuel mass flow and the CO and HCs emissions measured with the gas analyzer, the combustion efficiency is estimated as is shown in the following equation.

$$\eta_{Comb} = 1 - \frac{\dot{m}_{HC}(\dot{m}_{air} + \dot{m}_{fuel})}{\dot{m}_{fuel}} - \frac{\dot{m}_{CO}(\dot{m}_{air} + \dot{m}_{fuel})}{\dot{m}_{fuel}} \quad (5.1)$$

As mentioned above, during the first minutes of an engine cold start there are instabilities and degradations in the combustion. In Figure 5.6, it can be observed how the lowest values of efficiency are present until the 600 seconds approximately. In addition, performing LP EGR from the beginning of the engine cold start could affect the combustion process due to the combustion degradation. By this reason, it can be observed how the reference test without EGR presents a bit higher efficiency. Following the coolant temperature in order to take a reference of when the engine warm-up finishes, approximately at 60°C and after the second 800, the combustion is stable and the temperature in the cylinder is better for the engine operation, besides, during the end of the cycle, it can be observed how performing LP EGR and activating the bypass could improve the combustion efficiency due to the internal higher temperatures reached [66]. Nevertheless, the variations observed in the combustion efficiency and the fuel consumption are in the order of 5%. In general, the engine torque and the fuel consumption are similar comparing the different experiments.

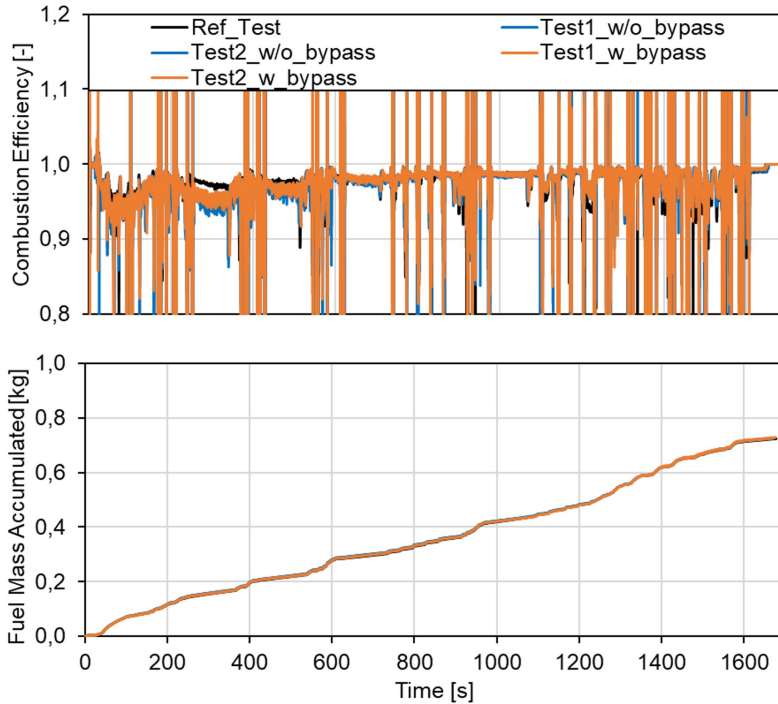


Figure 5.6: Combustion Efficiency and Accumulated Fuel Consumption

A small advantage could be observed performing the bypass activation in terms of combustion efficiency when the engine warm-up process finishes, this behavior could benefit the fuel consumption that should be affected by the combustion degradation during the engine cold start period.

5.4 Condensation and Fouling Analysis

The second objective of this experimental work is the analysis of two events presented when an IC engine is operating at very low ambient temperatures, in this case at -7°C . First, the condensation due to the hot gas coming from the fuel combustion, which has an important water content. The high humidity ratio in the exhaust gas produces condensation if the gas temperature is reduced below the dew point. And second, the fouling deposits, which could affect the EGR systems due to Hydrocarbons (HC) depositions on its principal components (i.e. EGR valve, EGR cooler).

5.4.1 Visualization of Condensates

With the aim of visualizing the condensation phenomena inside the Low-pressure EGR cooler bypass, different frame rates from the videos and pictures recorded with the endoscope cameras are presented.

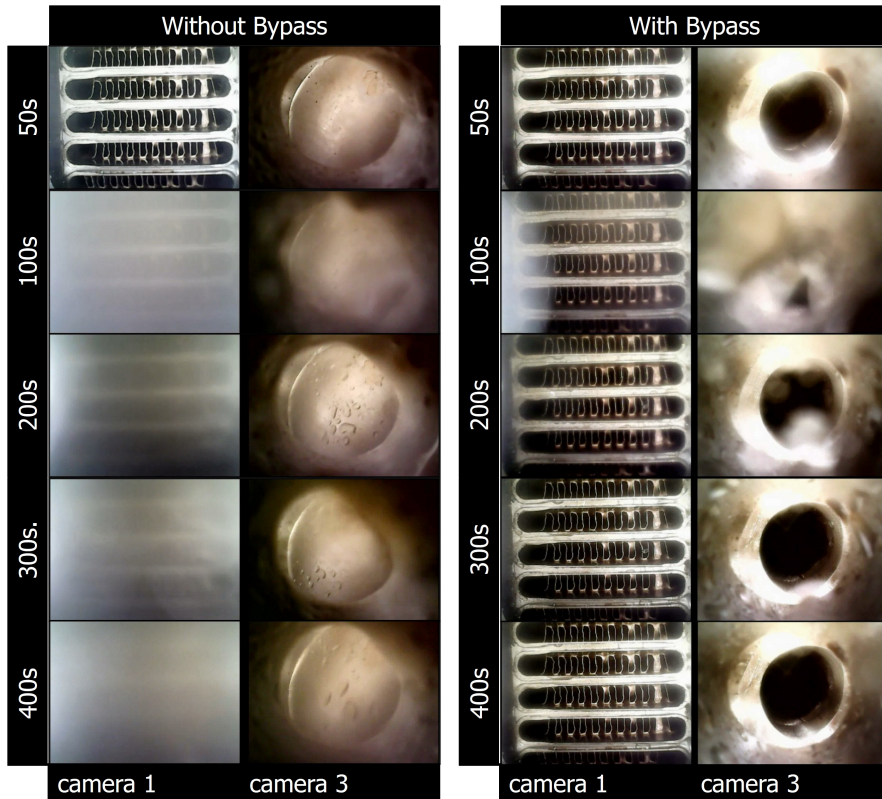


Figure 5.7: Video frames comparing two tests performed without (left) and with (right) bypass activation in the second 100, 200, 300 and 400

These frames allow to visualize the inlet of the cooler and the bypass flap of the system. The Figure 5.7 shows a sequence of frames of two tests performed in order to visualize the condensation phenomena inside the Low-pressure EGR bypass through the endoscope cameras. The frames at the left of the figure correspond to a test performing LP EGR and without activating the bypass system. The frames at the right of the figure correspond to a test performing LP EGR and activating the bypass system. The first frame (top of the figure) corresponds to a frame of the first seconds of the experiment, showing the initial conditions before the cycle begins. The second frame of the figure shows the images of the cooler and the bypass flap at 100 seconds. At this point in time, a

severe fog appears on the images and the first drops precipitate on the bypass surface, as shown by the bright spots on the surface of the camera 3. The third frame shows the images at the second 200 of the cycle. As [Figure 5.7](#) shows, at this time the temperature in the exhaust gas has increased enough to avoid condensation conditions.

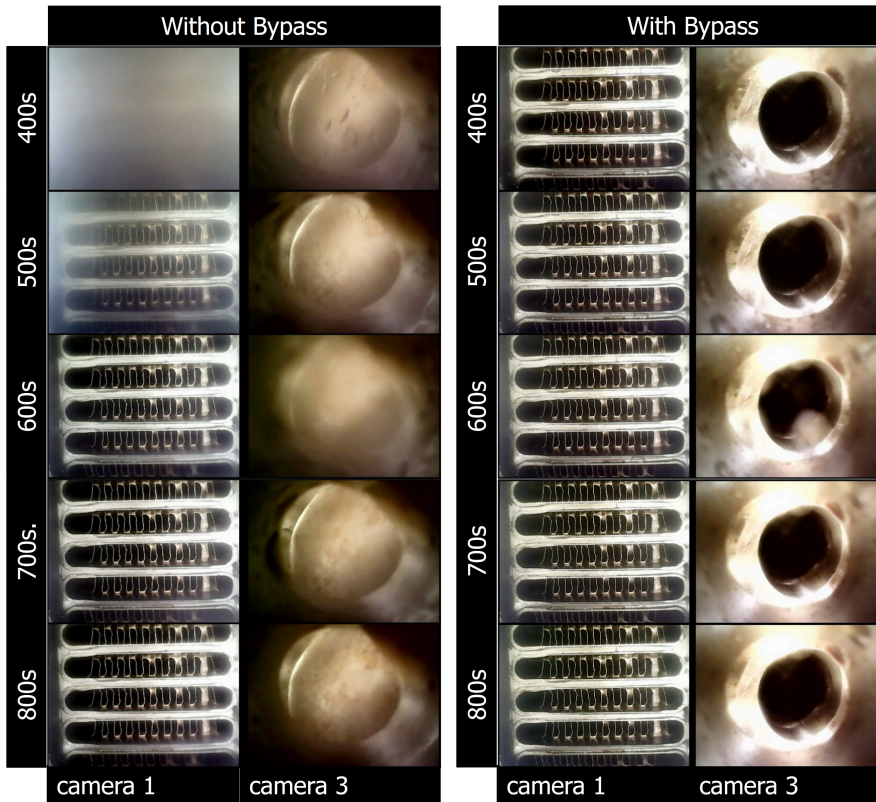


Figure 5.8: Video frames comparing two tests performed without (left) and with (right) bypass activation in the second 500, 600, 700 and 800

However, close to the surfaces, the temperature is lower and condensation conditions appear. As the bypass activation allows to increase the exhaust gas temperature, it is possible to observe a reduction in the fog in the frames at the right of the figure, while at the left of the figure, the fog is constant due to the lower exhaust gas temperature reached in the LP EGR cooler. The fourth and fifth frames show the images at 300 and 400 seconds of the cycle. At these moments, the fog practically disappears using the bypass activation. As [Figure 5.7](#) shows, although the temperature of the gas has increased considerably at these moments and no fog is formed in the exhaust gases, the temperature in the

bypass surfaces continue warming-up and drops of condensates can be observed. With the bypass deactivated, it is still possible to observe fog and condensation conditions at the cooler outlet at this time.

Figure 5.8 shows a sequence of frames of the following seconds of the two tests above mentioned. The first frame (top of the figure) corresponds to a frame at 400 seconds. Although at this time there are no condensation conditions on the exhaust gas using the bypass activation, dew conditions are produced in all the bypass walls and water drops appear in the bypass surface. The second frame of the figure shows the images of the cooler outlet and the bypass flap at the 500 seconds. At this time, the warm-up process reduces the relative humidity and dew conditions start to disappear. At the left of the figure, it is possible to observe a reduction in the fog and in the quantity of liquid in the bypass wall, especially in Camera 1. The last three frames, third, fourth and fifth, show the images at the 600, 700 and 800 seconds respectively. These images show a progressive reduction of the liquid drops on the bypass surface. This reduction is clear in the cooler outlet and in the bypass flap for both configurations, where the relative humidity decreases and condensation conditions disappear. It can be observed that the condensation time is lower by activating the bypass strategy. A reduction in time, of approximately 250 seconds could be reached due to the higher temperatures in the engine.

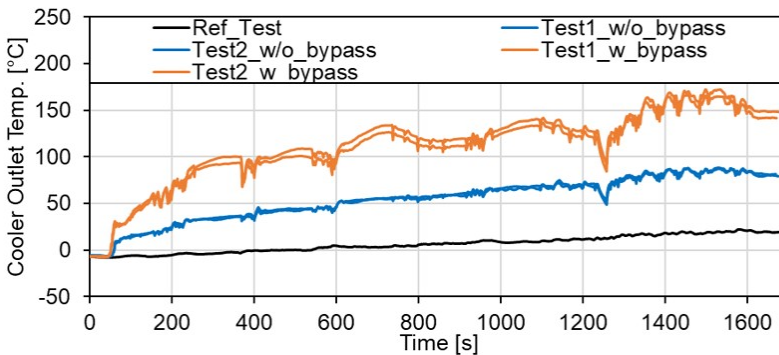


Figure 5.9: LP EGR Cooler Outlet Temperature (Gas Temperature)

This reduction could be explained by analyzing the exhaust gas temperature at the Low-pressure EGR cooler outlet. Figure 5.9 shows an increase of approximately 50°C activating the bypass (with bypass) with respect to perform LP EGR in the standard configuration, that is, using the EGR cooler (without bypass). Besides this temperature increment, it can be observed how a reduction in exhaust gas heating time is noticed, temperatures beyond 50°C are reached close to 200 seconds with the bypass configuration and after 600 seconds without the bypass

configuration. This could explain the condensation reduction observed through the endoscopes cameras and also could justify how local temperatures beyond 40-50°C contribute to leave the dew point and consequently avoid condensation conditions as could be observed in the previous Chapter 4.

5.4.2 Chemical analysis of condensates

Apart from visualizing the condensation phenomenon inside the Low-pressure EGR cooler bypass by means of the endoscope cameras, a sample of approximately 15 milliliters of condensates was collected through the sampling point mentioned in the experimental setup. A Thermal Gravimetric Analysis (TGA) and a Gas Chromatography – Mass Spectroscopy (GC – MS) analysis of the condensates collected during the experiments were performed. These analyses have the purpose of identifying which HC species are present in the condensates when the Low-pressure EGR is activated at cold conditions. The TGA analysis evaluates the mass loss when a substance is heated at a given heating rate. For this experimental work, the characterization of absorbed species and mineral fraction is assessed.

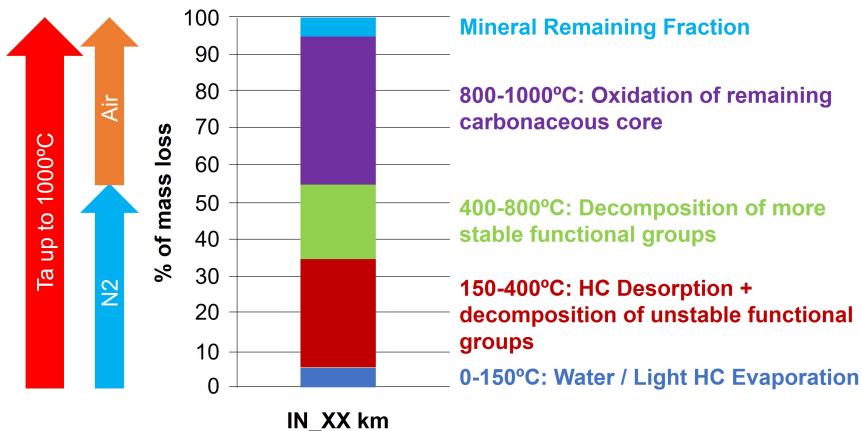


Figure 5.10: Thermal Gravimetric Analysis (TGA) Profile

Figure 5.10 shows the TGA analysis profile and its interpretation. Samples could be analyzed in an inert atmosphere (nitrogen) increasing the temperature until 800°C and in an oxidative atmosphere (synthetic air) increasing the temperature until 1000°C. The weight loss up to about 150°C is attributable to the water evaporation-desorption, the weight loss between 200 and 400°C is related to hydrocarbon desorption or decomposition of unstable functional groups (hydroxyls, carboxylic, carbonylic, . . .), the weight loss between 400 and

800°C is related to decomposition of stable functional groups and the weight loss from 800 to 1000°C is related to the oxidation of the carbonaceous core [36].

The TGA analysis performed in the condensates sample shows that approximately 98% of the weight loss is associated to water and light HC evaporation, and only the remaining 2% is related to decomposition of functional groups. That could explain the drops observed in [Figure 5.7](#) and [Figure 5.8](#) which are similar to water drops but what after several working hours can produce deposits accumulations related with the remaining HC species identified.

The GC-MS analysis allows to determine different compounds, like aromatic molecules or aliphatic compounds that can be examined in a very precise way. The aim of this analysis is the quantification of C1 – C2 and C3 – C10 aldehydes with an approach to Volatile Organic Compounds (VOC's).

[Table 5.1](#) shows the results of the GC-MS analysis with the total amount of each hydrocarbon present in milligrams per liter (mg/l). The main species found in the condensates were aliphatic HCs, specially, C1 – C2 aldehydes (formaldehyde and acetaldehyde) with a 74% of the total hydrocarbons. C3 – C10 aldehydes are present in a 14percent of the total hydrocarbons and the remaining 12% correspond to aromatics and other species. Regarding the volatile organic compounds, its presence is minimal and irrelevant in this study. Nevertheless, these results are in agreement with the HC species identified by Furukawa et al. [15], which reacting with other species could produce sticky fouling and deposits that could affect the normal operation of engine components as EGR valves and coolers.

Table 5.1: Gas Chromatography – Mass Spectroscopy (GC – MS) Results

	Total VOC's	Total Aliphatic	Total Aromatic
Condensates Sample (<i>mg/l</i> → <i>ppm</i>)	0.4503	54.5918	0.2128

5.4.3 Fouling Analysis

After 30 tests performing LP EGR at cold conditions, due to the condensation and the HCs depositions abovementioned, fouling conditions on the LP EGR line components are observed. [Figure 5.11](#) shows a sequence of the initial and final conditions of the LP EGR cooler and the bypass flap. It can be observed the fouling depositions on the surface comparing the reference test (without LP EGR) with four different tests performing LP EGR and activating or deactivating the bypass strategy. At the bottom of the figure, it can be observed the final conditions of the surfaces, where it is possible to evidence fouling and deposits due to reactions between the chemical components in the exhaust gas. Furthermore, following the highlighted zone in the pictures recorded with the

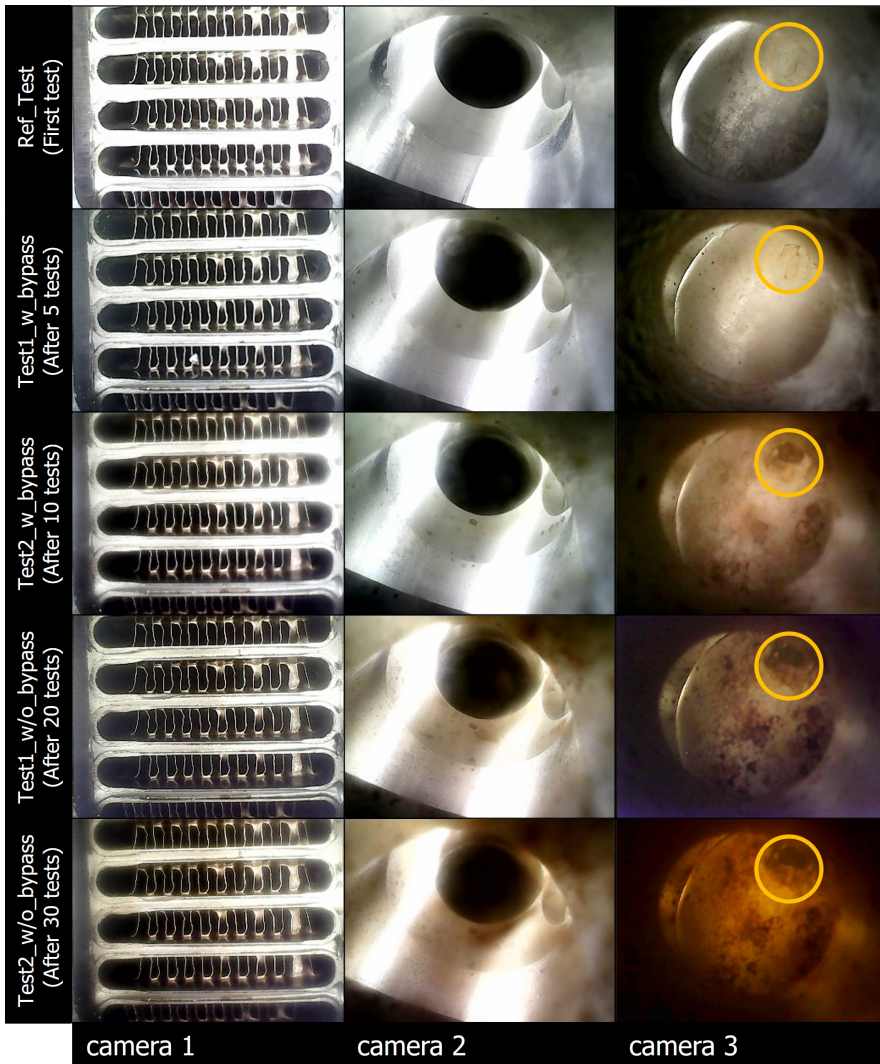


Figure 5.11: Pictures of fouling conditions after tests performed with and without bypass activation

camera 3, it is possible to identify local points on the surface where fouling depositions has increased and accumulated after each test.

Figure 5.12 shows a detail of the final conditions of the bypass flap. From the figure, it can be observed a golden layer of fouling, with apparently, burned depositions on its surface, probably from the accumulation of some species as could be observed in Figure 5.11.



Figure 5.12: Detail of fouling observed on the bypass flap

A similar golden layer of fouling at the LP EGR cooler outlet can be observed in [Figure 5.13](#). The initial condition of the LP EGR cooler before to start the experiments is presented at the left of the figure. The final conditions of the LP EGR cooler outlet after 30 tests performed at -7°C and activating the LP EGR during the whole cycle is shown at the right of the figure. It can be appreciated a uniform fouling layer on the internal surface of the cooler that could be related with the condensates observed through the endoscope cameras in the previous section.

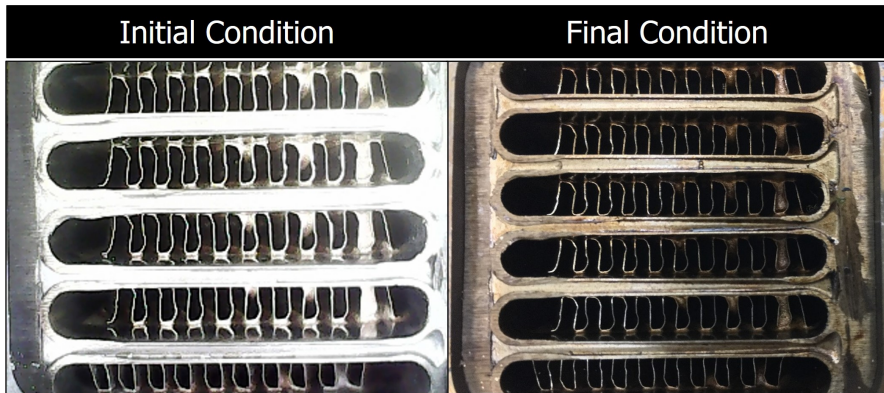


Figure 5.13: Initial (left) and final (right) conditions of the LP EGR cooler

The chemical analysis and fouling deposits show the presence of mainly formaldehyde and acetaldehyde in its composition. These species are produced by an incomplete combustion that reacting with acid substances could produce the sticky soot observed in the experiments. The golden color associated to these deposits could be related with the HCs aromatics and other products of the combustion as was founded in the literature.

5.5 Summary

This chapter presented the evaluation of a new compact line fitted with a bypass system for the cooler, implemented with the aim of accelerating the engine warm-up process as compared to the original low-pressure EGR line. The system was evaluated following two strategies, first performing EGR without bypass and then performing EGR bypassing the cooler.

The results are summarized in the next points:

- Activating the low-pressure EGR from the engine cold start leads a significant NO_x emissions reduction of approximately 60%. Moreover, the bypass activation leads to increase the engine intake temperature, reducing the engine warm-up time in 60 seconds and the CO emissions in approximately 12% due to a better combustion efficiency.
- Condensation phenomena and fouling depositions are visualized by means of endoscope cameras in order to identify the condensation time and the final conditions of the elements. Following this method, it could be observed that the period where condensation is produced, could be reduced by activating the bypass system in approximately 250 seconds.
- A chemical analysis of some condensates collected during the experiments and a comparison versus other species found in the literature is presented. This analysis shows that the main species produced in these experiments were aliphatic hydrocarbons, especially C1 – C2 aldehydes (formaldehyde and acetaldehyde).

5.6 References

- [36] C. Arnal, Y. Bravo, C. Larrosa, V. Gargiulo, M. Alfè, A. Ciajolo, M. U. Alzuet, Ángela Millera, and R. Bilbao. “Characterization of Different Types of Diesel (EGR Cooler) Soot Samples”. In: *SAE Technical Paper 2015-01-1690*. United States, 2015, p. 11 (cit. on pp. 10, 14, 68).
- [64] F. Payri, P. Olmeda, J. Martín, and R. Carreño. “Experimental analysis of the global energy balance in a DI diesel engine”. In: *Applied Thermal Engineering* 89 (2015), pp. 545–557 (cit. on p. 59).
- [65] J. M. Luján, H. Climent, V. Dolz, A. Moratal, J. Borges-Alejo, and Z. Soukeur. “Potential of exhaust heat recovery for intake charge heating in a diesel engine transient operation at cold conditions”. In: *Applied Thermal Engineering* 105 (2016), pp. 501–508 (cit. on p. 59).
- [66] F. Payri, A. Broatch, J. R. Serrano, L. F. Rodríguez, and A. Esmorís. “Study of the Potential of Intake Air Heating in Automotive DI Diesel Engines”. In: *SAE Technical Paper 2006-01-1233*. United States, 2006, p. 13 (cit. on p. 62).

CHAPTER **6**

Cylinder Deactivation Strategy

6.1 Introduction

IN the previous chapter, an experimental strategy using a new compact design of a bypass system for the Low-pressure EGR cooler was presented. In this chapter, a new method of deactivating cylinders, called “EGR DEACT”, is proposed. Meaning that the cylinders are not deactivated by the valves closure, but with the 100% of exhaust gas recirculation dedicated to the deactivated cylinders. This strategy allows to keep positive in-cylinder pressure (no blow-by risk) and could be presented as a cheaper solution compared to the intake and exhaust valve closing solution. According to this, the study of the cylinder deactivation strategy becomes especially interesting as a solution to reduce the warm-up process and decrease the after-treatment systems activation when IC engines operate at cold conditions (-7°C).

The main parts of this experimental study are summarized below:

- [section 6.2](#) describes the different methodologies and strategies followed to perform the physical experiments.
- [section 6.3](#) presents the results of a preliminary experimental study, evaluating the pumping losses in the cylinders and the engine response at steady and transient conditions when the deactivation cylinder strategy EGR DEACT at standard ambient conditions (20°C) is performed.
- [section 6.4](#) shows the effects of using the EGR DEACT strategy at steady conditions and during the engine cold start (-7°C) on the regulated diesel emissions and the engine thermal efficiency.

6.2 Methodology and Strategies

With the aim of comparing the engine performance in terms of pollutant emissions and exhaust gas temperatures for the EGR DEACT engine (2 cylinders firing) and standard engine (4 cylinders firing), steady and transient points were measured at an engine speed of 1500 rpm and a constant load of approximately 30 Nm at 20°C. For transient conditions, a standard engine start is performed until the warm-up process finishes, that is when the engine coolant temperature reaches 72°C. Then, the same methodology is applied to perform the study at cold conditions (-7°C). This engine operating point is a representative working point during the diesel engines homologation in the Worldwide harmonized Light vehicle Test Procedure (WLTP). Moreover, it is a representative working point studied in previous research works [67].

For the EGR DEACT configuration at 20°C and -7°C, it was necessary to modify the engine calibration with the purpose of following the fuel injection strategy and the EGR strategy of the standard engine configuration. The standard engine calibration is not configured for working with deactivated cylinders at cold conditions and presented some constraints in the fuel delivery and boost pressure [51]. These modifications were done with the purpose of keeping iso-torque conditions (constant load) for both configurations, offering to the customer the same engine performance when the EGR DEACT strategy is activated.

Figure 6.1 shows the standard and the EGR DEACT fuel injection strategy. Working with the standard engine (4 cylinders), two pre-injections of fixed quantity (1.5 mg/stroke) followed by a main injection, with a fixed separation of 650 μ s are performed. Working with the EGR DEACT engine (2 cylinders), two pre injections of fixed quantity (1.5 mg/stroke) followed by a main injection, with a fixed separation of 650 μ s and a post injection of fixed quantity (10 mg/stroke) without separation are performed. This additional fuel was added due to the engine calibration limitations and with the aim of reaching a similar torque and working with similar air fuel ratio (A/F) values than the standard engine configuration (4 cylinders).

Regarding the boost constraints, the exhaust gas flow rate through the deactivated cylinders (2 and 3) was controlled by the position of the EGR DEACT valve, while the turbine vanes were actuated manually trying to follow the requested boost pressure. The increased exhaust mass flow resulting from the displacement of intake air in the fired cylinders (1 and 4) and the exhaust mass flow regulation in the deactivated cylinders (2 and 3), could contribute directly to modify the engine pumping losses and the pressure before turbine. The torque limitations as a function of the variable geometry turbine (VGT) position and the engine pumping losses are presented in Figure 6.2. This figure illustrates the

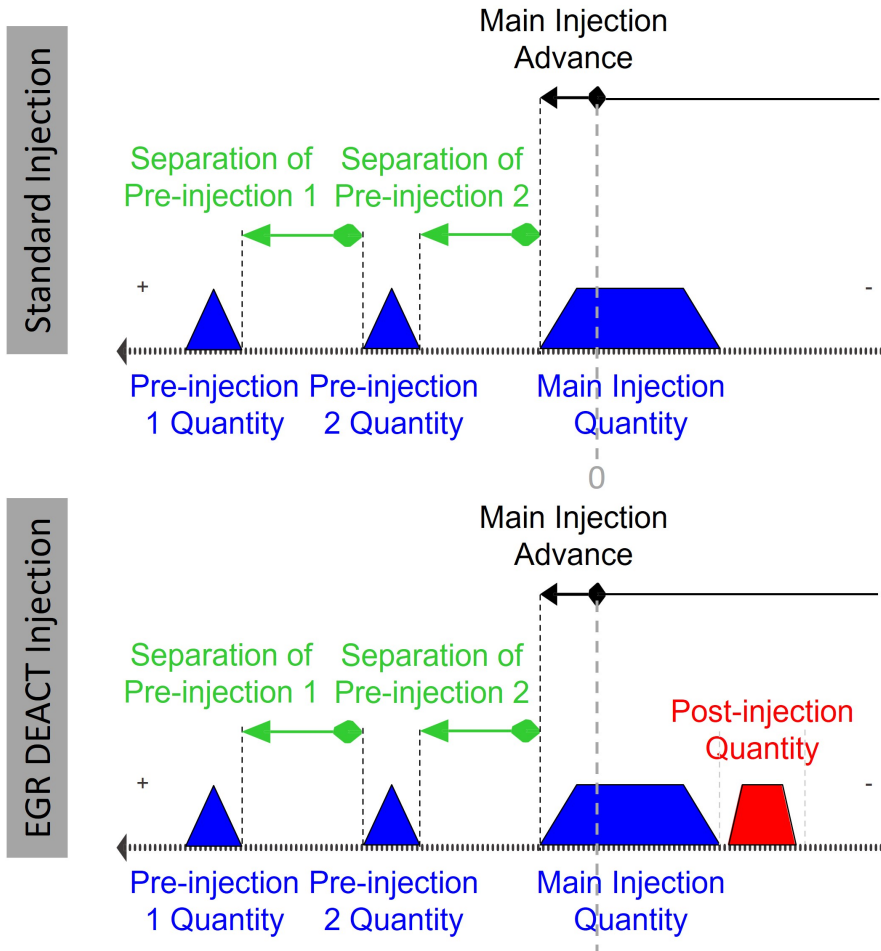


Figure 6.1: Standard and EGR DEACT Fuel Injection Strategy

trade-off between the boost setting and the pumping loss when running on EGR DEACT engine (2 cylinders). It can be observed how the measured points in the central part of the map, closing the turbine vanes from 40 percent onwards and EGR DEACT valve positions between 30 and 70%, present the higher torque values for this engine configuration. These values have been taken as reference parameters in order to perform this experimental work.

Besides of controlling the fuel injection settings and VGT position, variables like the LP EGR valve position and exhaust throttle (ET) valve position have been controlled in order to look for an optimal engine calibration in terms of pollutant emissions and thermal management.

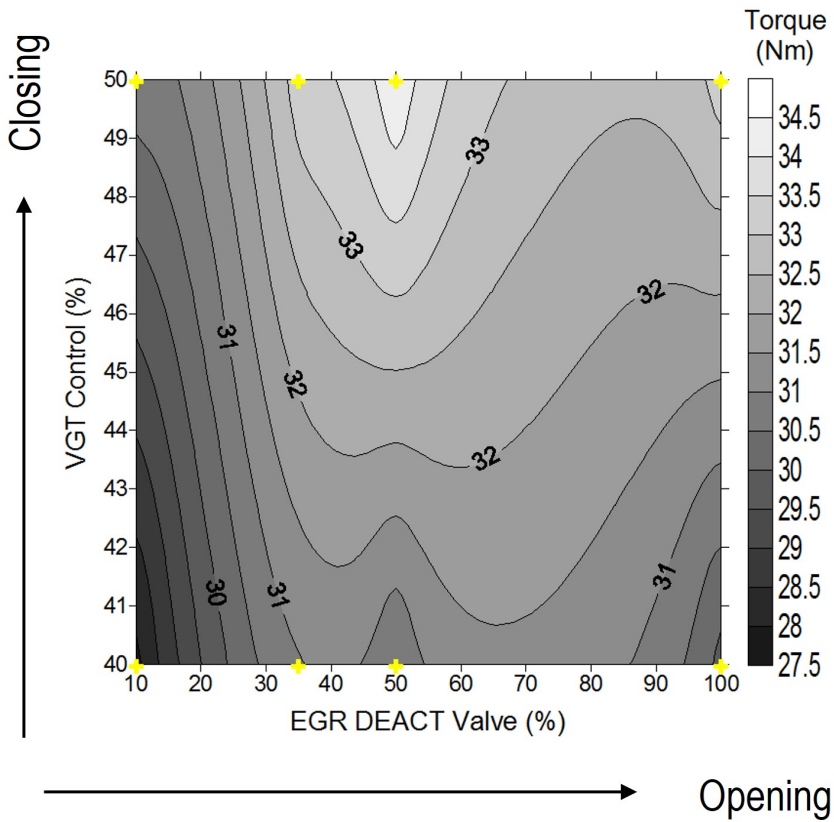


Figure 6.2: Torque limitations as function of VGT and EGR DEACT Valve position – 1500rpm

6.3 Experimental study at ambient temperature (20°C)

Steady and transient points have been measured at ambient temperature (20°C) with the aim of identifying the engine response when it works with the EGR DEACT configuration. This is performed with the purpose of comparing the standard engine operation with the modified strategy, analyzing the in-cylinder pressures, the pollutant emissions and the engine thermal efficiency, to subsequently replicate these results working at cold conditions (-7°C).

6.3.1 Pumping Losses Analysis

First, in order to analyze the pumping losses induced by the deactivation of cylinders 2 and 3, an estimation of the indicated work per cycle as a function of EGR DEACT valve position is presented. Then, the pollutant emissions trends and the thermal analysis at steady and transient conditions is discussed. It is important to highlight the fact that this analysis was done to assess the pumping losses consequently introduced by the EGR DEACT routing, having an unrepresentative EGR routing permeability layout (mass production EGR valve, recirculation across to small HP EGR holes, etc.)

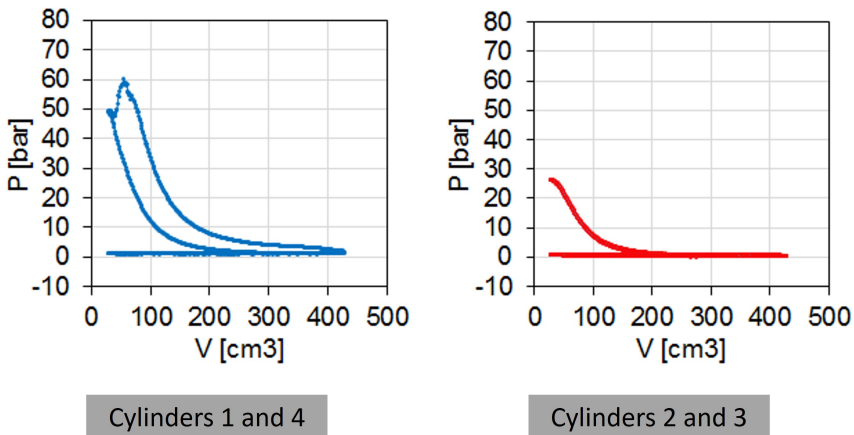


Figure 6.3: Indicated Diagram Profile (P – V) for the EGR DEACT Configuration

Figure 6.3 shows an example of the indicated diagram profile measured when the cylinder presents a combustion and under the EGR DEACT configuration. This diagram is used to estimate the indicated work per cycle and the pumping work considered also as mechanical losses. In fired cylinders (1 and 4), it could be assumed the compression and power strokes as the positive work obtained

from the cycle while the exhaust and intake strokes as the negative work. In deactivated cylinders (2 and 3), due to the fuel cut, there is not a power stroke in the cylinders and by this reason the complete cycle could be considered as a negative work that should be countered and minimized.

Taking this into account, using the indicated diagram, the in-cylinder pressures measured in the four cylinders and the engine cylinder capacity, the indicated work per cycle and the pumping work are estimated as is shown in the following equation.

$$W_i = \int_0^{\infty} P dv \quad (6.1)$$

Working with the standard engine (4 cylinders firing) a total indicated work per cycle of approximately 700 J is estimated. This value is the sum of the indicated work estimated by each cylinder. On the other hand, [Table 6.1](#) shows that working with the EGR DEACT strategy (2 cylinders firing) and regulating the EGR DEACT valve position between 35% and 50%, allows to reach a maximum indicated work of approximately 655 J and a considerable reduction of the pumping losses of 50%. However, the exhaust gas temperature is reduced due to a higher mass of gas recirculating in the deactivated cylinders (2 and 3). Moreover, a reduction in the effective work (engine torque) delivered by the engine using this configuration is noted. Taking this into account, some discrepancies are observed between the evolution of the indicated work and pumping work, which are estimated from the instantaneous pressures in the cylinder, and the torque, which is measured directly on the shaft. If the 35% and 50% EGR points are compared, when the indicated work increases and the pump work decreases, the torque decreases slightly, which does not make sense. Although the estimations of indicated work and pumping work were made by averaging the value of different cycles to avoid dispersion errors, these small discrepancies could not be avoided. Due to these discrepancies, it was preferred to use torque, which is a direct measure, as a parameter to optimize. Consequently, 35% EGR was chosen as the optimum operating point as it presented the point with the maximum torque and showed high values of temperature in the exhaust.

Table 6.1: Indicated work and pumping losses estimation

EGR DEACT Valve Position (%)	Turbine Outlet Temperature (°C)	Indicated Work (J)	Pumping Work (J)	Torque (Nm)
10	298	637.4	74	27.8
35	275	654.4	48.6	30.9
50	247	656.4	37.7	30.4
100	245	653	32.1	29.8

6.3.2 Results at steady-state conditions

Steady state points measured at 1500 rpm and constant load using the EGR DEACT engine configuration (2 cylinders firing) are compared with the standard engine configuration (4 cylinders firing). These tests are performed with the engine in hot conditions (85°C coolant temperature) and ambient temperature (20°C), measuring raw pollutant emissions and using the EGR DEACT injection strategy mentioned in the section 2.2. In addition, parameters like post injected fuel of 10 mg/stroke, VGT opening at 50percent, EGR DEACT valve position at 35percent and LP EGR valve opening at 60percent are fixed.

Table 6.2 shows the torque, exhaust gas temperature and pollutant emissions for the tests in both configurations. Keeping a constant torque value of approximately 30 Nm for both configurations, an increase of 70°C in the turbine outlet temperature (after-treatment inlet) was achieved using the EGR DEACT strategy. In addition, a reduction of 50% and 40% of the HC and CO emissions, respectively, was achieved. However, noticeable NO_x emissions increase and a fuel mass increase of 15% were found using this engine configuration. The NO_x emissions increase could be related with the boost limitations and the lower EGR rate performed in the firing cylinders. Under standard engine configuration, EGR rates of approximately 50% are reached. Besides, according with the literature the new exhaust gas recirculation distribution and its dispersion could contribute to increase the NO_x and PM emissions depending of the mixing behavior [68] [69].

Table 6.2: Engine performance at 20°C

	Standard Engine (4 Cylinders)	EGR DEACT Engine (2 Cylinders)
Torque (Nm)	30.5	31
Turbine Outlet T. (°C)	229	299
NO_x (g/kWh)	0.6	4.8
HC (g/kWh)	1.8	0.95
CO (g/kWh)	6.5	3.9
Fuel Mass (kg/h)	1.36	1.61

6.3.3 Results at transient conditions

Once the engine response at steady-state conditions and working under EGR DEACT configuration is known, the engine warm-up process at transient conditions is evaluated.

Figure 6.4 presents the engine torque response along the first minutes of an engine ambient start at 20°C. First, a reference test (*RefTest*) working with the standard engine at 1500 rpm was carried out. Then, two tests working with the EGR DEACT engine (Test 1 and Test 2) were performed trying to follow the reference test. The net pollutant emissions where measured during the Test 1

and the raw pollutant emissions were measured during the Test 2. To follow this operating condition, the parameters established at steady-state conditions in the methodology section are replayed working under this transient condition.

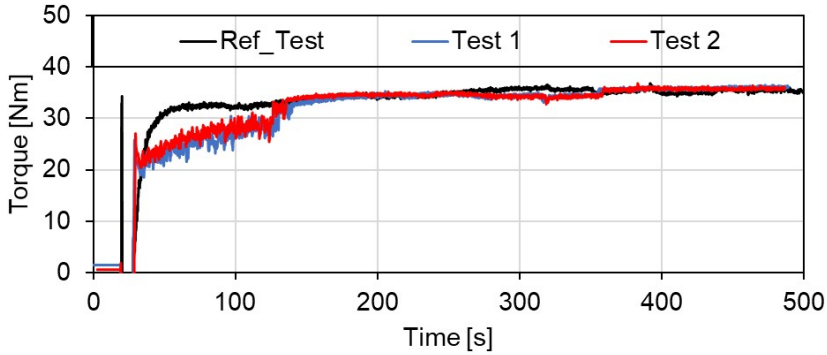


Figure 6.4: Torque at 20°C

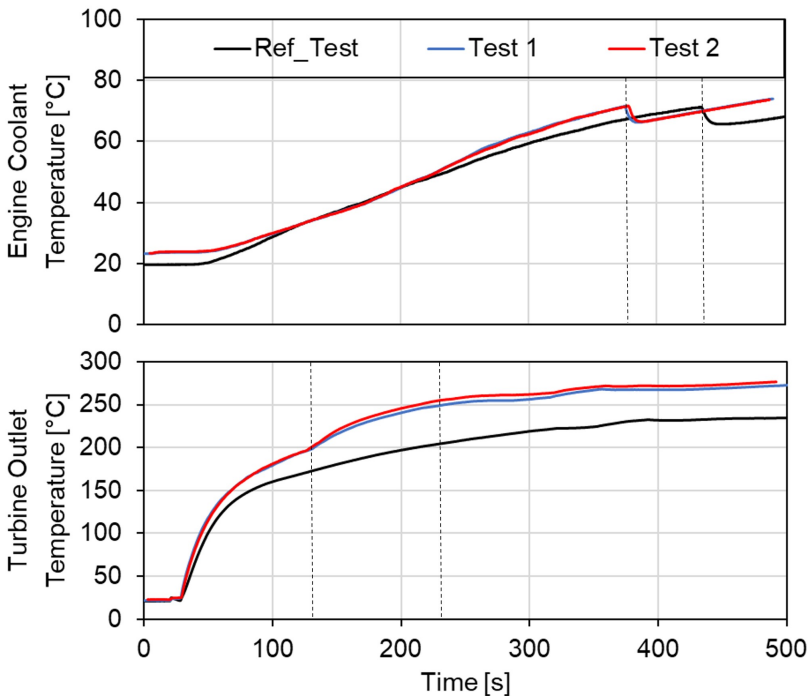


Figure 6.5: Engine coolant and turbine outlet temperature at 20°C

The engine thermal efficiency and the early activation of the after-treatment

system depends on the engine warm-up and the outlet temperatures reached in the exhaust line. **Figure 6.5** shows the engine coolant temperature and the exhaust temperature measured at the turbine outlet (DOC inlet) to check the after-treatment activation period and its efficiency. A temperature increment of approximately 60°C can be observed in the exhaust gases after the engine cold start (second 120) due to the EGR DEACT method implementation. This advantage could reduce the engine warm-up process up to 60 seconds and the after-treatment activation up to 100 seconds, improving the thermal efficiency of the DOC and its functioning. Oxidation catalyst and lean NOx trap (LNT) devices deliver its maximum efficiency when the exhaust gas temperature is beyond 200°C [70][71].

Due to the higher exhaust temperatures, a reduction in HC and CO emissions should be expected. **Figure 6.6** presents the pollutant emissions measurements upstream and downstream of the after-treatment system. On the top of the graph, it can be observed considerable NOx emissions increase due to the EGR limitations. Fixing the LP EGR valve position at 60% and activating the exhaust throttle (ET) valve also at 60%, a maximum EGR rate of 15% was performed. This limitation could be related to a low-pressure difference between the intake and exhaust manifolds due to the boost limitations evidenced before. **Table 6.3** presents how closing the ET valve is an alternative to increase the EGR rate performed.

Table 6.3: EGR rate limitations

LP EGR Valve Position (%)	Exhaust Throttle Valve Position (%)	EGR Rate (%)
60	50	11.4
60	60	14.2
60	70	20.3

On the other hand, CO and HC emissions present a significant reduction during the engine cold start of 60% and 50% respectively. This benefit could be directly related with the higher exhaust temperatures evidenced before. In addition, comparing net and raw CO emissions, a reduction in the DOC light-off period (instant when the working temperature is reached) of approximately 250 seconds can be observed.

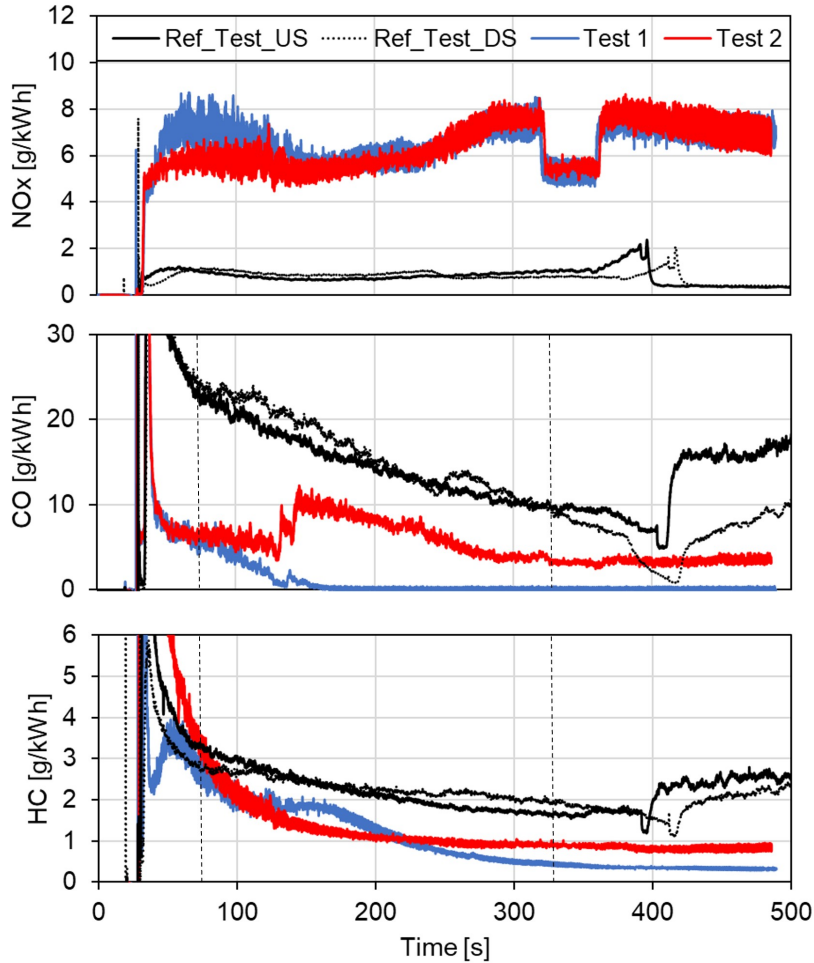


Figure 6.6: Engine pollutant emissions at 20°C

6.4 Experimental study at cold conditions (-7°C)

A significant contribution of this experimental work is to evaluate the EGR DEACT strategy under low ambient temperature (-7°C). Taking this into account, and using the study performed at ambient temperature (20°C) as a reference, the engine is tested at steady-state and transient conditions under these particular conditions, trying to follow a similar performance than the observed before.

6.4.1 Results at steady-state conditions

Steady points measured at 1500 rpm and constant load using the EGR DEACT engine configuration are compared to the standard engine configuration.

The main results of this experiment are presented in Table 6.4. Keeping a constant value of approximately 38 Nm of torque for both configurations, a noticeable increase of 120°C in the turbine outlet temperature (after-treatment inlet) was achieved. In addition, a reduction of 70% and 40% in HC and CO emissions, respectively, was found. A NO_x emissions reduction of 16% and an acceptable fuel mass increase of 15% was achieved working at -7°C. This reduction in NO_x is achieved taking as a reference that the engine is not prepared to perform exhaust gas recirculation at this particular temperature. In the 20°C case the engine performed exhaust gas recirculation from the engine start. However, these results shows the potential of the EGR DEACT strategy to increase the exhaust gases temperature and its benefits when the ICE is working at low ambient temperatures.

Table 6.4: Engine performance at -7°C

	Standard Engine (4 Cylinders)	EGR DEACT Engine (2 Cylinders)
Torque (Nm)	38.1	37.2
Turbine Outlet T. (°C)	214	336.5
NO _x (g/kWh)	3.2	2.7
HC (g/kWh)	1.9	0.6
CO (g/kWh)	10	6.3
Fuel Mass (kg/h)	1.59	1.91

6.4.2 Results at transient conditions

Working in transient conditions and starting the engine at a very low ambient temperature (-7°C) with exhaust gas recirculation from the beginning of the test causes instabilities and degradations of the combustion process. Figure 6.7 shows a reference test of an engine cold start performed with the standard engine (4 cylinders firing) and a single test performed with the EGR DEACT strategy (2 cylinders firing). Tests are performed using the same engine parameters fixed in the experimental study at 20°C. Following the torque evolution, it can be observed that working with the EGR DEACT configuration the warm up process of the engine is critical even decreasing the total work delivered by the engine, especially during the initial seconds of the test. This behavior is due to the early EGR activation and the lower capacity of the engine when it works with only two cylinders. Nevertheless, once the engine temperature increases and the warm up process finishes around the 200 seconds, the engine behavior begin to be stable.

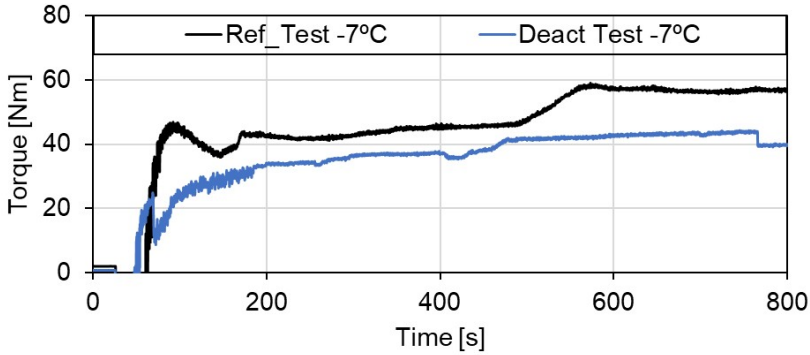


Figure 6.7: Torque at -7°C

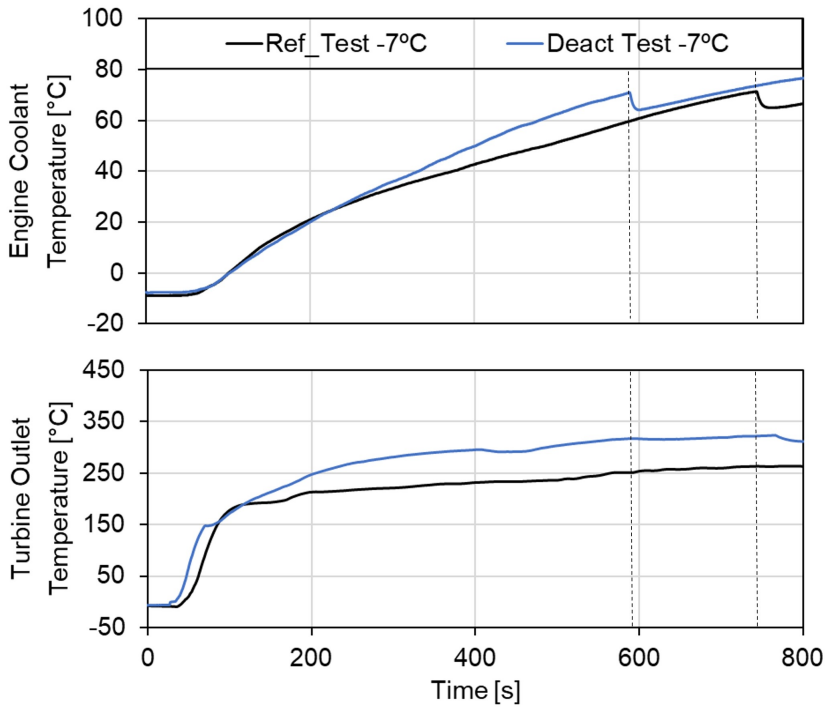


Figure 6.8: Engine coolant and turbine outlet temperature at -7°C

One improvement of this strategy is the reduction of the warm up process under these conditions. Figure 6.8 shows how the exhaust gas temperature is increased around 100°C reducing the engine warm up period in approximately 180 seconds (3 minutes) with respect to the reference case, noticeable time reduction that allows to improve the engine behavior and to reduce the activation

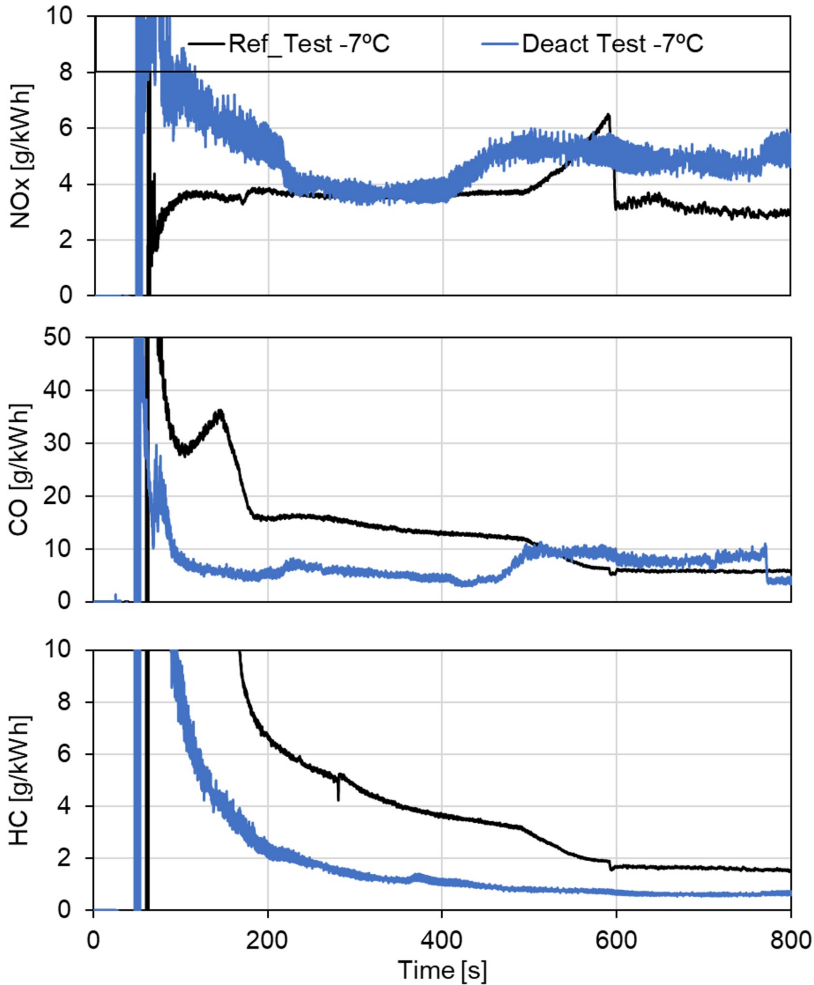


Figure 6.9: Engine pollutant emissions at -7°C

time of the after-treatment systems with the consequently benefits in pollutant emissions.

Figure 6.9 presents the raw pollutant emissions measurements of these tests. Higher values of NOx are evidenced during the first minutes of the cold start engine for the EGR DEACT strategy. However, when temperatures begin to increase, these levels decrease compared to the reference test. As it was founded at transient conditions and working at ambient temperature (20°C), CO and HC emissions are reduced in approximately 50% due to the higher temperatures reached in the exhaust gases.

6.5 Summary

This chapter presented the impact of using a new cylinder deactivation strategy on a IC engine running under cold conditions (-7°C) with the aim of improving the engine warm-up process. This evaluation has been performed in two parts. First, testing the strategy at ambient standard conditions (20°C) and then, activating the strategy at low ambient temperature (-7°C).

The results are summarized in the next points:

- An experimental study is performed at 20°C to analyze the effect of the cylinder deactivation strategy at steady-state and during an engine cold start at 1500 rpm and constant load. In particular, the pumping losses, pollutant emissions levels and engine thermal efficiency are analyzed.
- The engine behavior is analyzed at steady-state and transient conditions under very low ambient temperatures (-7°C). In these conditions, the results show an increase of the exhaust temperatures of around 100°C , which allows to reduce the diesel oxidation catalyst light-off by 250 seconds, besides of reducing the engine warm-up process in approximately 120 seconds.
- The CO and HC emissions have been reduced by 70% and 50%, respectively, performing this new strategy. However, due to the limited EGR distribution between cylinders, NO_x emissions present and slightly increase.

6.6 References

- [51] J. Zammit, M. McGhee, P. Shayler, and I. Pegg. “Internal Combustion Engines: Performance, Fuel Economy and Emissions”. In: Woodhead Publishing, 2013 (cit. on pp. 12, 75).
- [67] P. Mock, J. Kühlwein, U. Tietge, V. Franco, A. Bandivadekar, and J. German. “The WLTP: How a new test procedure for cars will affect fuel consumption values in the EU”. In: *The International Council on Clean Transportation - Working Paper 2014.9* (2014), pp. 1–20 (cit. on p. 75).
- [68] V. Macián, J. M. Luján, H. Climent, J. Miguel-García, S. Guilain, and R. Boubennec. “Cylinder-to-cylinder high-pressure exhaust gas recirculation dispersion effect on opacity and NO_x emissions in a diesel automotive engine”. In: *International Journal of Engine Research* 22.4 (2021), pp. 1154–1165 (cit. on p. 80).
- [69] J. Galindo, H. Climent, R. Navarro, and G. García-Olivas. “Assessment of the numerical and experimental methodology to predict EGR cylinder-to-cylinder dispersion and pollutant emissions”. In: *International Journal of Engine Research* 22.10 (2021), pp. 3128–3146 (cit. on p. 80).
- [70] P. Piqueras, A. García, J. Monsalve-Serrano, and M. J. Ruiz. “Performance of a diesel oxidation catalyst under diesel-gasoline reactivity controlled compression ignition combustion conditions”. In: *Energy Conversion and Management* 4 (2019), pp. 18–31 (cit. on p. 82).
- [71] J. Serrano, P. Piqueras, E. Sanchis, and B. Diesel. “A modelling tool for engine and exhaust aftertreatment performance analysis in altitude operation”. In: *Results in Engineering* 4.100054 (2019), pp. 1–11 (cit. on p. 82).

CHAPTER

7

DPF Regeneration with High-pressure EGR

7.1 Introduction

IN the previous chapter, the EGR DEACT strategy as an alternative solution for accelerating the engine warm-up process was presented. In this chapter, a possible engine configuration to be present when an internal combustion engine is operating at low ambient temperatures (-7°C) is evaluated. This configuration is the High-pressure EGR activation while the diesel particulate filter (DPF) is under active regeneration process.

The main parts of this experimental study are summarized below:

- [section 7.2](#) describes the different methodologies and strategies followed to perform the physical experiments.
- [subsection 7.3.1](#) presents the impacts on the engine behavior working under this configuration. The DPF regeneration process, the combustion efficiency and the pollutant emissions are evaluated. In addition, the DPF regeneration process efficiency is analysed.
- [subsection 7.3.2](#) shows the impacts on the EGR components, the fouling depositions and an approximated estimation of the soot mass and volume collected from the High-pressure EGR line during the experimental campaign.

7.2 Methodology and Strategies

Tests have been performed in steady-state conditions with an engine speed of 2000 rpm and 4 bar of brake mean effective pressure (BMEP). The engine working condition was defined as a representative point for the DPF regeneration, comparable to a real engine operation on a highway at 120 km/h with medium load.

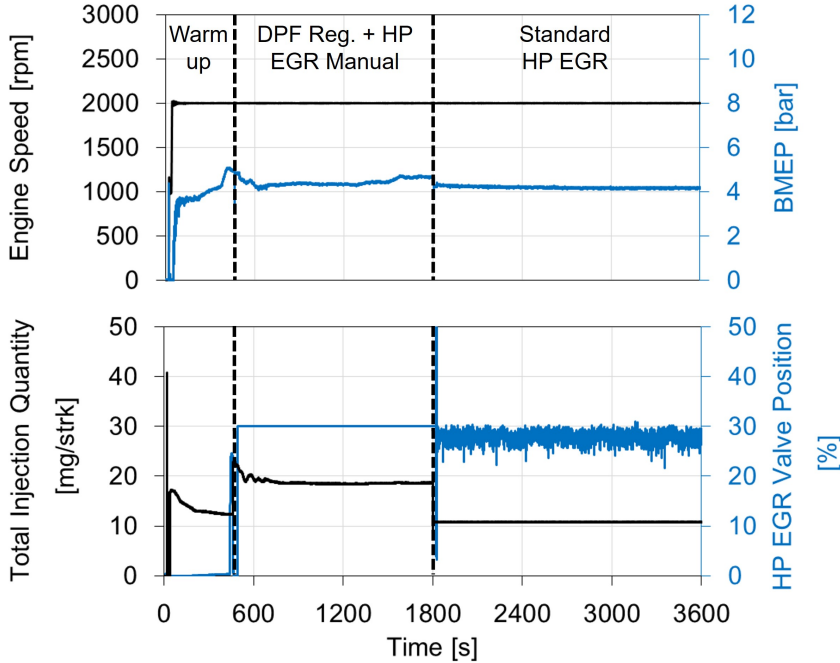


Figure 7.1: Profile of the tests performed

The Original Equipment Manufacturer (OEM) engine calibration is not prepared to perform LP EGR at low ambient temperatures. Under the standard engine calibration, only the HP EGR is enabled after the engine coolant temperature is increased. For this experimental work, the engine has been running during 40 hours at -7°C activating the HP EGR, 20 of them activating the regeneration mode together. Figure 7.1 shows the process to carry out each test. First, the engine warm-up process is performed in standard conditions (without EGR and without regeneration) until the engine coolant temperature reaches 60°C , then, a 20% of HP EGR rate is activated by the ECU and the active regeneration mode is forced manually. A post injection is enabled in this mode with the aim of increasing the exhaust gas temperature and burn the soot particles off bonded on the DPF. This condition is maintained along 30 minutes

and then the regeneration mode is deactivated, returning to the standard engine calibration. To hold fouling conditions in the DPF at the end of each test is the aim of working with the base calibration (only HP EGR performed), this methodology allows to check the DPF regeneration process during the first 30 minutes of the test. This procedure is repeated continuously until reaching a testing time of one hour per test.

To achieve an efficient DPF regeneration process, some relevant variables are followed during the experiments. The post injected fuel quantity and the turbine outlet temperature are verified [11]. These parameters allow to control a key condition to conduct a DPF regeneration process, as the exhaust gas temperature. In order to check the DPF loading process, two reading calibration variables are recorded. First, the pressure difference (ΔP) between the DPF inlet and outlet (measured by a differential pressure sensor), as an indicator of the back pressure generated in the engine exhaust line that could modify the HP EGR rate performed and as a consequence the engine intake temperatures. And second, the particulate filter soot mass estimated by the ECU, as a reference parameter to check the DPF loading conditions. This estimated value is an internal calculation, based on the DPF status and several variables calculated and measured by the ECU, as per example, DPF pressure difference, upstream and downstream temperatures, engine working conditions, DPF diagnosis, etc.

Due to the impossibility to obtain a HP EGR rate estimation from the CO₂ measurement, it was necessary to estimate the engine volumetric efficiency for this engine configuration at 2000 rpm with no EGR and constant load. Following the methodology described in the [Chapter 3](#), a HP EGR rate mathematical estimation is assessed.

Finally, to visualize the impact of performing HP EGR combined with the DPF regeneration at cold conditions (-7°C) on some engine components (i.e. HP EGR valve, HP EGR Rail, WCAC), they were disassembled and cleaned before starting with the experimental work.

7.3 Results and Discussions

To present how the use of the HP EGR combined with the active regeneration mode could affect the engine behavior and its performance under cold operating conditions (-7°C), this section is divided into two different parts. In the first [subsection 7.3.1](#), the impact of this configuration on the engine thermal behavior, DPF regeneration efficiency, pollutant emissions and fuel consumption is presented. In the second [subsection 7.3.2](#), the fouling phenomena evolution inside the EGR line components is presented.

7.3.1 Impact of the HP EGR combined with the regeneration mode on the engine behavior

Performing HP EGR while the DPF is being regenerated leads to a higher temperature in the engine intake line. In order to show the main results of this work in terms of repeatability and dispersion between tests, a group of representative tests is selected. First, a reference test performed at -7°C activating the regeneration mode at the end of the engine warm-up (500 s) and only performing HP EGR in standard engine conditions after the second 1800. Later, a group of five tests using HP EGR with the regeneration mode activated between the second 500 and 1800 and finally, two tests where the DPF reached saturated conditions under similar working conditions. [Figure 7.2](#) shows the engine intake temperature measured in the intake manifold. Comparing the reference test with the tests performing HP EGR together with regeneration mode, it can be observed how the intake temperature increases approximately by 30°C . Thanks to keeping the same WCAC regulation between tests, in the [Figure 7.2](#), it can be observed how the engine intake temperature increases progressively above the reference test due to the HP EGR activation. These higher temperatures could increase the in-cylinder temperature improving the engine combustion efficiency.

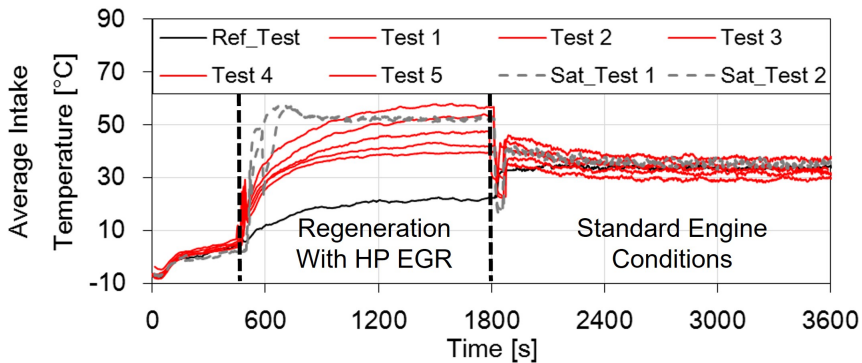


Figure 7.2: Engine intake temperature

[Figure 7.3](#) shows the HP EGR rate estimated through the Eq. 3. The HP EGR rate performed together with the regeneration mode is a similar rate than the used by the ECU in standard engine conditions. The EGR rate remains approximately constant at 20%. However, the saturated tests present an EGR rate higher than 20% due to a possible DPF saturation or soot accumulation in the HP EGR line, which increases the backpressure in the exhaust line.

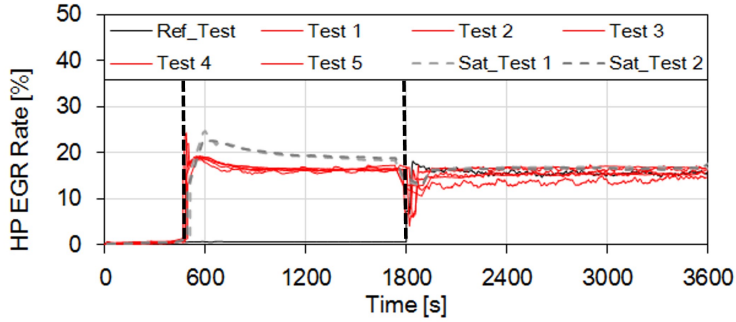


Figure 7.3: HP EGR rate performed

The higher backpressure could lead to variations in the turbocharger speed and pressure ratios. Figure 7.4 presents the VGT position (top of the graph) and the turbocharger speed (bottom of the graph). Due to the low engine operating point selected for this experimental study, there is no evidence of representative variations on the VGT position. Pressure ratios on the turbocharger change with respect to the air mass flow and the HP EGR rate performed. In addition, following the turbocharger speed in the reference test, it can be observed how the higher air mass flow and fuel mass flow under regeneration process lead higher speeds on the turbocharger. Tests with lower air mass flow due to the HP EGR activation present lower speeds.

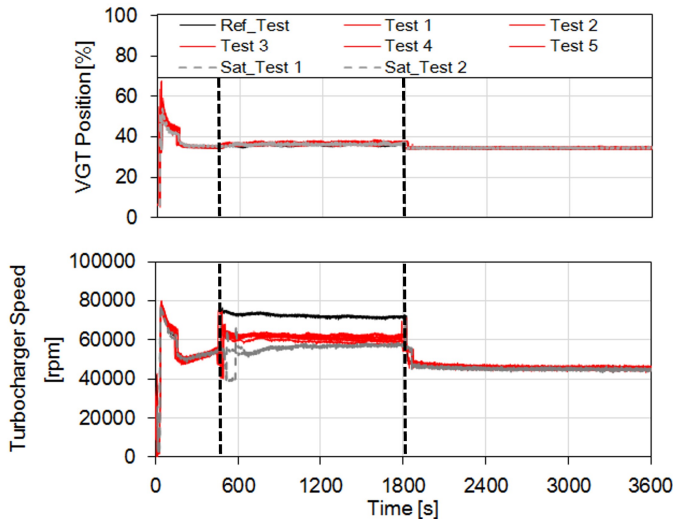


Figure 7.4: Turbocharger behavior

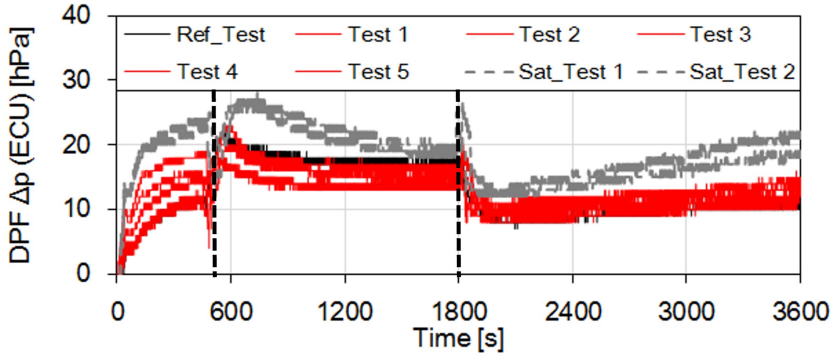


Figure 7.5: DPF difference pressure

7.3.1.1 DPF regeneration analysis

Experimentally, the DPF saturation can be followed through the differential pressure sensor measurement (ΔP ECU) at the filter inlet and outlet and the soot mass estimation performed by the ECU. Figure 7.5 shows the DPF ΔP as a reference to identify if there are clogging conditions on the DPF. It can be observed how performing HP EGR while the DPF is under active regeneration allows to reduce the pressure difference below the reference test, indicating that the regeneration process is efficient. The soot mass variable recorded from the ECU confirmed this statement. Nevertheless, under standard engine calibration (right of the figure), performing HP EGR and operating under cold ambient conditions could produce a DPF saturation condition increasing this ΔP value. It is important to highlight that the exhaust gases carried through the high pressure circuit are not cleaned in the engine after treatment system and could affect the combustion process considerably. For this reason, the EGR rate control, the EGR line temperatures and the engine intake temperature is a key factor to ensure a reliable DPF regeneration process.

Regarding the saturated tests (dashed lines), the higher EGR rate due to a higher-pressure difference, it is evidence of the soot accumulation on the DPF and the consequence of a higher intake temperature. This fact can improve the combustion efficiency under controlled conditions, but out of control, it could affect the thermal efficiency of the components (i.e. EGR valve and EGR cooler), thus affecting their normal operation.

In addition to the abovementioned ECU variables, other important variable that allows to follow the regeneration process efficiency is the DPF inlet temperature [72]. Figure 7.6 shows that, even activating the HP EGR together with the regeneration mode, the DPF inlet temperature remains constant around 470°C for this engine configuration. This high temperature allows to clean the soot

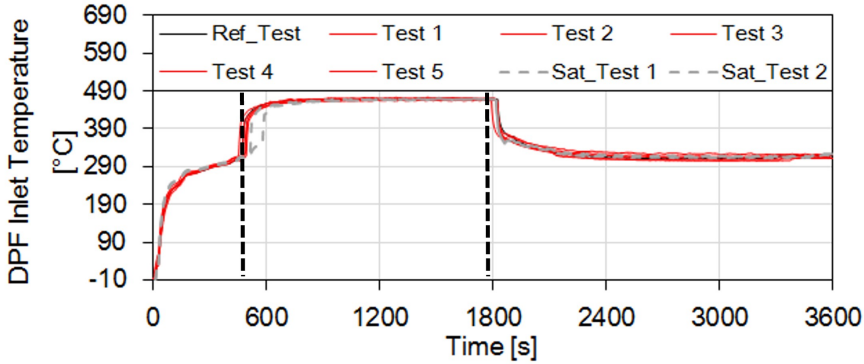


Figure 7.6: DPF inlet temperature

particles accumulated in the DPF and to keep an optimal operation condition for the diesel oxidation catalyst.

Although these variables provide experimental information about the DPF status, it is possible to perform a mathematical analysis in order to sustain these results. Fig. 8 shows the pressure drop dimensionless coefficient (α) calculated as a theoretical indicator of the flow resistance through the DPF. This coefficient is estimated as a function of the delta pressure (ΔP) and the volumetric flow rate through the DPF, as is shown in the Equation 7.1.

$$\Delta P = \alpha \frac{1}{2} \rho v^2 \quad (7.1)$$

The gas density (ρ) is calculated as a function of the pressure and temperature (P, T) at the inlet of the DPF and the gas velocity (v) is calculated as a function of the exhaust gasses mass flow, the gas density and the section area of the filter. Taking this into account, an increase in the pressure drop dimensionless coefficient indicates a higher flow resistance through the DPF (saturation) and a decrease in the coefficient indicates a lower flow resistance (cleaning). In Figure 7.7, it can be evidenced how, under standard engine calibration (right of the figure), the DPF is saturated due to the HP EGR activation at cold ambient conditions. On the other hand, the regeneration process in combination with the HP EGR activation (left of the figure) presents a slight tendency to decrease, indicating that exists a reduction in the amount of soot clogged on the filter, as could be observed experimentally.

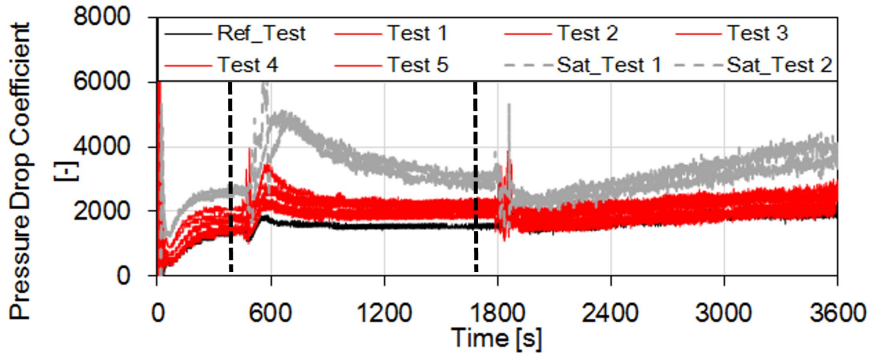


Figure 7.7: Pressure drop dimensionless coefficient

7.3.1.2 Pollutant emissions

Measured values of NO_x, HC and CO emissions collected upstream the after-treatment system are presented in [Figure 7.8](#). The aim of performing EGR is to obtain a significant NO_x emissions reduction under cold operating conditions. Nevertheless, one disadvantage of this strategy is the combustion degradation, increasing the unburned HCs and PMs. The top graph of [Figure 7.8](#) shows the measured values of NO_x emissions. With the standard calibration at cold conditions, the engine is prepared to perform HP EGR and keep a NO_x values of approximately 2.5 g/kWh. During the DPF regeneration mode in combination with the HP EGR this value is reduced to approximately 1.25 g/kWh. This value represents a reduction of 50%. In terms of HC emissions, a significant increase is observed compared to the standard calibration due to the additional post injected fuel used during the DPF regeneration. However, comparing the DPF regeneration with and without HP EGR, it could be observed that the proposed configuration could help to reduce this issue thanks to a small reduction in the post injected fuel and the higher intake temperatures reached.

Finally, activating the HP EGR during a regeneration process, keeping an appropriate main injection advance, and thanks to the higher intake temperature reached with this proposed configuration, the CO emissions could be reduced significantly, as it can be observed by comparing the use of the HP EGR or not. It is possible to estimate an approximate reduction of about 60%. This reduction allows to reach close values to the values performed under the standard engine calibration, besides, the aftertreatment system could also reduce significantly these values.

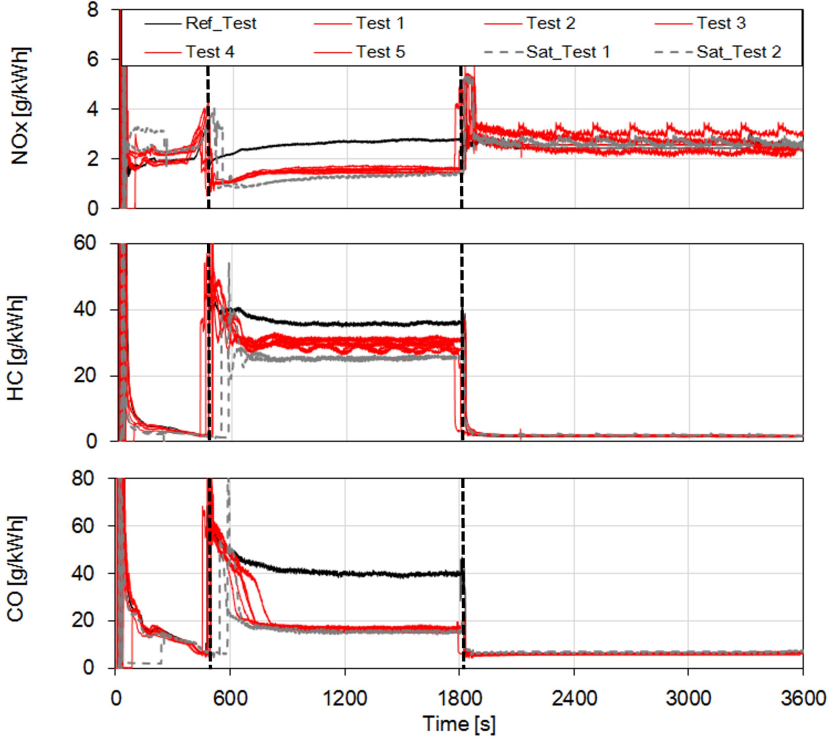


Figure 7.8: Raw pollutant emissions measurements

7.3.1.3 Combustion efficiency and fuel consumption

Equation 7.2 shows the combustion efficiency and the brake specific fuel consumption (BSFC) for the different tests. The combustion efficiency estimates the quantity of fuel burned during the combustion process and it is calculated by means of the engine-out emissions measurements, as is shown in the Equation 7.2.

$$\eta_{Comb} = 1 - \frac{\dot{m}_{HC}(\dot{m}_{air} + \dot{m}_{fuel})}{\dot{m}_{fuel}} - \frac{\dot{m}_{CO}(\dot{m}_{air} + \dot{m}_{fuel})}{4\dot{m}_{fuel}} \quad (7.2)$$

As mentioned above, operating at very low ambient temperatures cause instabilities and degradations in the combustion process. In Equation 7.2, it can be observed how the combustion efficiency increases progressively with the engine warm-up until the 500 s approximately. Performing a DPF regeneration could affect the combustion process due to the additional fuel injected when the post injection is activated. For this reason, it can be observed how the reference test without EGR presents the lower efficiency. Activating the HP

EGR together with the regeneration mode results in a slight improvement of the combustion efficiency. This improvement is due to a higher intake temperature and a quite reduction in the post injected fuel during the regeneration mode. Therefore, the consequent higher in-cylinder temperature promotes a better combustion process. In addition, the observed reduction in the brake specific fuel consumption is coherent with this behavior.

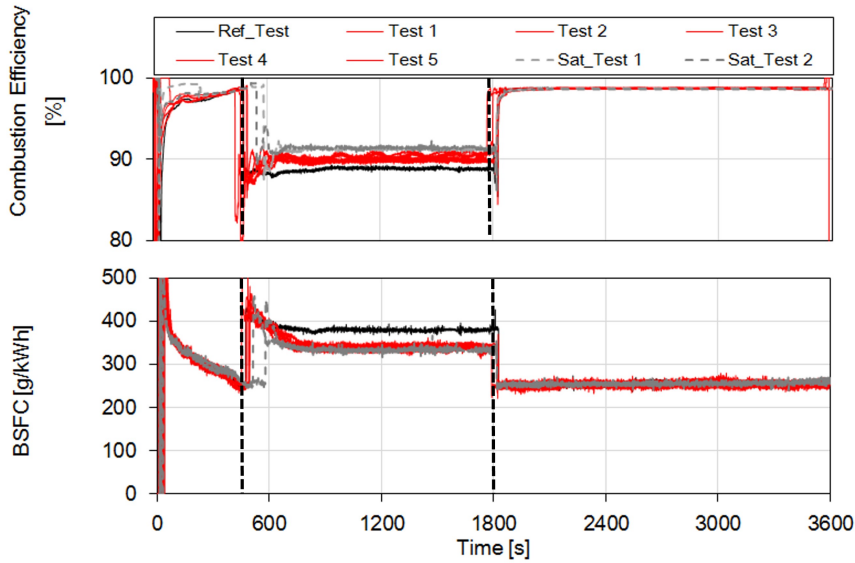


Figure 7.9: Combustion efficiency and BSFC

Working with the standard engine calibration, both, combustion efficiency and BSFC present optimal values, considering that this operation is at low ambient temperature (-7°C).

7.3.2 Impact of the HP EGR combined with the regeneration mode on the engine components

The second goal of this experimental study is to perform a brief analysis of a known event presented when an IC engine is operating with exhaust gas recirculation (EGR) at very low ambient temperatures. These are the fouling deposits, which could affect the EGR systems due to unburned HC and PM depositions on its main components (i.e. EGR valve and EGR cooler).

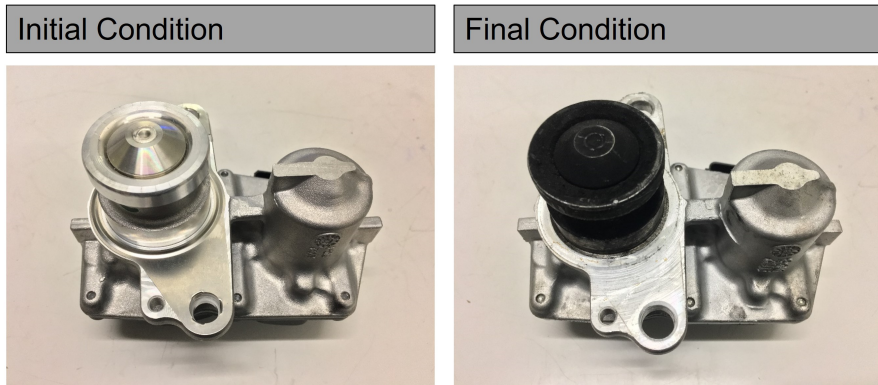


Figure 7.10: Fouling observed on the HP EGR valve

After 40 hours performing HP EGR at cold conditions, 20 of them with active DPF regeneration, fouling depositions on the HP EGR line components are observed. Figure 7.10 and Figure 7.11 shows an images of the initial and final conditions of the HP EGR valve and a section of the HP EGR rail of the circuit. It can be observed a black soot on the actuator surface comparing the reference (initial condition) with the final condition. This is a typical soot as found in EGR circuits of IC engines, with similar features, like matte black color, carbon texture and rough surface.

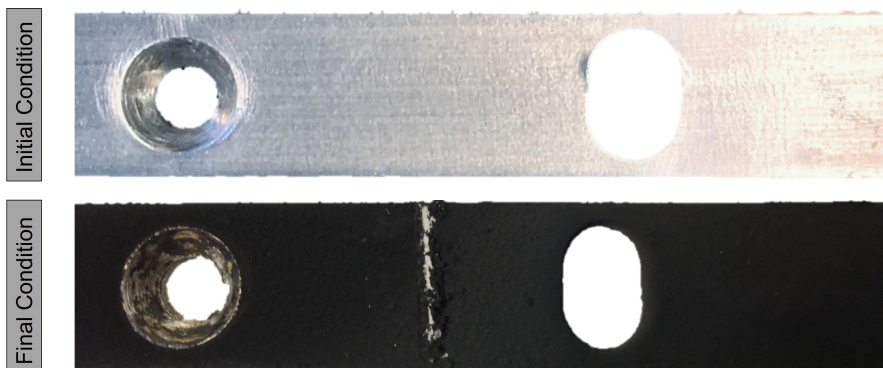


Figure 7.11: Fouling observed on the section of the HP EGR rail

In order to obtain a quantitative estimation of the amount of soot produced during this experimental campaign, the layer of soot observed on the surface of the elements is considered as a geometrical area with the same shape of the element. For example, the EGR valve actuator observed in Figure 7.10 is considered as a tube with cover. Then, the soot volume is estimated by measuring the thickness of the soot layer. This estimation is performed with

the aim of obtaining and order of magnitude represented in a numerical value of the soot produced after this experimental campaign. On the other hand, in order to know the mass of soot, approximately 50% of the soot particles has been removed and collected from the HP EGR components (i.e. EGR valve, ducts, rail and intake manifold), the particles collected from each element are weighted in a precision scale and multiplied by two in order to obtain an estimation of the 100% of the mass.

Approximately, the deposition of 30 cm^3 of soot, equivalent to a 6 gr of soot mass, has been estimated after 40 hours performing HP EGR and DPF regeneration at cold conditions. This calculated value can be considered as an acceptable amount of soot produced when exhaust gas recirculation is used. Typical saturation values in diesel engines to conduct DPF regeneration are close to 20 gr of soot.

7.4 Summary

This chapter presented the impact of using the high-pressure exhaust gas recirculation strategy while the diesel particulate filter is under active regeneration mode. This strategy is evaluated under 40 hours of operation, 20 of them using the two systems in combination.

The results are summarized in the next points:

- The activation of the high-pressure exhaust gas recirculation during the particulate filter regeneration process leads to a 50% NO_x emissions reduction with respect to a reference case without exhaust gas recirculation. Moreover, the modification of some engine parameters compared to the base calibration, as the exhaust gas recirculation rate, the main fuel injection timing and the post injection quantity, allows to optimize this strategy by reducing the CO emissions up to 60%. Regarding the HC emissions and fuel consumption, a small advantage could be observed using this strategy.
- The activation of the high-pressure exhaust gas recirculation at low temperatures can produce fouling deposits and condensation on the engine components (valve, cooler, intake manifold, etc.) and can contribute to reach saturation conditions on the DPF. For these reasons, the regeneration efficiency is followed during the experiments through the filter status, concluding that the use of low high-pressure exhaust gas recirculation rates, beyond 20%, in combination with the regeneration mode also allows to clean the soot particles of the particulate filter.
- The soot depositions are visualized and presented at the end of the work with a brief analysis of the soot characteristics and a quantitative estimation of the total soot volume produced during the experimental campaign. A fouling quantity of $30cm^3$ and $6gr$ was estimated, observing that the principal components where soot is deposited were the HP EGR rail and the engine intake manifold.

7.5 References

- [72] J. R. Serrano, P. Piqueras, J. de la Morena, and E. J. Sanchis. “Late Fuel Post-Injection Influence on the Dynamics and Efficiency of Wall-Flow Particulate Filters Regeneration”. In: *Applied Sciences* 9.24 (2019), p. 5348 (cit. on p. 95).

CHAPTER 8

Conclusions and Future Works

8.1 Introduction

DURING this research work, a scientific contribution has been done for the improvement of the Internal Combustion Engine (ICE) considering its operation at very low ambient temperatures (-7°C). The strategies employed throughout the document are based on:

- High-pressure EGR
- Low-pressure EGR
- Cylinder Deactivation
- DPF Regeneration

In the first part, a simple mathematical model able to predict whether or not there is condensation inside the High-pressure EGR line is presented. The second part presents a new prototype of the Low-pressure EGR line fitted with a bypass system. The third part is focused on a new configuration of the cylinder deactivation strategy called EGR DEACT. The last part evaluates the impacts of introducing high-pressure EGR while the DPF is under active regeneration in the ICE.

8.2 Main contributions

The main contributions of the different experimental strategies evaluated and implemented along this scientific work are presented hereunder:

8.2.1 Condensation Model

A simple model to predict condensation conditions in EGR flow and in the duct walls of the high-pressure EGR line has been developed and validated experimentally. The model predicts in which states the condensation conditions may appear or disappear. Besides, an experimental measurement technique has been developed to check the condensation.

The condensation conditions depend on the engine working conditions (air to fuel ratio, EGR rate. . .), ambient humidity and local conditions of temperature and pressure at the point where this condensation phenomena is analyzed. For this work, two different positions for the EGR thermocouples were used, one at the center of the EGR rail ports (gas side) and a second position, close to the EGR rail wall (wall side). The main conclusion of this work is that a simple model, as the model described in the [chapter 4](#), can be used to easily predict at different points of the EGR line, the mist conditions in gases and also the drops attached to the walls in the ducts.

This research work could be used to establish strategies to avoid or cause the appearance of the condensation in EGR circuits of IC engines. The model is enough simple to be used combined with control strategies to avoid or cause these condensation conditions in the gas side and in the duct walls. This is very interesting from the point of view of the new approval emissions regulations that will require more aggressive EGR strategies at low temperatures where condensation could appear.

It could be stated that for this particular working conditions (for an engine warm-up at -7°C , a symmetric rail to distribute the EGR and measuring temperatures at the HP-EGR outlet), the condensation conditions in the gas side are present until the gas temperature reaches 50°C at cylinders 1 and 4 and 60°C at cylinders 2 and 3. In our particular test, the EGR flow reaches these conditions in the second 300 approximately. In the wall side case, the condensation conditions are present until the wall temperature reaches values around 40°C at cylinders 1 and 4, and 30°C at cylinders 2 and 3. The walls reach these conditions in the second 800 approximately. Once these conditions have been reached, the relative humidity is below one and the dew point, which is a parameter that depends on pressure and humidity, indicates that no condensation phenomenon occurs in these parts of the EGR line.

8.2.2 LP-EGR Bypass

The advantages and impacts of using a new concept of a Low-pressure EGR line fitted with a cooler bypass during engine cold operating conditions have been studied and analyzed. The impact in pollutant emissions, fuel consumption and engine warm-up process are presented. Besides, a chemical analysis to identify HC species due to condensation and fouling depositions has been performed.

The main objective of performing Low-pressure EGR at cold conditions is to reduce NO_x emissions thanks to the oxygen concentration reduction of the working fluid in the combustion chamber. In this work, a noticeable NO_x emissions reduction of approximately 60% with respect to a reference case without Low-pressure EGR has been achieved. On the other hand, one disadvantage of this strategy is an increment in CO and HC emissions during the first part of the warmup process, due to the combustion degradation. However, the reduction in the warm-up process period, when EGR is performed, could compensate that negative effect and produce a neutral effect in the accumulated values of these pollutant emissions, at the end of the cycle.

The purpose of the bypass implementation is to reach higher temperatures at the engine intake in order to accelerate the warm-up process (from the cold start until optimal working temperature). Activating the bypass system the engine intake temperature has been increased 30°C, leading a CO emissions reduction of approximately 12%, if it is compared this case with bypass with the case where the bypass is deactivated and the exhaust gas passes through the EGR cooler. Although it is possible to reduce CO emissions by using the bypass strategy, comparing to the reference test, similar values has been reached in both cases. Taking the coolant temperature as a reference of the engine warm-up process, a reduction in time of approximately 60 seconds with the bypass activated and 100 seconds with the bypass deactivated have been achieved.

An additional parameter to take into account in this experimental work is the fuel consumption and the combustion efficiency. Any significant benefit or disadvantage could be observed in terms of fuel consumption. However, analyzing the combustion efficiency it was identified that the bypass strategy could improve the combustion temperature once the warm-up process has finished.

The second aim of this research work is the analysis and visualization of condensation and fouling phenomena produced by the Low-pressure EGR activation at cold conditions. It could be stated for this particular work (for an engine warm-up at -7°C, activating the LP EGR from the engine cold start and using a bypass system for the LP EGR cooler) that the period where condensation is produced, that is, when the relative humidity is above one, could be reduced by activating the bypass in approximately 250 seconds. In addition, using the endoscope cameras was possible to observe how the fouling deposits increased

after each test. These deposits have been analyzed chemically concluding that the main species produced in these experiments were aliphatic hydrocarbons, especially C1 – C2 aldehydes (formaldehyde and acetaldehyde). These species in reaction with acids and other HCs could produce sticky soot as the reported in other research works contributing to blocking EGR valve.

8.2.3 Cylinder Deactivation

The main advantages and disadvantages of implementing a new method of the cylinder deactivation strategy, called EGR DEACT, in a diesel engine working at very low ambient temperature (20°C and -7°C) have been studied and analyzed. The impacts in pollutant emissions, pumping losses and engine warm-up process were presented.

From the experimental study performed at 20°C, the main conclusions are related with the engine performance:

- The EGR DEACT engine behavior (2 cylinders) could be improved by optimizing the injection settings in the ECU (e.g. total injected fuel, injection time, etc.), in order to reproduce same conditions than the standard engine (4 cylinders).
- In order to reproduce the same turbocharger conditions, the VGT can be closed between 30% and 50%, increasing the turbocharger speed to the turbocharger standard conditions, but also increasing the A/F ratio.
- In order to reduce A/F ratio and reproduce similar EGR rates, the Low-pressure EGR valve can be opened to higher values, but it does not increase the EGR ratios in the cylinders 1 and 4 (there is not enough delta pressure between exhaust and intake lines to increase EGR rate). Maximum values of LP EGR rates in cylinders 1 and 4 are close to 10%, which is lower than with the standard engine case (50%). However, closing the exhaust throttle valve it can be possible to obtain an additional delta pressure and increase the EGR rate ratio to 20% reducing at the same time the NO_x emissions levels.
- The pumping losses is another important parameter to take into account when the EGR DEACT strategy is activated. Using this particular engine configuration (not “tailor made” EGR routing), it is necessary to find a trade-off between the mass flow recirculated in the deactivated cylinders and the maximum torque delivered by the engine in order to reduce the negative impact produced by the pumping work. A fully adapted EGR routing layout combined with a simpler ON/OFF actuator should solve this issue.

- The EGR DEACT engine configuration (2 cylinders) in transient conditions (engine start) allow to advance the DOC light-off period in 250 seconds approximately compared with the standard engine configuration (4 cylinders).

The main findings of this work, taking the previous study as a reference and evaluating the engine performance working at cold conditions (-7°C), are the noticeable increment in the exhaust gas temperature at the after-treatment inlet in approximately 100°C , reducing the activation period of the device and reducing the engine warm-up process significantly. The CO and HC emissions reduction of 70% and 50% respectively is another important benefit using this engine configuration. Regarding the NO_x emissions, they remain more or less constant in comparison with the reference test at -7°C , nevertheless, a NO_x after-treatment device could reduce these emissions levels.

8.2.4 DPF Regeneration

The advantages, disadvantages and impacts of performing High-pressure EGR together with the DPF regeneration mode during engine cold operating conditions have been studied. The impact in regeneration efficiency, pollutant emissions and fuel consumption were presented. Besides, a brief analysis of the impact of fouling depositions on the engine components have been performed.

The main objective of performing High-pressure EGR at cold conditions (-7°C) is to reduce the NO_x emissions thanks to the oxygen concentration reduction of the working fluid in the combustion chamber. In this work, a noticeable NO_x emissions reduction of approximately 50% with respect to a reference case without High-pressure EGR during a DPF regeneration process has been achieved. Regarding HC and CO emissions, another advantages were found with this proposed configuration. A significant CO emissions reduction of 60% was achieved performing High-pressure EGR and fixing a main injection advance of -10° CAD. In terms of HC emissions, a reduction of 15% was observed due to the improvements in combustion efficiency and fuel consumption. Besides, the after treatment system could also reduce significantly these values. During the DPF regeneration, the additional fuel injected in the post injection affected the combustion efficiency due to the late combustion of this fuel during the exhaust stroke. A quite benefit could be observed due to a slight improvement in the combustion temperature when the High-pressure EGR is activated.

On the other hand, performing High-pressure EGR without the regeneration mode at cold conditions could contribute to the DPF saturation and degradation, the accumulation of soot increases the pressure difference in the DPF and as a consequence an increment in the EGR rate performed and in the EGR temperatures was registered.

In order to avoid the previous conclusion, the regeneration efficiency was evaluated through the DPF pressure difference, the soot mass estimated by the ECU, the High-pressure EGR rate and the flow resistance through the DPF. It was found that the activation of only the HP EGR at cold conditions with EGR rates beyond 20% contributed to increase the soot depositions and to saturate the DPF early. By this reason, if the purpose is to activate the High-pressure EGR to reduce NO_x emissions, the EGR rate and the intake temperatures must be controlled and limited. The Low-pressure EGR could be presented as another option to decrease this impact. However, performing a low HP EGR rate in combination with the regeneration mode could reduce the post injected fuel and the exhaust gas temperature, but anyway continue keeping the regeneration efficiency in acceptable values. This was confirmed verifying the DPF status through the ECU variables (DPF deltaP and soot estimation) and the pressure drop dimensionless coefficient estimated. It allowed to obtain the noticeable NO_x emission reduction abovementioned.

The second aim of this research work is the analysis and visualization of fouling phenomena produced by the High-pressure EGR activation at cold conditions. After 40 hours of tests, soot particles were found on the High-pressure EGR line of the engine. These particles match with typical fouling observed in IC engines. A fouling quantity of $30cm^3$ and 6 gr was estimated, observing that the principal components where soot is deposited were the HP EGR rail and the engine intake manifold.

8.3 Future works

The internal combustion engine continue taking precedence in the automotive industry and is still presented as the more utilized powertrain for the current means of transportation. By this reason, all the improvements and research works performed on these systems, will contribute to the continue development of more efficient and less contaminatives engines. The exhaust gas recirculation (EGR), the cylinder deactivation and new techniques as the water injection combustion, can demonstrate that the IC engine is able to fulfill with the current and future enviromental regulations and can be presented as a good alternative solution inside the transition process of vehicles electrification.

Experimental future works

- Experimental evaluation of switching strategies of the bypass system, closing and opening the valve during the engine warm-up process with the aim of finding a trade-off between time reduction and pollutant emissions reduction.
- Perform a more agressive cylinder deactivation campaing, testing the new engine calibration and the EGR DEACT configuration with the aim of checking the repeatability of the tests and finding an optimal engine calibration for these particular conditions.
- Experimental evaluation of the different strategies at lower ambient temperatures (-10°C) and maybe considering high altitudes in operation.

Theoretical future works

- Improvement of the condensation model considering real combustion efficiencies and condensation coming from the chemical reactions of the gases inside the engine components. The experimental validation on the Low-pressure EGR line will complete this work.
- Perform Computational Fluid Dynamics (CFD) simulations of the new Low-pressure EGR line fitted with the bypass, with the aim of understand the fluid behavior inside the prototype and its experimental validation.

Bibliography

- [1] **Luján, J. M., Dolz, V., Monsalve, J., and Bernal, M. A.**
“High-pressure exhaust gas recirculation line condensation model of an internal combustion diesel engine operating at cold conditions”
in: *International Journal of Engine Research* 22.2 (2021), pp. 407–416
(cit. on p. vii)
- [2] **Galindo, J., Dolz, V., Monsalve, J., Bernal, M. A., and Odillard, L.**
“Advantages of using a cooler bypass in the low-pressure exhaust gas recirculation line of a compression ignition diesel engine operating at cold conditions”
in: *International Journal of Engine Research* 22.5 (2020), pp. 1624–1635
(cit. on p. vii)
- [3] **Galindo, J., Dolz, V., Monsalve, J., Bernal, M. A., and Odillard, L.**
“EGR cylinder deactivation strategy to accelerate the warm-up and restart processes in a Diesel engine operating at cold conditions”
in: *International Journal of Engine Research* 23.4 (2022), pp. 614–623
(cit. on p. vii)
- [4] **Galindo, J., Dolz, V., Monsalve, J., Bernal, M. A., and Odillard, L.**
“Impacts of the exhaust gas recirculation (EGR) combined with the regeneration mode in a compression ignition diesel engine operating at cold conditions”
in: *International Journal of Engine Research* 22.12 (2021), pp. 3548–3557
(cit. on p. vii)
- [5] **Galindo, J., Dolz, V., Monsalve, J., Bernal, M. A., and Odillard, L.**
“Exhaust gas recirculation combined with regeneration mode in a compression ignition diesel engine operating at cold conditions”
in: *THIESEL 2020. Thermo-and Fluid Dynamic Processes in Direct Injection Engines. 8th-11th September*. Valencia, Spain 2021, pp. 359–369
(cit. on p. vii)

- [6] **Michigan Michigan Engineering, U. of**
Video: 100% renewable diesel cars can reduce carbon emissions while waiting for electric vehicles
2021. URL: <https://news.engin.umich.edu/2021/09/100-renewable-diesel-cars-can-reduce-carbon-emissions-while-waiting-for-electric-vehicles/>
(cit. on p. 2)
- [7] **Yang, Z., Liu, Y., Wu, L., Martinet, S., Zhang, Y., Andre, M., and Mao, H.**
“Real-world gaseous emission characteristics of Euro 6b light-duty gasoline- and diesel-fueled vehicles”
in: *Transportation Research Part D: Transport and Environment* 78.– (2020), p. 102215
(cit. on p. 8)
- [8] **Hooftman, N., Messagie, M., Van Mierlo, J., and Coosemans, T.**
“A review of the European passenger car regulations – Real driving emissions vs local air quality”
in: *Renewable and Sustainable Energy Reviews* 86.– (2018), pp. 1–21
(cit. on p. 8)
- [9] **Luján, J. M., Pla, B., Bares, P., and Pandey, V.**
“Adaptive calibration of Diesel engine injection for minimising fuel consumption with constrained NOx emissions in actual driving missions”
in: *International Journal of Engine Research* 22.6 (2021), pp. 1896–1905
(cit. on p. 8)
- [10] **A, C.-A., J, H., J, R.-F., M, L., A, R., and J, B.**
“Effect of advanced biofuels on WLTC emissions of a Euro 6 diesel vehicle with SCR under different climatic conditions”
in: *International Journal of Engine Research* 22.12 (2021), pp. 3433–3446
(cit. on p. 8)
- [11] **Parliament, E. U.**
REGULATION (EU) 2019/631 OF THE EUROPEAN PARLIAMENT AND OF THE COUNCIL
2019. URL: <https://eur-lex.europa.eu/legal-content/EN/TXT/?uri=CELEX%3A32019R0631&qid=1666123169654>
(cit. on p. 8)
- [12] **Luján, J. M., Climent, H., Ruiz, S., and Moratal, A.**
“Pollutant emissions and diesel oxidation catalyst performance at low ambient temperatures in transient load conditions”
in: *Applied Thermal Engineering* 129.– (2018), pp. 1527–1537
(cit. on p. 8)

- [13] **Arnau, F. J., Martín, J., Piqueras, P., and Auñón, Ángel**
“Effect of the exhaust thermal insulation on the engine efficiency and the exhaust temperature under transient conditions”
in: *International Journal of Engine Research* 22.9 (2021), pp. 2869–2883
(cit. on p. 8)
- [14] **Galindo, J., Navarro, R., Tarí, D., and Moya, F.**
“Development of an experimental test bench and a psychrometric model for assessing condensation on a low-pressure exhaust gas recirculation cooler”
in: *International Journal of Engine Research* 22.5 (2021), pp. 1540–1550
(cit. on p. 8, 13)
- [15] **Torregrosa, A. J., Broatch, A., Olmeda, P., and Romero, C.**
“Assessment of the Influence of Different Cooling System Configurations on Engine Warm-up, Emissions and Fuel Consumption”
in: *International Journal of Automotive Technology* 9.4 (2008), pp. 447–458
(cit. on p. 8)
- [16] **Millo, F., Giacominetto, P. F., and Bernardi, M. G.**
“Analysis of different exhaust gas recirculation architectures for passenger car Diesel engines”
in: *Applied Energy* 98.– (2012), pp. 79–91
(cit. on p. 8)
- [17] **Thangaraja, J. and Kannan, C.**
“Effect of exhaust gas recirculation on advanced diesel combustion and alternate fuels - A review”
in: *Applied Energy* 180.– (2016), pp. 169–184
(cit. on p. 8)
- [18] **Desantes, J. M., Luján, J. M., Pla, B., and Soler, J. A.**
“On the combination of high-pressure and low-pressure exhaust gas recirculation loops for improved fuel economy and reduced emissions in high-speed direct-injection engines”
in: *International Journal of Engine Research* 14.1 (2013), pp. 3–11
(cit. on p. 9)
- [19] **Luján, J. M., Guardiola, C., Pla, B., and Reig, A.**
“Switching strategy between HP (high pressure)- and LPEGR (low pressure exhaust gas recirculation) systems for reduced fuel consumption and emissions”
in: *Energy* 90.– (2015), pp. 1790–1798
(cit. on p. 9)
- [20] **Park, Y. and Bae, C.**
“Experimental study on the effects of high/low pressure EGR proportion in a passenger car diesel engine”
in: *Applied Energy* 133.– (2015), pp. 308–316
(cit. on p. 9)

- [21] **Moroz, S., Bourgoïn, G., Luján, J. M., and Pla, B.**
“Acidic Condensation in Low Pressure EGR Systems using Diesel and Biodiesel Fuels”
in: *SAE International Journal of Fuels and Lubricants* 2.2 (2010), pp. 305–312
(cit. on pp. 9, 11)
- [22] **Chalgren, R. D., Parker, G. G., Arici, O., and Johnson, J. H.**
“A Controlled EGR Cooling System for Heavy Duty Diesel Applications Using the Vehicle Engine Cooling System Simulation”
in: *SAE Technical Paper 2002-01-0076*. United States 2002, p. 28
(cit. on p. 9)
- [23] **Magand, S., Watel, E., Castagné, M., Soleri, D., Grondin, O., Devismes, S., and Moroz, S.**
“Optimization of a Low NO_x Emission HCCI Diesel Prototype Vehicle”
in: *Proceedings of the THIESEL Congress 2008*. Valencia, Spain 2008, pp. –
(cit. on p. 9)
- [24] **Yu, X., Yu, S., and Zheng, M.**
“Hydrocarbon impact on NO to NO₂ conversion in a compression ignition engine under low-temperature combustion”
in: *International Journal of Engine Research* 20.2 (2019), pp. 216–225
(cit. on p. 9)
- [25] **Furukawa, N., Goto, S., and Sunaoka, M.**
“On the mechanism of exhaust gas recirculation valve sticking in diesel engines”
in: *International Journal of Engine Research* 15.1 (2014), pp. 78–86
(cit. on pp. 9, 11)
- [26] **Boldaji, M. R., Sofianopoulos, A., Mamalis, S., and Lawler, B.**
“Computational fluid dynamics investigations of the effect of water injection timing on thermal stratification and heat release in thermally stratified compression ignition combustion”
in: *International Journal of Engine Research* 20.5 (2019), pp. 555–569
(cit. on p. 9)
- [27] **Vaudrey, A.**
“Thermodynamics of indirect water injection in internal combustion engines: Analysis of the fresh mixture cooling effect”
in: *International Journal of Engine Research* 20.5 (2019), pp. 527–539
(cit. on p. 9)
- [28] **Tsuruta, T. and Nagayama, G.**
“A microscopic formulation of condensation coefficient and interface transport phenomena”
in: *Energy* 30.6 (2005), pp. 795–805
(cit. on p. 9)

- [29] **Tauzia, X., Maiboom, A., Karaky, H., and Chesse, P.**
“Experimental analysis of the influence of coolant and oil temperature on combustion and emissions in an automotive diesel engine”
in: *International Journal of Engine Research* 20.2 (2019), pp. 247–260
(cit. on p. 9)
- [30] **Serrano, J. R., Piqueras, P., Angiolini, E., Meano, C., and Morena, J. D. L.**
“On Cooler and Mixing Condensation Phenomena in the Long-Route Exhaust Gas Recirculation Line”
in: *SAE Technical Paper 2015-24-2521*. United States 2002, p. 15
(cit. on pp. 9, 10)
- [31] **Serrano, J., Piqueras, P., Navarro, R., Tarí, D., and Meano, C.**
“Development and verification of an in-flow water condensation model for 3D-CFD simulations of humid air streams mixing”
in: *Computers Fluids* 167 (2018), pp. 158–165
(cit. on p. 9)
- [32] **Yang, B.-J., Mao, S., Altin, O., Feng, Z.-G., and Michaelides, E. E.**
“Condensation Analysis of Exhaust Gas Recirculation System for Heavy-Duty Trucks”
in: *ASME. J. Thermal Sci. Eng. Appl.* 3.4 (2011), p. 9
(cit. on p. 10)
- [33] **Warey, A., Balestrino, S., Szymkowicz, P., and Malayeri, M.**
“A One-Dimensional Model for Particulate Deposition and Hydrocarbon Condensation in Exhaust Gas Recirculation Coolers”
in: *Aerosol Science and Technology* 46.2 (2012), pp. 198–213
(cit. on p. 10)
- [34] **Warey, A., Long, D., Balestrino, S., Szymkowicz, P., and Bika, A. S.**
“Visualization and Analysis of Condensation in Exhaust Gas Recirculation Coolers”
in: *SAE Technical Paper 2013-01-0540*. United States 2013, p. 12
(cit. on p. 10)
- [35] **Bravo, Y., Lázaro, J. L., and García-Bernad, J. L.**
“Study of Fouling Phenomena on EGR Coolers due to Soot Deposits. Development of a Representative Test Method”
in: *SAE Technical Paper 2005-01-1143*. United States 2005, p. 8
(cit. on p. 10)
- [36] **Arnal, C., Bravo, Y., Larrosa, C., Gargiulo, V., Alfè, M., Ciajolo, A., Alzuet, M. U., Millera, Ángela, and Bilbao, R.**
“Characterization of Different Types of Diesel (EGR Cooler) Soot Samples”
in: *SAE Technical Paper 2015-01-1690*. United States 2015, p. 11
(cit. on pp. 10, 14, 68)

- [37] **Warey, A., Bika, A. S., Long, D., Balestrino, S., and Szymkowicz, P.**
“Influence of water vapor condensation on exhaust gas recirculation cooler fouling”
in: *International Journal of Heat and Mass Transfer* 65 (2013), pp. 807–816 (cit. on pp. 10, 11)
- [38] **Qiu, L., Reitz, R., Eagle, E., and Musculus, M.**
“Investigation of Fuel Condensation Processes under Non-reacting Conditions in an Optically-Accessible Engine”
in: *SAE Technical Paper 2019-01-0197*. United States 2019, p. 12 (cit. on p. 10)
- [39] **Bermúdez, V., Lujan, J. M., Pla, B., and Linares, W. G.**
“Effects of low pressure exhaust gas recirculation on regulated and unregulated gaseous emissions during NEDC in a light-duty diesel engine”
in: *Energy* 36.9 (2011), pp. 5655–5665 (cit. on p. 10)
- [40] **Lance, M. J., Mills, Z. G., Seylar, J. C., Storey, J. M., and Sluder, C. S.**
“The effect of engine operating conditions on exhaust gas recirculation cooler fouling”
in: *International Journal of Heat and Mass Transfer* 126 (2018), pp. 509–520 (cit. on p. 11)
- [41] **Lapuerta, M., Ramos, Ángel, Fernández, D., and González, I.**
“High-pressure versus low-pressure exhaust gas recirculation in a Euro 6 diesel engine with lean-NO_x trap: Effectiveness to reduce NO_x emissions”
in: *International Journal of Engine Research* 20.1 (2019), pp. 155–163 (cit. on p. 11)
- [42] **Dimitriou, P., Turner, J., Burke, R., and Copeland, C.**
“The benefits of a mid-route exhaust gas recirculation system for two-stage boosted engines”
in: *International Journal of Engine Research* 19.5 (2018), pp. 553–569 (cit. on p. 11)
- [43] **Vos, K. R., Shaver, G. M., Ramesh, A. K., and Jr., J. M.**
“Impact of Cylinder Deactivation and Cylinder Cutout via Flexible Valve Actuation on Fuel Efficient Aftertreatment Thermal Management at Curb Idle”
in: *Frontiers in Mechanical Engineering* 5.52 (2019), pp. 1–18 (cit. on p. 12)
- [44] **Arnau, F. J., Martín, J., Pla, B., and Auñón, Ángel**
“Diesel engine optimization and exhaust thermal management by means of variable valve train strategies”

- in: *International Journal of Engine Research* 22.4 (2020), pp. 1196–1213
(cit. on p. 12)
- [45] **Vos, K. R., Shaver, G. M., Joshi, M. C., Ramesh, A. K., and Jr., J. M.**
“Strategies for using valvetrain flexibility instead of exhaust manifold pressure modulation for diesel engine gas exchange and thermal management control”
in: *International Journal of Engine Research* 22.3 (2021), pp. 755–776
(cit. on p. 12)
- [46] **Gosala, D. B., Shaver, G. M., Jr., J. M., and Lutz, T. P.**
“Fuel-efficient thermal management in diesel engines via valvetrain-enabled cylinder ventilation strategies”
in: *International Journal of Engine Research* 22.2 (2021), pp. 430–442
(cit. on p. 12)
- [47] **Gosala, D. B., Allen, C. M., Ramesh, A. K., Shaver, G. M., Jr., J. M., Stretch, D., Koeberlein, E., and Farrell, L.**
“Cylinder deactivation during dynamic diesel engine operation”
in: *International Journal of Engine Research* 18.10 (2017), pp. 991–1004
(cit. on p. 12)
- [48] **Ramesh, A. K., Gosala, D. B., Allen, C., Joshi, M., Jr., J. M., Farrell, L., Koeberlein, E. D., and Shaver, G.**
“Cylinder Deactivation for Increased Engine Efficiency and Aftertreatment Thermal Management in Diesel Engines”
in: *SAE Technical Paper 2018-01-0348*. United States 2018, p. 10
(cit. on p. 12)
- [49] **McCarthy, J.**
“Cylinder deactivation improves Diesel aftertreatment and fuel economy for commercial vehicles”
in: *17. Internationales Stuttgarter Symposium. Proceedings*. Springer Vieweg, Wiesbaden 2017, pp. 1013–1039
(cit. on p. 12)
- [50] **Allen, C. M., Joshi, M. C., Gosala, D. B., Shaver, G. M., Farrell, L., and Jr., J. M.**
“Experimental assessment of diesel engine cylinder deactivation performance during low-load transient operations”
in: *International Journal of Engine Research* 22.2 (2021), pp. 606–615
(cit. on p. 12)
- [51] **Zammit, J., McGhee, M., Shayler, P., and Pegg, I.**
“Internal Combustion Engines: Performance, Fuel Economy and Emissions”
in: Woodhead Publishing 2013
(cit. on pp. 12, 75)

- [52] **Gritsenko, A. V., Glemba, K. V., and Petelin, A. A.**
“A study of the environmental qualities of diesel engines and their efficiency when a portion of their cylinders are deactivated in small-load modes”
in: *Journal of King Saud University - Engineering Sciences* 33.1 (2021), pp. 70–79 (cit. on p. 12)
- [53] **Zamboni, G. and Capobianco, M.**
“Experimental study on the effects of HP and LP EGR in an automotive turbocharged diesel engine”
in: *Applied Energy* 94 (2012), pp. 117–128 (cit. on p. 12)
- [54] **Bermúdez, V., García, A., Villalta, D., and Soto, L.**
“Assessment on the consequences of injection strategies on combustion process and particle size distributions in Euro VI medium-duty diesel engine”
in: *International Journal of Engine Research* 21.4 (2020), pp. 683–697 (cit. on p. 12)
- [55] **Fontanesi, S., Pecchia, M. D., Pessina, V., Sparacino, S., and Iorio, S. D.**
“Quantitative investigation on the impact of injection timing on soot formation in a GDI engine with a customized sectional method”
in: *International Journal of Engine Research* 23.4 (2022), pp. 624–637 (cit. on p. 12)
- [56] **Kang, W., Pyo, S., and Kim, H.**
“Comparison of intake and exhaust throttling for diesel particulate filter active regeneration of non-road diesel engine with mechanical fuel injection pump”
in: *International Journal of Engine Research* 22.7 (2021), pp. 2337–2346 (cit. on p. 13)
- [57] **Liu, Z., Shah, A. N., Ge, Y., Ding, Y., Tan, J., Jiang, L., Yu, L., Zhao, W., Wang, C., and Zeng, T.**
“Effects of continuously regenerating diesel particulate filters on regulated emissions and number-size distribution of particles emitted from a diesel engine”
in: *Journal of Environmental Sciences* 23.5 (2011), pp. 798–807 (cit. on p. 13)
- [58] **Abarham, M., Chafekar, T., Hoard, J. W., Salvi, A., Styles, D. J., Sluder, C. S., and Assanis, D.**
“In-situ visualization of exhaust soot particle deposition and removal in channel flows”

- in: *Journal of Environmental Sciences* 87 (2013), pp. 359–370
(cit. on p. 13)
- [59] **Fang, J., Meng, Z., Li, J., Du, Y., Qin, Y., Jiang, Y., Bai, W., and Chase, G. G.**
“The effect of operating parameters on regeneration characteristics and particulate emission characteristics of diesel particulate filters”
in: *Applied Thermal Engineering* 148 (2019), pp. 860–867
(cit. on p. 13)
- [60] **Lapuerta, M., Rodríguez-Fernández, J., and Oliva, F.**
“Effect of soot accumulation in a diesel particle filter on the combustion process and gaseous emissions”
in: *Energy* 47.1 (2012), pp. 543–552
(cit. on p. 13)
- [61] **Lapuerta, M., Hernández, J. J., and Oliva, F.**
“Strategies for active diesel particulate filter regeneration based on late injection and exhaust recirculation with different fuels”
in: *International Journal of Engine Research* 15.2 (2014), pp. 209–221
(cit. on p. 13)
- [62] **Payri, F. and Desantes, J. M.**
Motores de Combustión Interna Alternativos
1st ed. Editorial Reverté 2011
(cit. on p. 28)
- [63] **Kuehn, T. H., Ramsey, J., and Threlkeld, J. L.**
Thermal Environmental Engineering
3rd ed. Pearson 1998
(cit. on p. 42)
- [64] **Payri, F., Olmeda, P., Martín, J., and Carreño, R.**
“Experimental analysis of the global energy balance in a DI diesel engine”
in: *Applied Thermal Engineering* 89 (2015), pp. 545–557
(cit. on p. 59)
- [65] **Luján, J. M., Climent, H., Dolz, V., Moratal, A., Borges-Alejo, J., and Soukeur, Z.**
“Potential of exhaust heat recovery for intake charge heating in a diesel engine transient operation at cold conditions”
in: *Applied Thermal Engineering* 105 (2016), pp. 501–508
(cit. on p. 59)
- [66] **Payri, F., Broatch, A., Serrano, J. R., Rodríguez, L. F., and Esmoris, A.**
“Study of the Potential of Intake Air Heating in Automotive DI Diesel Engines”
in: *SAE Technical Paper 2006-01-1233*. United States 2006, p. 13
(cit. on p. 62)

- [67] **Mock, P., Kühlwein, J., Tietge, U., Franco, V., Bandivadekar, A., and German, J.**
“The WLTP: How a new test procedure for cars will affect fuel consumption values in the EU”
in: *The International Council on Clean Transportation - Working Paper* 2014.9 (2014), pp. 1–20 (cit. on p. 75)
- [68] **Macián, V., Luján, J. M., Climent, H., Miguel-García, J., Guilain, S., and Boubennec, R.**
“Cylinder-to-cylinder high-pressure exhaust gas recirculation dispersion effect on opacity and NO_x emissions in a diesel automotive engine”
in: *International Journal of Engine Research* 22.4 (2021), pp. 1154–1165 (cit. on p. 80)
- [69] **Galindo, J., Climent, H., Navarro, R., and García-Olivas, G.**
“Assessment of the numerical and experimental methodology to predict EGR cylinder-to-cylinder dispersion and pollutant emissions”
in: *International Journal of Engine Research* 22.10 (2021), pp. 3128–3146 (cit. on p. 80)
- [70] **Piqueras, P., García, A., Monsalve-Serrano, J., and Ruiz, M. J.**
“Performance of a diesel oxidation catalyst under diesel-gasoline reactivity controlled compression ignition combustion conditions”
in: *Energy Conversion and Management* 4 (2019), pp. 18–31 (cit. on p. 82)
- [71] **Serrano, J., Piqueras, P., Sanchis, E., and Diesel, B.**
“A modelling tool for engine and exhaust aftertreatment performance analysis in altitude operation”
in: *Results in Engineering* 4.100054 (2019), pp. 1–11 (cit. on p. 82)
- [72] **Serrano, J. R., Piqueras, P., Morena, J. de la, and Sanchis, E. J.**
“Late Fuel Post-Injection Influence on the Dynamics and Efficiency of Wall-Flow Particulate Filters Regeneration”
in: *Applied Sciences* 9.24 (2019), p. 5348 (cit. on p. 95)